Project No. 609687

FP7-ENERGY-2013-IRP

ELECTRA

European Liaison on Electricity Committed Towards long-term Research Activities for Smart Grids

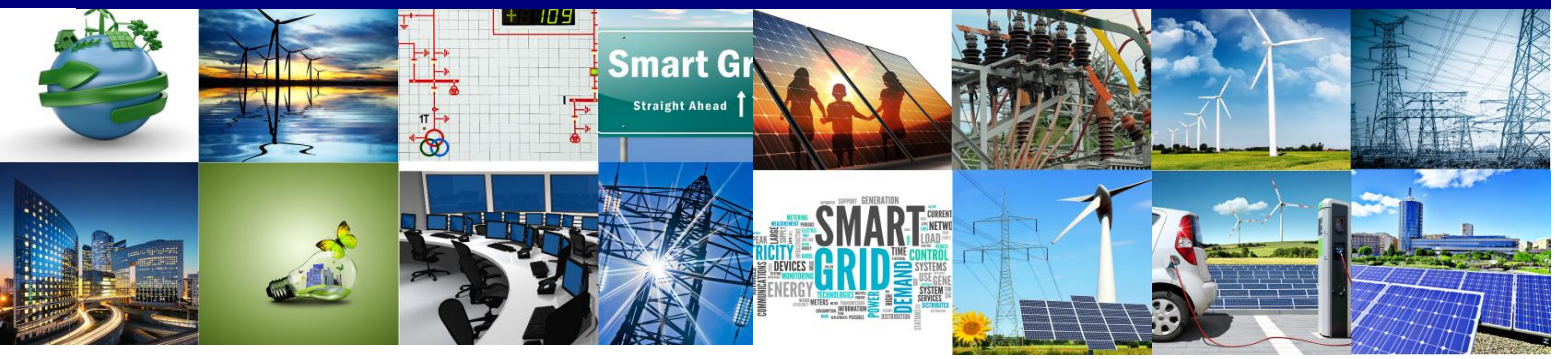

WP 6

Control schemes for the use of flexibility

Deliverable 6.2

Impact of network disturbances on the proposed voltage and frequency control solution

08/12/2017

ID&Title	**D6.2** Impact of network disturbances on the proposed voltage and frequency control solution	**Number of pages:**	110

Short description (Max. 50 words):

This report investigates trends in protection for future power systems, in the context of the ELECTRA "Web-of-Cell" control architecture. The impacts of faults and other disturbances on key protection and control functions are analysed.

Version	Date	Modification's nature
V0.1	04/01/2017	First draft
V0.2	08/02/2017	Revised draft
V0.3	31/03/2017	Updated draft
V0.4	07/06/2017	Updated SRPS definitions
V0.5	28/06/2017	Updated TUBITAK and VTT contributions
V0.6	12/07/2017	Updated USTRATH contribution
V0.7	25/07/2017	Updated USTRATH, TEC, IEN contributions
V0.8	09/08/2017	Added RSE contribution
V0.9	17/08/2017	Updated draft
V0.91	23/08/2017	Updated VTT contribution
V0.92	24/08/2017	Updated VTT and TUBITAK contributions
V0.93	30/08/2017	Updated IEN contribution
V0.94	31/08/2017	Updated executive summary
V0.95	01/09/2017	Updated executive summary
V0.96	26/09/2017	Updated IEN and TUBITAK contributions
V0.97	28/09/2017	Updated TECNALIA contribution
V1.00	02/10/2017	Under review
V1.01	27/11/2017	Updated following internal review
V1.02	28/11/2017	Updated contributions
V2.00	08/12/2017	Released

Accessibility

☒ PU, Public

☐ PP, Restricted to other program participants (including the Commission Services)

☐ RE, Restricted to other a group specified by the consortium (including the Commission Services)		
☐ CO, Confidential, only for members of the consortium (including the Commission Services)		
If restricted, please specify here the group:		
Owner / Main responsible:		
Task 6.3 Leader:	Steven Blair (USTRATH)	
Reviewed by:		
WP 6 Leader: Technical Project Coordinator: Project Coordinator:	Seppo Hänninen (VTT) Helfried Brunner (AIT) Luciano Martini (RSE)	17/11/2017
Final Approval by:		
ELECTRA Technical Committee TOQA appointed Reviewer:	-	08/12/2017

Authors

Name	Last Name	Organization	Country
Steven	Blair	USTRATH	UK
Seppo	Hänninen	VTT	Finland
Bartosz	Kedra	IEN	Poland
Michał	Kosmecki	IEN	Poland
Atte	Löf	VTT	Finland
Bengt	Lüers	OFFIS	Germany
Julia	Merino	TEC	Spain
Daniele	Pala	RSE	Italy
Riku	Pasonen	VTT	Finland
Armağan	Temiz	TUBITAK	Turkey

Copyright

Consisting of:

Coordinator	
Ricerca Sul Sistema Energetico – (RSE)	Italy
Participants	
Austrian Institute of Technology GmbH - (AIT)	Austria
Vlaamse Instelling Voor Technologisch Onderzoek N.V. - (VITO)	Belgium
Belgisch Laboratorium Van De Elektriciteitsindustrie - (LABORELEC)	Belgium
Danmarks Tekniske Universitet - (DTU)	Denmark
Teknologian Tutkimuskeskus - (VTT)	Finland
Commissariat A L'Energie Atomique Et Aux Energies Alternatives - (CEA)	France
Fraunhofer-Gesellschaft Zur Förderung Der Angewandten Forschung E.V – (IWES)	Germany
Centre For Renewable Energy Sources And Saving - (CRES)	Greece
Agenzia Nazionale per Le Nuove Tecnologie, L´Energia E Lo Sviluppo Economico Sostenibile - (ENEA)	Italy
Fizikalas Energetikas Instituts - (IPE)	Latvia
SINTEF Energi AS - (SINTEF)	Norway
Instytut Energetyki - (IEN)	Poland
Instituto De Engenharia De Sistemas E Computadores Do Porto - (INESC_P)	Portugal
Fundacion Tecnalia Research & Innovation - (TECNALIA)	Spain
Joint Research Centre European Commission - (JRC)	Belgium
Nederlandse Organisatie Voor Toegepast Natuurwetenschappelijk Onderzoek – (TNO)	Netherlands
Turkiye Bilimsel Ve Teknolojik Arastirma Kurumu - (TUBITAK)	Turkey
University Of Strathclyde - (USTRATH)	UK
European Distributed Energy Resources Laboratories (DERlab)	Germany
Institute for Information Technology at University of Oldenburg (OFFIS)	Germany

Executive Summary

This deliverable provides guidance for the key areas of protection research that will underpin the realisation of stable and efficient future power systems, particularly considering the proposed ELECTRA IRP Web of Cells (WoC) control architecture [1]. For such a radical decentralised control paradigm, it is critical that the impact of disturbances, such as power system faults, is minimised through novel protective systems and systematic validation. Industry challenges arising from the large-scale integration of renewable energy sources are already apparent, such as the difficulties in specifying backup protection settings to achieve timely and correct fault isolation, and the maloperation of loss of mains protection relays during large loss of generation events.

In the context of the WoC architecture, this report demonstrates how to rapidly and efficiently respond to disturbances by:

- Utilising adaptive and wide area protection schemes;
- Proactive control of available grid resources (such as managing the response of converter-interfaced generation) to optimise protection functionality; and
- Initiating post-fault action to ensure system stability and optimal system operation.

The methodology for this work has involved three stages:

1. Identification and information capture of all relevant state-of-the-art protection and control “functions” i.e. research activities, methods, and algorithms.
2. Qualitative analysis and multi-criteria ranking of the most “impactful” of the identified protection and control functions. The criteria includes factors relating to the WoC control architecture.
3. Detailed, quantitative studies of the key, high-priority functions. This includes integration of applicable WoC control use cases.

Therefore, detailed studies are provided in this report for the following areas of research, which have been identified through the methodology: fast-acting wide area protection methods using Phasor Measurement Units (PMUs); adaptive and “self-organising” protection under varying system conditions; enhanced fault ride-through capabilities; fault location for self-healing systems; and fault pattern recognition.

The report illustrates how the increased availability of measurements and communications can be exploited to provide optimised and more resilient protection functionality, which is especially important to accommodate the connection of highly-distributed generation at medium- and low-voltages. Methods are demonstrated which can dynamically adapt to changes in distribution systems and cater for arbitrary changes in power flows and topology in transmission systems; these developments are critical for mitigating the inherent uncertainty in future power system generation sources. Furthermore, the potential for loss of communications and the scalability to a large number of measurement locations are explicitly catered for in the design of a novel wide area protection scheme.

The WoC architecture provides a convenient division of a large grid into smaller areas that can accommodate scalability of the low-latency requirements for wide area protection and the coordination of adaptive protection in distribution systems with high levels of distributed generation. It is shown how wide area protection can be designed to operate efficiently within the WoC architecture, including protecting tie-lines between cells, but further work is required to establish the performance under realistic communications delays and “weak” networks associated with the presence of converter-interfaced renewable generation.

The pervasiveness of renewable generation interfaced to the grid via power electronic converters, coupled with the projected reduction in system inertia, will alter long-standing assumptions about the voltage and current behaviour during power system faults and is already creating significant industry challenges. A method is proposed to provide new indictors of high-impedance faults in such circumstances, and wide area protection provides a promising supervisory technique for such systems. However, further work is required to analyse and model power systems and the proposed protection solutions in more diverse scenarios.

It has been shown that there is a potential conflict between wind farm fault ride through (FRT) capability and ELECTRA Primary Voltage Control (PVC) due to the similar operational timescales. This requires careful design of the PVC control parameters and analysis of the interaction with FRT.

Terminologies

Abbreviations

AC	Alternating Current
ANN	Artificial Neural Network
BP	Boundary Point
BRC	Balance Restoration Control
BSC	Balance Steering Control
CCC	Cell Central Controller
CIM	Common Information Model
CT	Current Transformer
CTL	Control Topology Level
CTS	Control Time Scale
DC	Direct Current
DG	Distributed Generation
DER	Distributed Energy Resource
DIFG	Double Fed Induction Generator
DoW	Description of Work
DT	Definite Time
ELECTRA IRP	European Liaison on Electricity Committed Towards long-term Research Activities for Smart Grids Integrated Research Programme
FC	Full Converter
FCC	Frequency Containment Control
FL	Fuzzy Logic
FRT	Fault Ride Through
GOOSE	Generic Object Oriented Substation Events
GPS	Global Positioning System
HIF	High Impedance Fault
HV	High Voltage
HVDC	High Voltage Direct Current
ICT	Information and Communications Technology
IDMT	Inverse Definite Minimum Time
IED	Intelligent Electronic Device
IRPC	Inertia Response Power Control
LIF	Low Impedance Fault
LV	Low Voltage
LVRT	Low Voltage Ride Through

MV	Medium Voltage
NO	Normally Open (Point In The Network)
OCR	Over Current Relay
OPF	Optimal Power Flow
PDC	Phasor Data Concentrator
PS	Primary Substation
PC	Pick-up Current
PMU	Phasor Measurement Unit
PPVC	Post Primary Voltage Control
PVC	Primary Voltage Control
ROCOF	Rate of Change of Frequency
RTDS	Real Time Digital Simulator
SCIG	Squirrel Cage Induction Generator
SIPS	System Integrity Protection Scheme
SRPS	Single Reference Power System
SS	Secondary Substation
TCP	Transmission Control Protocol
TMS	Time Multiplier Settings
UDP	User Datagram Protocol
VPN	Virtual Private Network
WAN	Wide Area Network
WoC	Web of Cells
WT	Wavelet Transform

Table of Contents

List of Figures and Tables

1 Introduction

The unprecedented large-scale integration of distributed, renewable energy sources presents significant challenges for the real-time control and protection of electrical power systems. In the coming decades, there will be a sharp rise in the number of available grid measurements and controllable resources [2], such as converter-interfaced generation, energy storage, and demand-side response. In particular, the stability of future grid operation will be enhanced by providing more and faster-acting ancillary services [3], and this will be delivered through a large number of diverse resources, rather than centralised generation sources. However, such services must be designed in a manner that is computationally feasible and efficient, and where real-time control and protection actions are not unduly delayed by communications systems or other factors.

A radical new control architecture has been designed within the ELECTRA IRP research project to directly address the challenges associated with the real-time operation of grids with highly-distributed resources. This architecture decentralises critical system functions – such as the provision of inertia, frequency containment, and balancing – into zones or "cells" which are smaller than conventional Load Frequency Control (LFC) areas. Each cell is responsible for the provision and activation of internal flexibility of any type available and communicating with neighbouring cells where necessary; this process will be automated by cell controllers rather than depending on manual input. This "divide and conquer" approach, which has been named the Web of Cells (WoC), is designed to allow the grid to efficiently scale to a very large number of measurable and controllable devices – without excessive computational requirements or communications delays.

Under such a radical new control paradigm, protection and automation strategies are required to detect emergent issues in real-time and instruct a fast-acting response utilising flexible grid resources. It is important to rapidly and efficiently respond to disturbances by, for example: utilising adaptive, wide-area protection schemes; proactive control of available grid resources (such as managing the fault level contribution from converter-interfaced generation) to optimise protection functionality and provide a faster-acting response; and taking post-fault action to ensure protection stability and optimal system operation.

This report documents the work within the ELECTRA IRP to minimise the impact of disturbances in future highly-distributed power systems. An analysis of the impact of suitable protection schemes in such power systems has been conducted using the following methodology:

1. Identification of all relevant developments in the state of the art in power system protection.
2. Qualitative analysis of the highest impact protection "functions" for future highly-distributed power systems such as the WoC, using inputs from multiple EU research institutes.
3. Investigation of "high-impact" protection functions through detailed simulation studies, using representative grid models. Quantitative factors, such as reduced protection trip times, will be used to evaluate the performance of the proposed functions. Where appropriate, these simulations will be demonstrated using laboratory experiments.

This work thereby provides guidance for diverse areas of protection research that will underpin the realisation of stable and efficient future power systems. This report assesses in detail the impact of network disturbances and how the proposed solutions react in those circumstances. Chapter 3 describes the research methodology, and Chapter 4 analyses a wide variety of relevant, emerging research activities. Chapter 5 summarises the common simulation models which underpin this work. Opportunities for adaptive protection in distribution systems are discussed in Chapter 6. Leading from this, Chapter 7 illustrates the use of information systems to automatically handle adaptive and dynamic power systems. Chapter 8 discusses the impact of fault ride-through

capability for wind energy integration. The large-scale use of Synchrophasor measurements is analysed in Chapter 9, including: feasible architectures for Phasor Measurement Units (PMUs); a computational platform for resilient and adaptive backup protection that leverages a multitude of Synchrophasor data; and a measurement method to validate real-time requirements and lead to efficient simulation techniques. Chapter 10 presents a new method for locating faults in distribution systems, and Chapter 11 examines methods for fault detection. Chapter 12 concludes and provides recommendations for how to minimise the effects of network disturbances. Results from this work have also been presented at the CIGRE Study Committee B5 (Protection and Automation) Colloquium in September 2017 [4].

2 Analysis of Technical Objectives

This section establishes the precise technical focus and the objectives of the work, and Figure 2-1 summarises the key technical objectives[1].

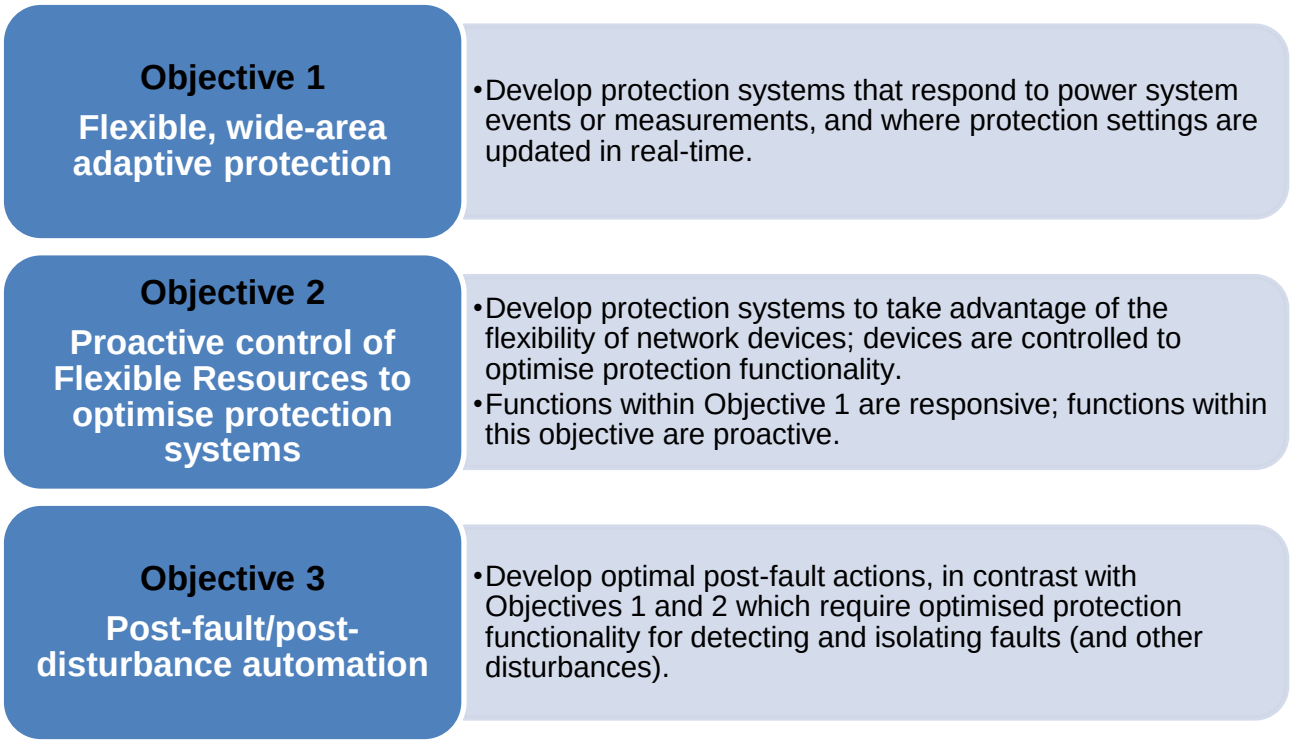

Figure 2-1: Key research objectives

These objectives represent the critical technical challenges for protection in future power systems, particularly considering the opportunities for flexibility, uncertainty relating to renewable energy generation, and the desire for more resilient power delivery systems. The work in this report has been tailored to address these key challenges.

[1] The outline of the research is based on the ELECTRA IRP Description of Work (DoW) documentation. Detailed analysis of the DoW is given in Chapter 13. Based on this analysis, the key objectives in Figure 2-1 have been established. This process ensured that the task objectives were clear and fully aligned with the internal DoW requirements.

3 Research Methodology

3.1 Overview

There are multiple technical objectives and other factors affecting this work, leading to the following requirements:

- Addressing all technical objectives identified within Chapter 2.
- Expanding on the state of the art for the protection of future highly-distributed power systems.
- Ensuring consistency with other aspects of the ELECTRA project, including the WoC architecture, the novel real-time control functionality (i.e. ELECTRA use cases[2]), and the use of common power system simulation models.
- Exploiting the authors' diverse expertise.
- Encouraging collaboration between the authors, where appropriate.
- Conduct complementary laboratory validation, using results or techniques developed within the research work.

To cater for all of these factors, the methodology summarised in Figure 3-1 has been used, with the detailed process given in Section 3.2.

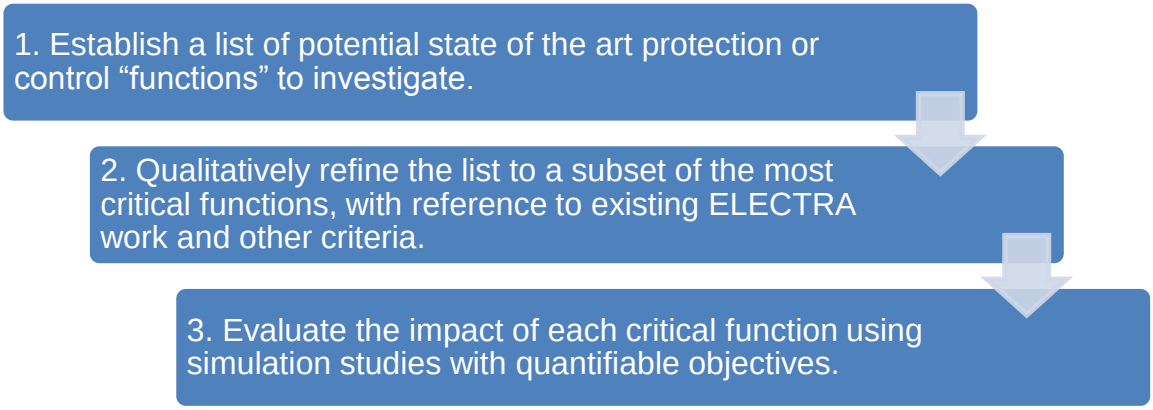

Figure 3-1: Overview of research methodology

3.2 Detailed Methodology

As summarised in Figure 3-1, the following methodology has been used to complete the research:

1. **Develop a comprehensive list of state of the art, or emerging, protection and control "functions"**. In this context, a "function" could include any relevant system or technique, for example: wide-area protection using Phasor Measurement Unit (PMU) data, controlling fault levels to optimise protection coordination, or adaptive overcurrent protection. The full list of functions resulting from this analysis is discussed in Chapter 4.
2. **Map each function to relevant concepts within ELECTRA and assess each function using several qualitative criteria**, as defined in Section 4.2. Based on this assessment, a

[2] In order to maintain frequency (balancing) and voltage control in the future power system, the WoC control scheme introduces six high-level use cases, which are Balance Restoration Control (BRC), Frequency Containment Control (FCC), Inertia Response Power Control (IRPC), Balance Steering Control (BSC), Primary Voltage Control (PVC), and Post Primary Voltage Control (PPVC)

subset of high-priority or high-impact functions are selected by the authors, and an explicit written justification for this selection is given. This process involves the following steps:

a. Map each function to one (or more) objectives described in Chapter 2, to ensure that the function is relevant, and to ensure that there is "coverage" of all three objectives. Where possible, each function should also be mapped to other related concepts within ELECTRA, specifically the Control Topology Level (CTL)[3] and to one or more real-time control Use Cases. This three-way mapping is illustrated in Figure 3-2. Note that CTLs which are not applicable are shaded in grey.
b. Ensure that each function fits within the expertise (and allocated person-months) of the authors, as indicated in Figure 3-3.
c. Qualitatively assess each function to determine the highest quality or highest impact functions for further study. This is illustrated in Figure 3-4.

3. **Detailed analysis of the "high impact" subset of protection and control functions**. From the subset of high-priority functions, a further subset is selected by the authors to be studied in detail using simulations, including quantitative evaluation. Quantitative factors may include, for example, reduced protection operation time resulting from the function under study. The full process is as follows:
    a. Prepare a brief literature review for each protection or control function.
    b. Define relevant performance metrics for each function, e.g., reduced protection trip time, minimal zone isolated by protection, or ability to ride-through a disturbance. Therefore, each function should be associated with a testable scenario with quantifiable outcomes. It should be possible to test the original base case, without the novel protection or control function integrated (i.e. using a "conventional" function), for comparison of the defined performance metrics. For example, the trip times for a novel wide-area backup protection scheme using PMUs might be compared to trip times for a conventional transmission line distance protection scheme.
    c. Draw overall conclusions and recommendations based on all research results.

[3] A characteristic "topology level" at which a control function operates within the WoC architecture. The following definitions have been established within the ELECTRA project:
CTL0: Physical, single device level
CTL1: Flexible (aggregate) resource level
CTL2: Cell level
CTL3: Inter-cell level

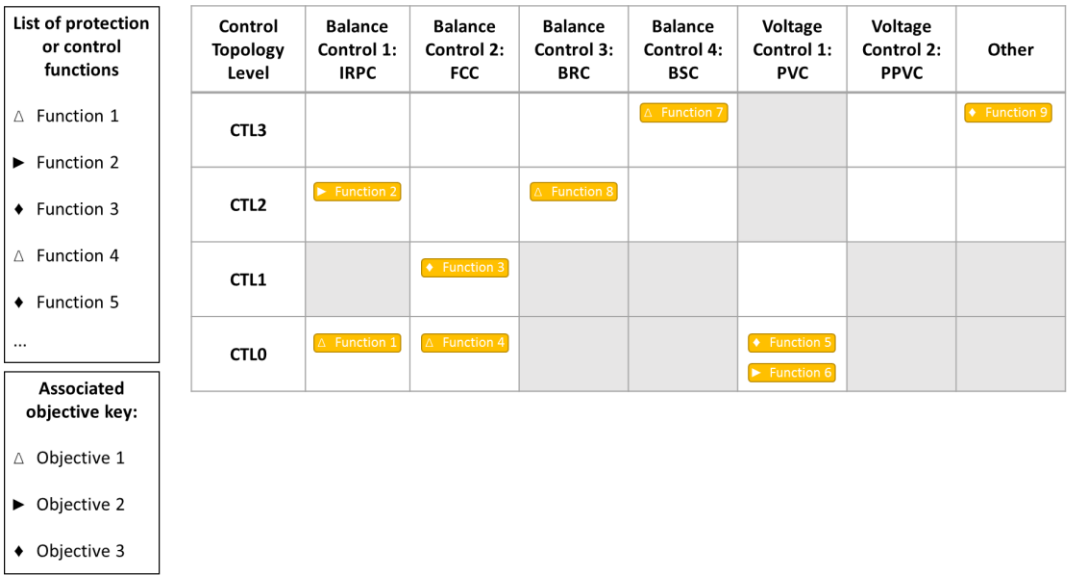

Figure 3-2: Ensure objective coverage

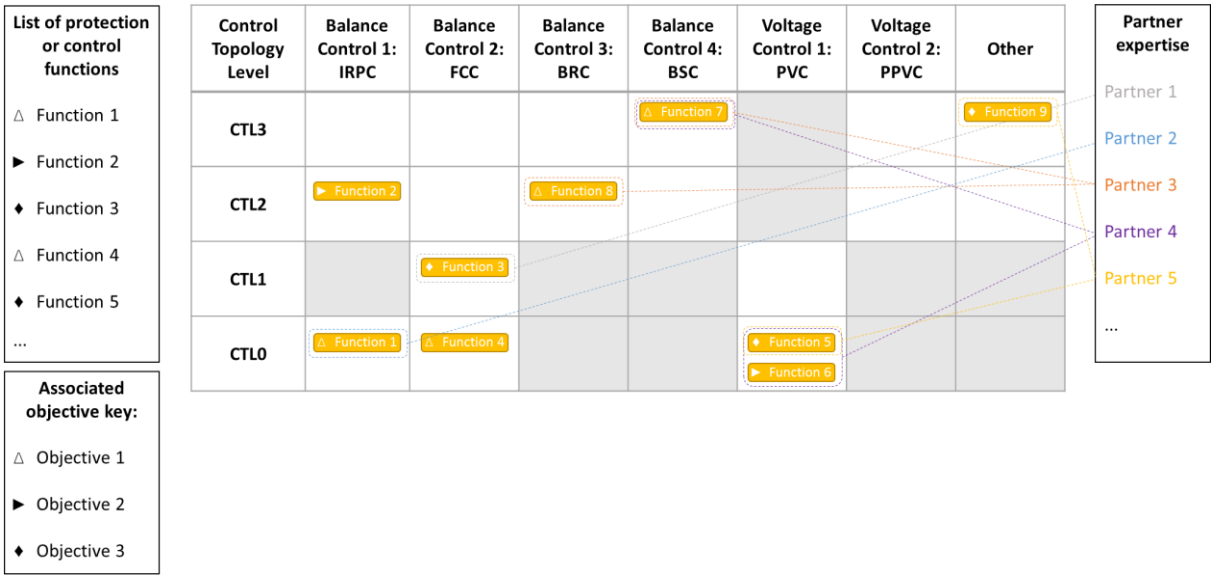

Figure 3-3: Ensure project partner coverage

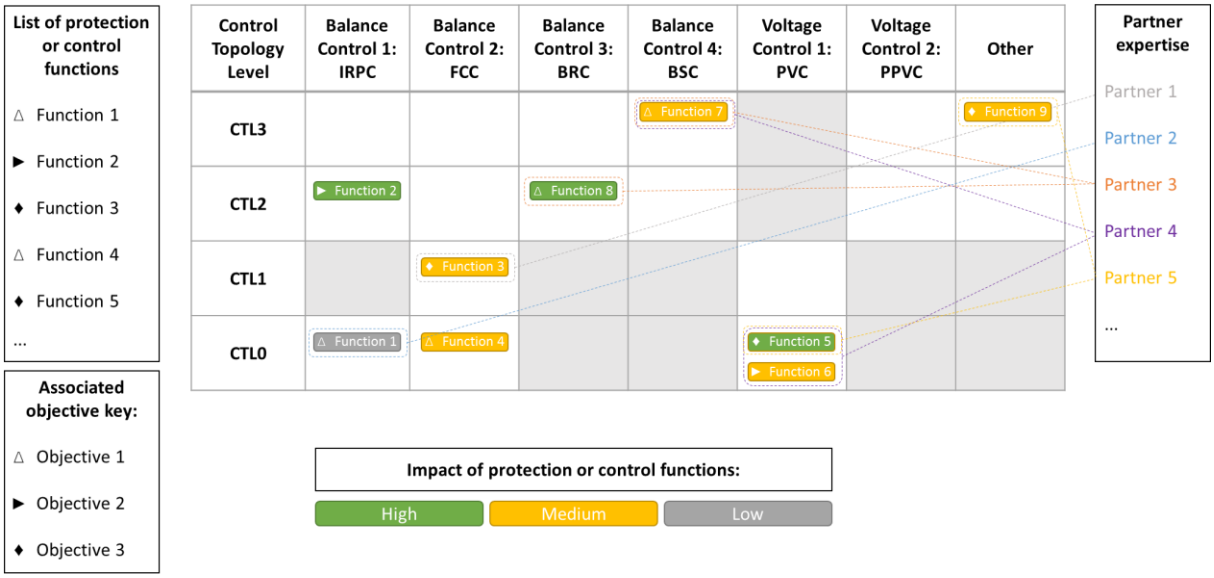

Figure 3-4: Assess impact of functions

4 Analysis of Protection and Control Functions

4.1 Key Identified Protection and Control Functions

The report authors collaboratively established a list of nineteen diverse research topics, which include promising developments in protection for future power systems. Due to the large number of items and assessment criteria, these results have been included in a separate spreadsheet document, which should accompany this report, although one full example is given in Section 4.3. The seven highest ranked protection and control function are included in Section 4.4 (Table 4-2).

4.2 Qualitative Criteria for Function Assessment

To comprehensively assess the impact of potential protection and control functions, a large number of criteria have been used. These criteria include the following (with the full list provided in the accompanying spreadsheet):

- Background information:
  - Role of function
  - Applicable voltage levels
  - Potential advantages
  - Communications requirements
  - References to key publications
- Relationship with ELECTRA:
  - Specific research challenges and novelty, in context of ELECTRA
  - Applicable objective (see Chapter 2)
  - Interaction with WoC architecture
  - Possible control conflicts
  - Appropriate simulations models, for consistency with the rest of the project
  - Relevant ELECTRA Use Cases
  - ELECTRA CTL mapping
- Qualitative assessment criteria:
  - Novelty
  - Relevant to ELECTRA
  - Feasibility of simulation-based implementation and testing
  - Feasibility of lab-based implementation and testing
  - Necessity (i.e. the perception of how urgently the function is required to be implemented)

For each of the “qualitative assessment criteria”, a score (low, medium, or high) has been attributed to each function. Attributing a value to each score level (low = 1, medium = 2, high = 3) allowed an aggregate score to be calculated for each function.

4.3 Example of Result of Qualitative Analysis

Table 4-1 summaries the results of the qualitative analysis for one of the identified protection or control functions. This information includes several background factors and the relationship of the protection/control function to the ELECTRA WoC concept and control use cases. To reiterate, this process has been completed for all nineteen candidate protection functions, but only one is highlighted here in detail due to the scale of the content.

Name of protection or control function	Detection and location of large disturbances (such as a large loss of generation, or loss of an inter-cell tie-line) in a web-of-cells architecture
Background information	
Description	Identification of the cell "responsible" for resolving a power imbalance so that, initially, that cell can attempt to resolve the issue (i.e. CTL2)
Role of function	Support function
What is protected, e.g., the network or a specific device?	N/A
What is the network or device protected against?	N/A
Applicable voltage levels	HV, MV
Geographic area of efficacy	Wide-area
Potential advantages	Ensure that cells are given the opportunity to resolve local problems locally
Communications requirements	Low-bandwidth, low-delay
Literature status (e.g. well-known, new)	New, but there is some existing work using PMU data for disturbance location
References from initial literature survey	[5], [6]
ELECTRA relationship	
Research challenges and novelty, in context of ELECTRA	Ensuring the correct and timely identification of the "responsible" cell
Relevant objective(s)	Objective 3
Potential interaction with ELECTRA WoC architecture	This function may also be required for correct reserves activation, and therefore could interact with FCC and BRC.
Difference between implementation today, and implementation for WoC	Decentralised design, which will dived the problem into smaller concerns, but may require real-time coordination between cells.
Possible conflicts with other control functions	N/A
Potential ELECTRA SRPS models	Pan European
Potential ELECTRA Use Case mapping	FCC, BRC
ELECTRA Control Topology Level mapping	CTL2, CTL3
Possible target for simulation development and demonstration?	Yes
Possible target for WP7 laboratory demonstration?	Yes
Laboratory demonstration options	Yes - RTDS-based study
Qualitative evaluation	
Novelty	High
Relevance to ELECTRA	High
Feasibility of simulation-based implementation and testing	High
Feasibility of lab-based implementation and testing	Medium
Necessity	High
Overall score (out of 15)	14

Table 4-1: Example of protection function qualitative analysis

4.4 Justification for Relevance to ELECTRA, the WoC, and Future Power Systems

Table 4-2 summarises the results of the qualitative assessment described in Section 4.2 i.e. the results of Stage 2 of the methodology given in Figure 3-1, and the functions which had the highest qualitative scores. The table therefore highlights the key protection functions which will be especially important in future highly-distributed power systems, and which are analysed in detail in this report.

Protection and Control Function	Description and Justification for Investigation	Report Chapter
Detection and location of large disturbances	Identification of events such as a large loss of generation, or loss of an inter-cell tie-line. This is important in a WoC architecture, because the "responsible" cell may need to be identified to correctly respond. Furthermore, signals from neighbouring cells may need to be considered.	Chapter 9
Protection with distributed Intelligent Electronic Devices (IEDs)	Self-healing concept and fault distance computation in MV overhead networks (in context of overcurrent protection).	Chapter 10
Wide-area protection using Phasor Measurement Units (PMUs)	The use of PMU voltage and/or current measurements to quickly detect and locate faults. Even considering communications delays, this has the potential to provide faster-acting protection than existing transmission system backup protection methods (e.g. within 150 ms). It is also important to be able to accurately characterise the latency of PMUs for real-time applications, and for informing simulation studies.	Chapter 9
Adaptive overcurrent protection	Primary protection of distribution networks with very high shares of distributed generation, by optimisation of the overcurrent relay time and pickup current settings.	Chapter 6
Fault Ride Through (FRT)	Impact of high penetration of wind energy on system behaviour during voltage disturbances.	Chapter 8
Pattern recognition based schemes	The detection of abnormal events in the system by analysing characteristic patterns, and the identification of the most interesting pattern (and variable) for fault location and detection in a WoC architecture.	Chapter 11
Self-organising protection	Automated configuration of protection for arbitrary, varying network topologies. Coordination of protection devices for detection and location of faults in case of a reconfigurable network such as the WoC.	Chapter 7

Table 4-2: Key identified protection and control functions

5 Simulation Models

5.1 Overview and Requirements

To provide consistency of the simulation results itself and to guarantee the coherence along the full project, two Single Reference Power System (SPRS) models have been selected for testing the proposed protection schemes and the control functions. These models are intended to provide representative examples of typical distribution system (based on a CIGRE medium voltage (MV) model), and a larger Pan-European transmission system. Both were selected as potential SRPS models in the framework of ELECTRA Work Package 5 relating to observing the state of the future power system.

5.2 CIGRE MV Model

The CIGRE MV grid was published in “Benchmark Systems for Network Integration of Renewable and Distributed Energy Resources”, Task Force C6.04, April 2014” [7] with the intention to provide a common basis for benchmarks in electric power systems. The publication shows a topological overview of the grid and specifies nodes, loads, generation, lines, switches, transformers and the slack. The benchmark gives flexibility to model radial and meshed grids according to the switches configuration. A scheme of the grid is shown in Figure 5-1.

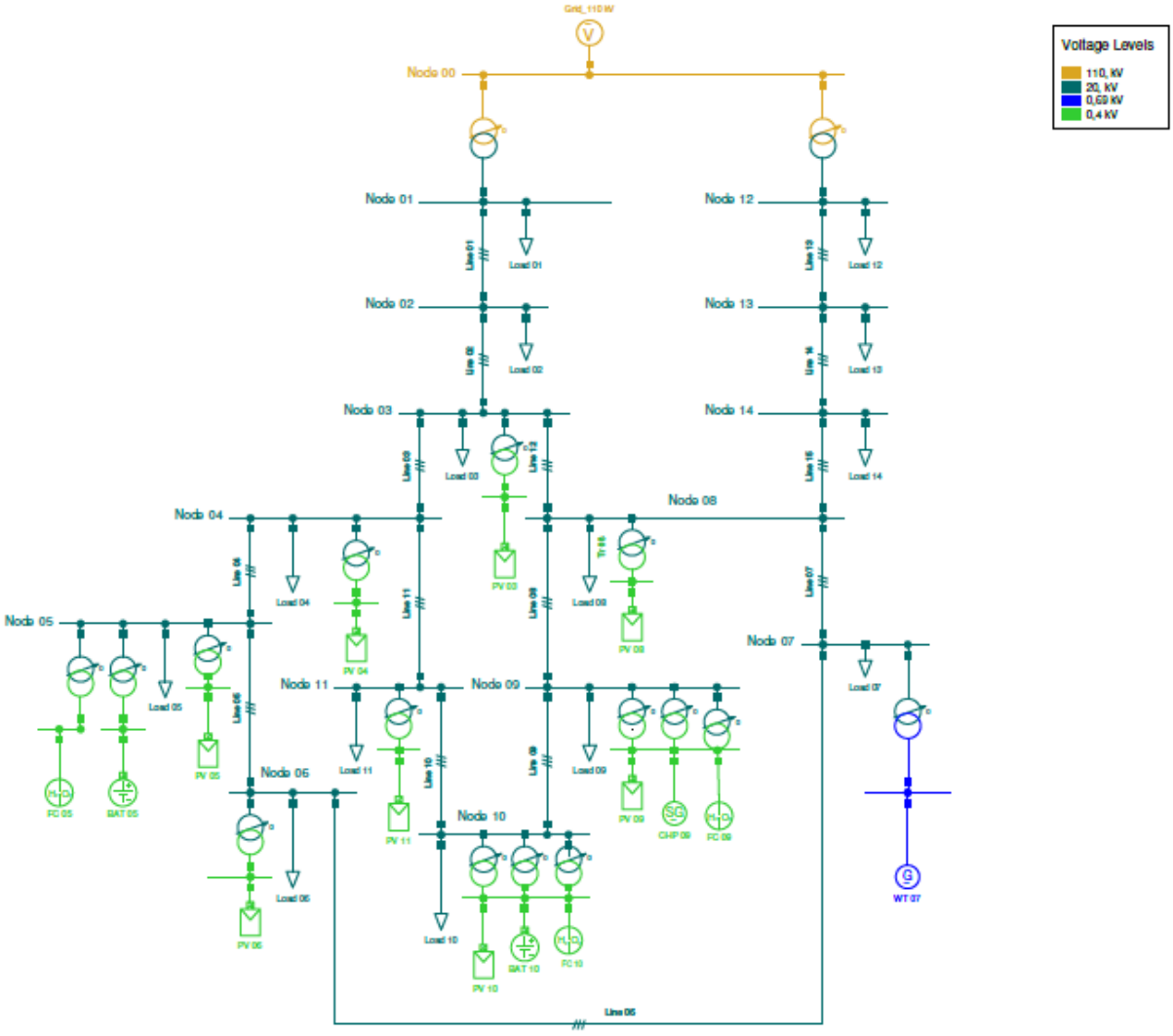

Figure 5-1: CIGRE MV model

From that base model, several modifications were made in order to introduce distributed energy resources (DERs). The connection to the High-Voltage (HV) grid is done from a single 110 kV busbar. Downstream the grid has two main MV feeders where the loads and the DERs are connected at 20 kV level. Both feeders are weakly linked. The DERs are mainly Photovoltaic (PV) installations on the Low-Voltage (LV) level (i.e., eight PV plants), but also batteries (two units), Combined-Heat Power (CHP) devices (two units) and fuel cells (two units) are connected at 0.4 kV and the wind turbine is connected at 0.69 kV.

5.3 Pan-European Model

The Pan-European model is based on the CIGRE HV grid. The original network represents three different geographical areas with 13 main buses. The modified version layout is shown in Figure 5-2, where also the division of the grid into cells is displayed. The model combines alternate current (AC) and direct current (DC) transmission systems at multiple voltage levels, with ranges from 0.4 kV to 400 kV in the AC system and a nominal voltage of the 650 kV for the DC one. The cells inside contain diverse DERs: batteries, PV panels and other power electronic converters, that are the extrema for controlling the power transmission through the high voltage direct current (HVDC) links.

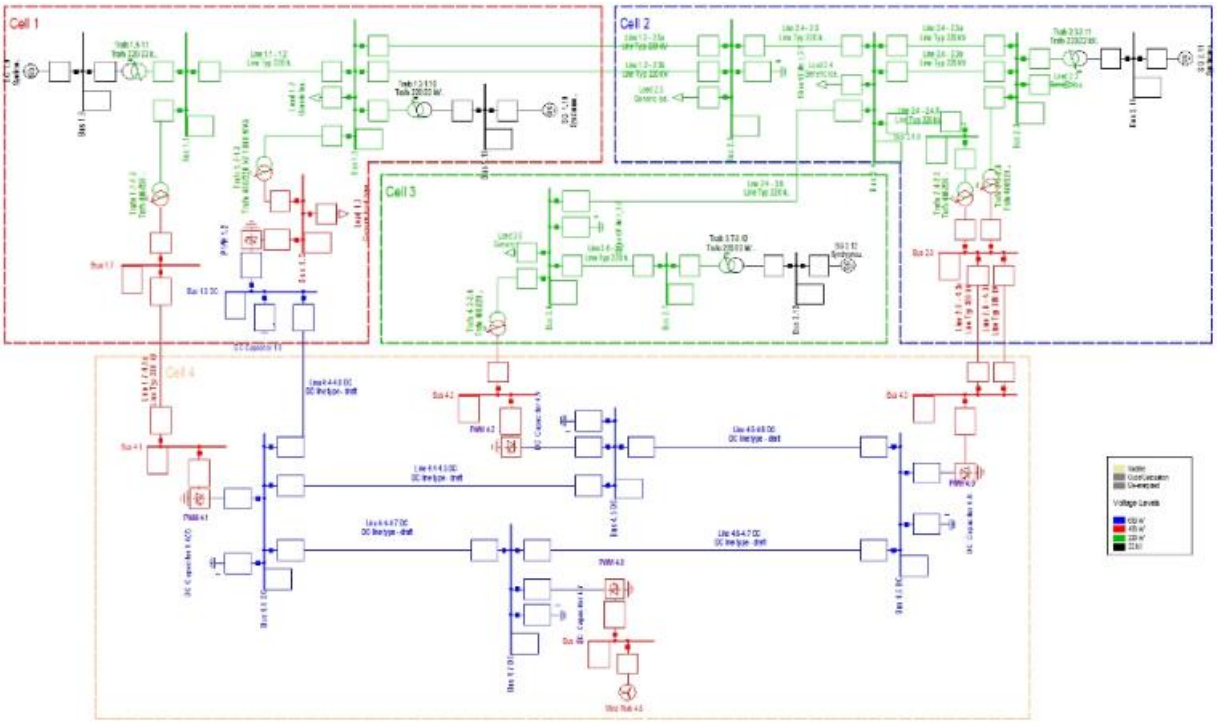

Figure 5-2: Pan-European model

6 Adaptive Overcurrent Protection and Operation with Post Primary Voltage Control

6.1 Introduction

The increasing amount of DER required in the 2030+ horizon of interest within ELECTRA IRP, and the decrease in the short-circuit (SC) current contribution of the DERs as well as their sensitive dynamics raises challenges for conventional protection schemes. This requires protection schemes to become adaptive in order to deal with the topology changes and to avoid false trips in case of internal faults within a cell or in any neighbouring cell. The aim of adaptive overcurrent protection is to determine the Pick-up Currents (PCs) and the time dial settings, also known as Time Multiplier Settings (TMS), of overcurrent relays (OCRs) in an adaptive way in order to maintain relay coordination following a network topology change and to provide a fast response to varying load demands and intermittent distributed generation.

Two different approaches have been investigated to deal with the adaptive overcurrent protection for the WoC. Both approaches have been developed considering the CIGRE MV grid as testing/reference grid for which the schemes have been designed. In both cases, slight modifications to fulfil the needs of the grid for the correct validation of the protection schemes have been proposed. The first approach (Section 6.2) considers the CIGRE MV grid as a single cell. In this approach, the protection scheme coordinates the trip of intelligent electronic devices (IEDs, i.e., overcurrent relays) considering the adaptive functionality based on a centralised communication control[4]. OCR parameters are calculated based on Definite Time (DTM) characteristics in the first approach. The second approach (Section 6.3) extends the adaptive protection concept to a multi-cell case and the adaptive functionality is triggered by a change of the status of a DER or due to a short circuit (SC) fault. In this approach, OCRs are used as Inverse Definite Time (IDTM) relays, and the tripping time is inversely proportional to SC fault currents. Additionally, two specific scenarios from Section 6.3 are evaluated under Section 6.4 considering the Post Primary Voltage Control (PPVC) response of multi-cell networks after adaptive overcurrent protection operations, which aims to assess a specific ELECTRA use case with a specific protection function under the WoC structure.

6.2 Single-Cell Evaluation with DTM Relay Settings

6.2.1 Overview and Modelling

In order to evaluate adaptive protection schemes in WoC structures considering various DER conditions, the base network model of the CIGRE MV benchmark is slightly modified. However, the network is kept as close as possible to the original benchmark being used for other developments within the project, thus, the only modification applied is to increase the nominal power and the generation capacities of PV panels connected in LV levels. In this way, the generation capacity in the cell will allow testing of adaptive protection schemes under several DERs penetration cases. The CIGRE benchmark allows the configuration on several topologies by opening/closing of two switches. Out of the several feasible structures, the line connecting Node 14 and Node 09 is opened as well as the line connecting Node 06 and Node 07, leading to the radial structure shown in Figure 6-1. The modified system eventually consists of two feeders with 14 nodes including a

[4] This work has been published in the conference paper: *A case study of an adaptive protection scheme for the Web-of-cells Concept*, in ISGT Europe 2017 (http://sites.ieee.org/isgt-europe-2017/) co-authored by Maria Valov (IWES-Fraunhofer) and Julia Merino (TECNALIA) in the framework of the REX Exchange Program (4th call).

broad set of DERs such as PV systems, fuel cells, batteries and a wind turbine. Due to the ELECTRA interest in grids with a high deployment of DERs, only the protection scheme of one feeder has been tested as there are no DERs in the other one (i.e., the right feeder in Figure 6-1). All simulations have been performed by DigSILENT Power Factory tool.

6.2.2 Proposed Adaptive Protection Scheme

The protection scheme considers the protection of DERs and MV lines. The protection of DERs responds to general principles applied to generation groups and thus, it is not affected by the system state. Due to this reason, the focus of this study includes the line overcurrent protection. The overall view of the protection scheme designed for the cell can be seen in Figure 6-1.

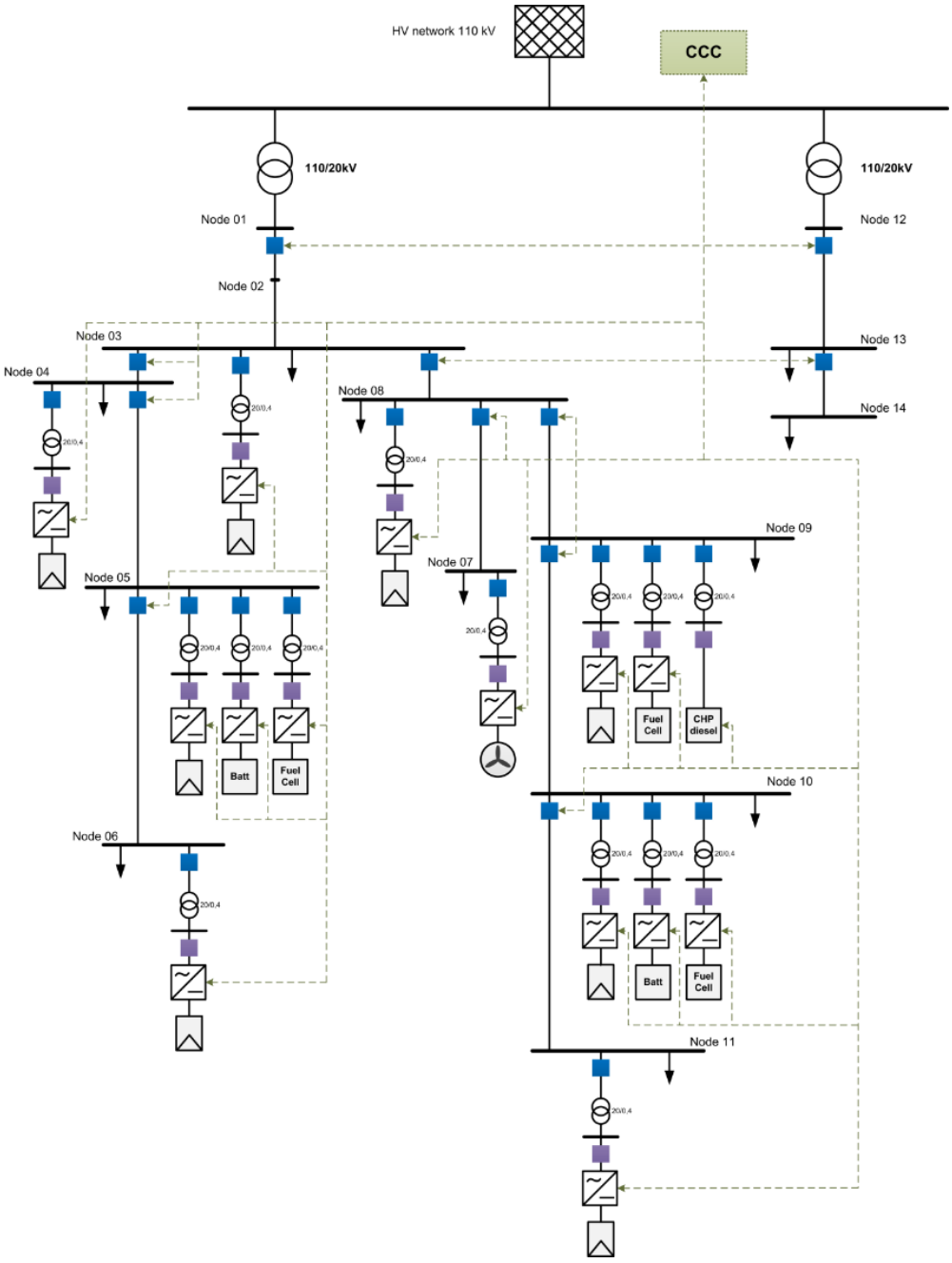

Figure 6-1: Proposed protection scheme for the cell

IEDs, widely used devices especially in the protection of MV grids, have been modelled in this study. The IEDs are based on a coordinated overcurrent principle with DT characteristics. However, in order to identify the abnormal situations, this model has been improved to include the

adaptive functionality. For the adaptive characteristic of IEDs, look-up tables have been used containing pre-defined setting groups. These groups can easily be switched to address the possible changes in the cell, guaranteeing fault isolation in any disturbed network condition. For the initial testing of the protection scheme within the cell, two overcurrent settings have been defined based on a SC fault analysis. The cell has a supervisory control function called Cell Controller (CC) which is under the responsibility of the cell system operator. The CC observes entire cell to estimate in advance the SC currents in case of internal faults and, consequently, to adapt IED settings accordingly. The flow chart of the CC operation to perform adaptive protection is shown in Figure 6-2.

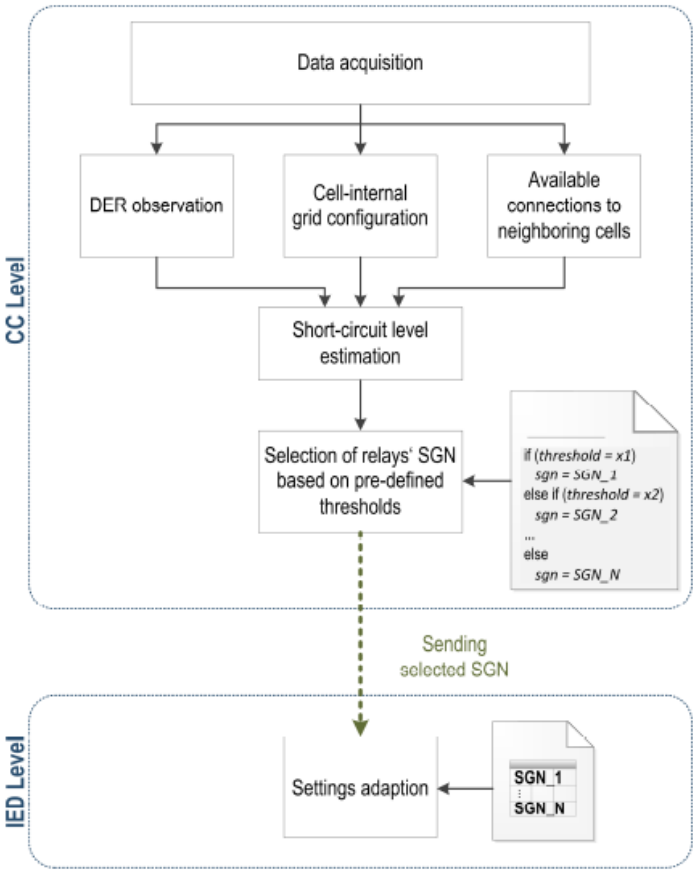

Figure 6-2: Flow chart of the adaptive protection by the CC

Benefiting from the high degree of observability of the WoC as well as the advanced existing communication technologies, the CC registers the required information: availability and feed-in of DERs and the status of network switches indicating existing grid topology. For the estimation of SC currents supplied to the cell by neighbouring cells, reliable communication links in the tie-lines should exist. With all the information, a decision-making algorithm decides relay settings for the prevailing cell state. The result is sent to IEDs that switch the tripping curves if necessary or keep the current settings.

6.2.3 Case Study

The simulation study has performed comparing the selective fault isolation accomplished by the IEDs with and without the adaptive functionality implemented in two scenarios. The response of the system to a three-phase SC fault has been simulated. In order to observe tripping curves of the coordinated overcurrent protection scheme (main/backup protection), a SC fault at the end of one feeder (Node 11) is applied.

6.2.3.1 Without Adaptive Functionality

The cell is protected by a standard protection scheme in this scenario. This scheme is designed for normal conditions to a connection with a neighbouring cell at the HV side. The “HV cell” provides most of the SC current to the fault. If a fault occurs, the SC current is detected by all IEDs, but only the corresponding IED based on the delay of DT curves initiates tripping signal to the corresponding circuit-breaker. The performance of this conventional scheme is presented in Figure 6-3. The value of the SC currents due to a fault as seen by any IED (on the primary side of the current transformers) has been represented with vertical lines, where the colours are those according to the respective relays. In Figure 6-3, it can be seen that the main IED (R10), the closest one to the SC fault, trips just after 100ms. The other relays along the feeder behave as the backup protection relays. The time grading (time between two relay operations) is taken as 300ms.

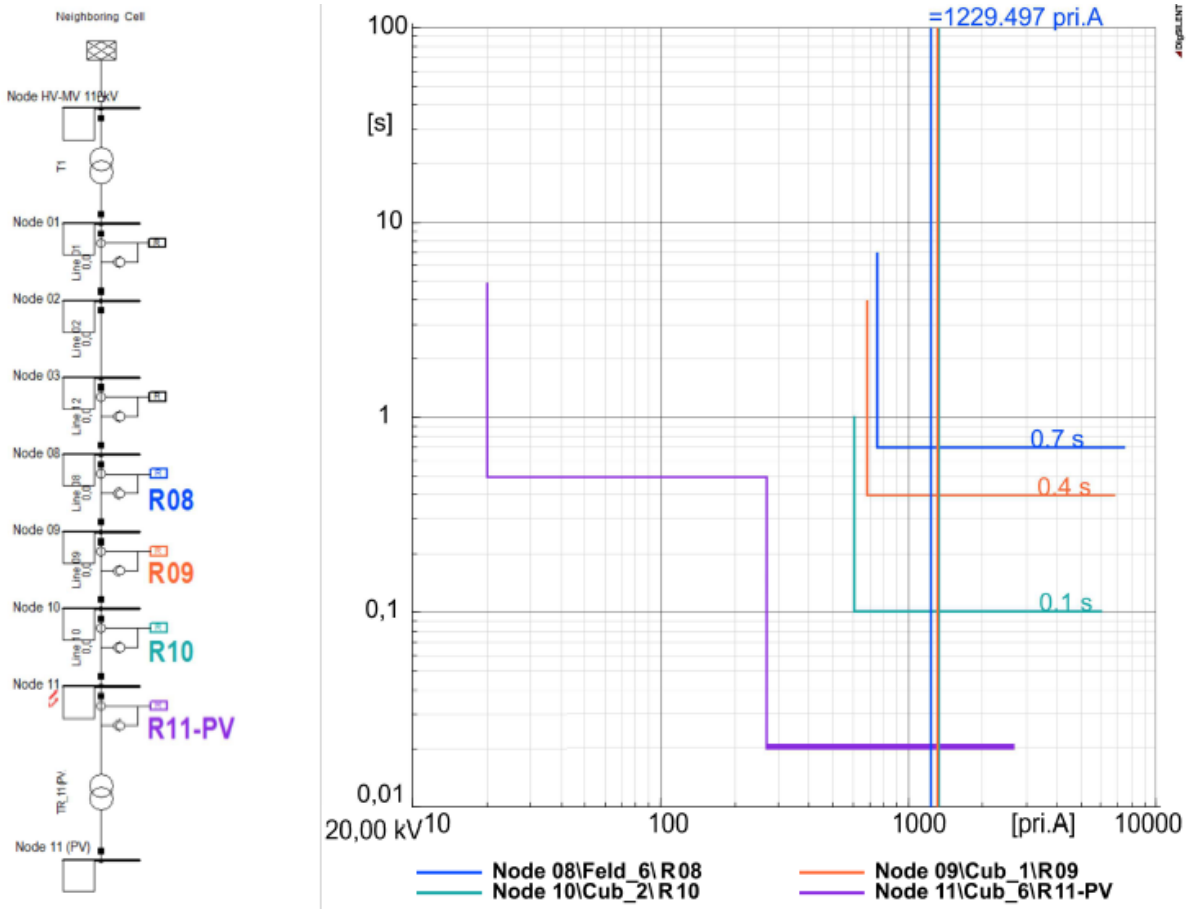

Figure 6-3: IED tripping curves for the cell tied to a neighbouring HV cell

If the main cell is isolated from the HV cell, SC currents in the cell drastically decrease since they are supplied by DERs only. The SC fault current values in this case become very close to the nominal load currents due to converter based generation, thus the relays would not trip (see Figure 6-4). Consequently, DT curves of IEDs need to be shifted to lower short-circuit levels securing fast fault isolation for this cell condition. An adaptive solution based on IEDs with different tripping settings pre-defined for each possible cell state seems to satisfy the condition.

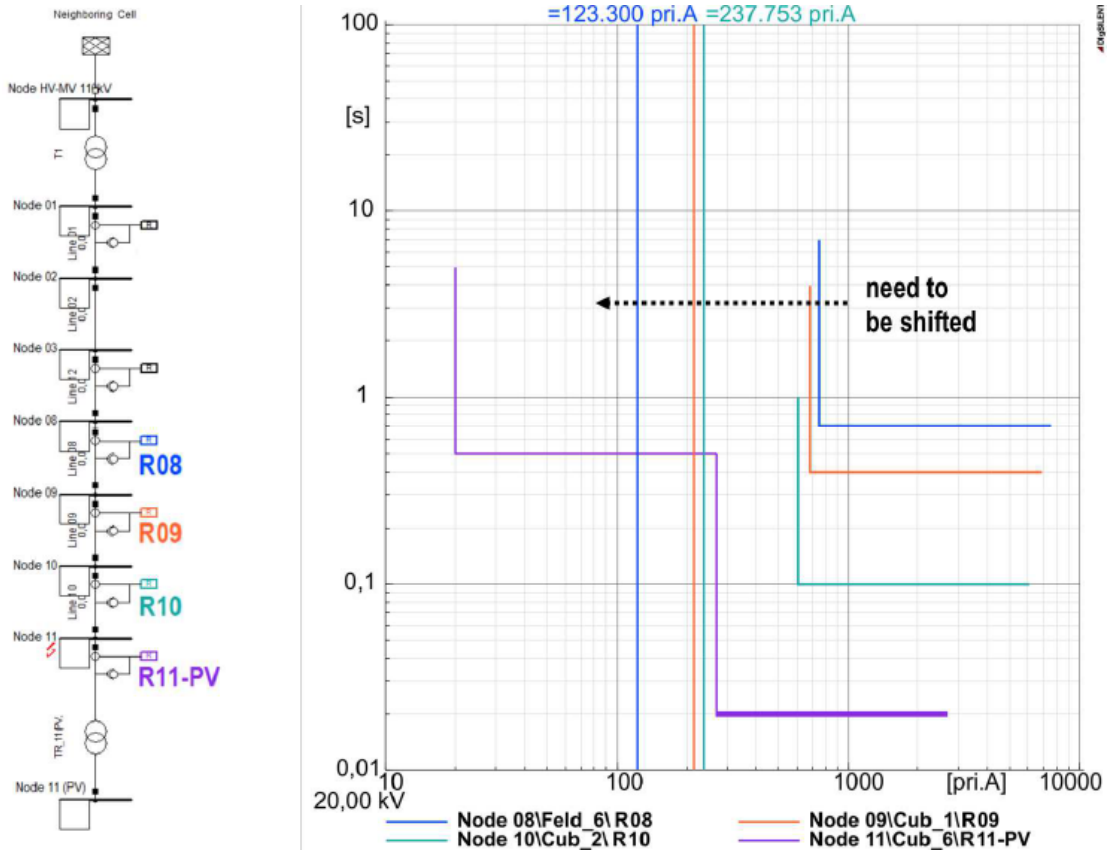

Figure 6-4: IED tripping curves for the isolated cell

6.2.3.2 With Adaptive Functionality

With the functionality of the CC proposed, the prevailing operating state of the cell with reduced short-circuit capability has been detected and then setting groups of the IEDs adapted properly, as shown in Figure 6-5. The results indicate that the CC enables automatic shifting of IEDs' tripping curves according to the SC fault level during the islanding condition of the cell. It has to be noticed that the adaptation of tripping curves to these lower settings can lead to false trips when the normal situation is restored. Therefore, when the main cell is re-connected to the HV cell, the tripping settings must be changed back to the pre-fault values, which is also the responsibility of the proposed adaptive protection system.

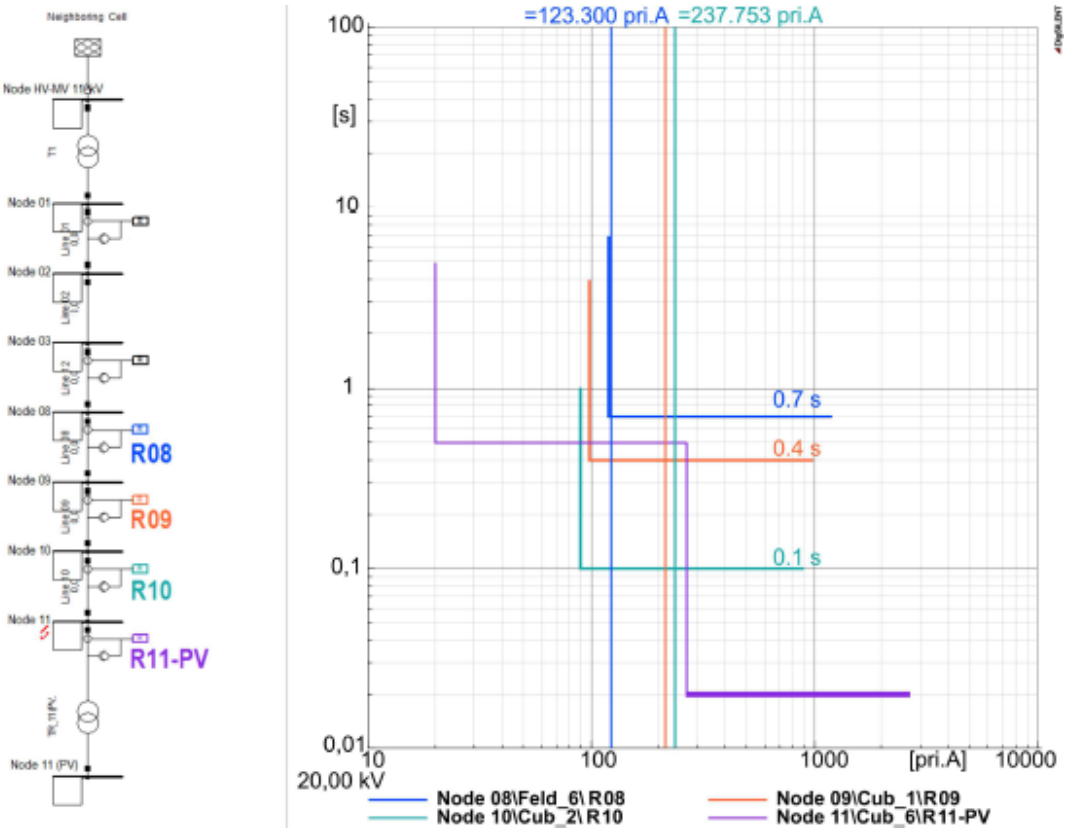

Figure 6-5: IED tripping curves for the isolated cell with adaptive functionality.

6.3 Multi-cell evaluation with IDTM relay settings

6.3.1 Overview and Modelling

The aim of adaptive overcurrent protection is to determine set points, i.e. Pick-up Currents (PCs) and Time Multiplier Settings (TMS), of overcurrent relays (OCRs) adaptively in order to fulfil the relay coordination following a network topology change and to provide a fast response to varying load demands and distributed generation. An adaptive overcurrent protection algorithm has been developed to be applied on the slightly modified reference CIGRE MV model. The network modifications described in Table 6-1 are applied on the reference network. The aim of network modification (i.e. self-organizing) is to provide secure network operation in case of topology change (i.e. the network becomes N-1 secure for some customers because supply can be restored via another path in the network in case of some specific fault locations) and to increase the presence of distributed generation in each cell.

Modified Element	Original Network	Modification
Load 12	20 MW, 4.7 Mvar	10 MW, 2.4 Mvar
Load 13	0.03 MW, 0.02 Mvar	3.4 MW, 2.1 Mvar
Load 14	0.54 MW, 0.26 Mvar	5.4 MW, 2.6 Mvar
DERs as static generators	Located at *almost* each node (only **~5%** of total load demand)	Located at *all* nodes (1 MW at each node to reach **~50%** of total load demand)
T1 transformer	1 single transformer	2 parallel transformers
Lines 02, 12, 13, 14, and 15	1 single line	2 parallel lines
Line 03	1 single line	3 parallel lines

Table 6-1: Modifications to the CIGRE MV reference network

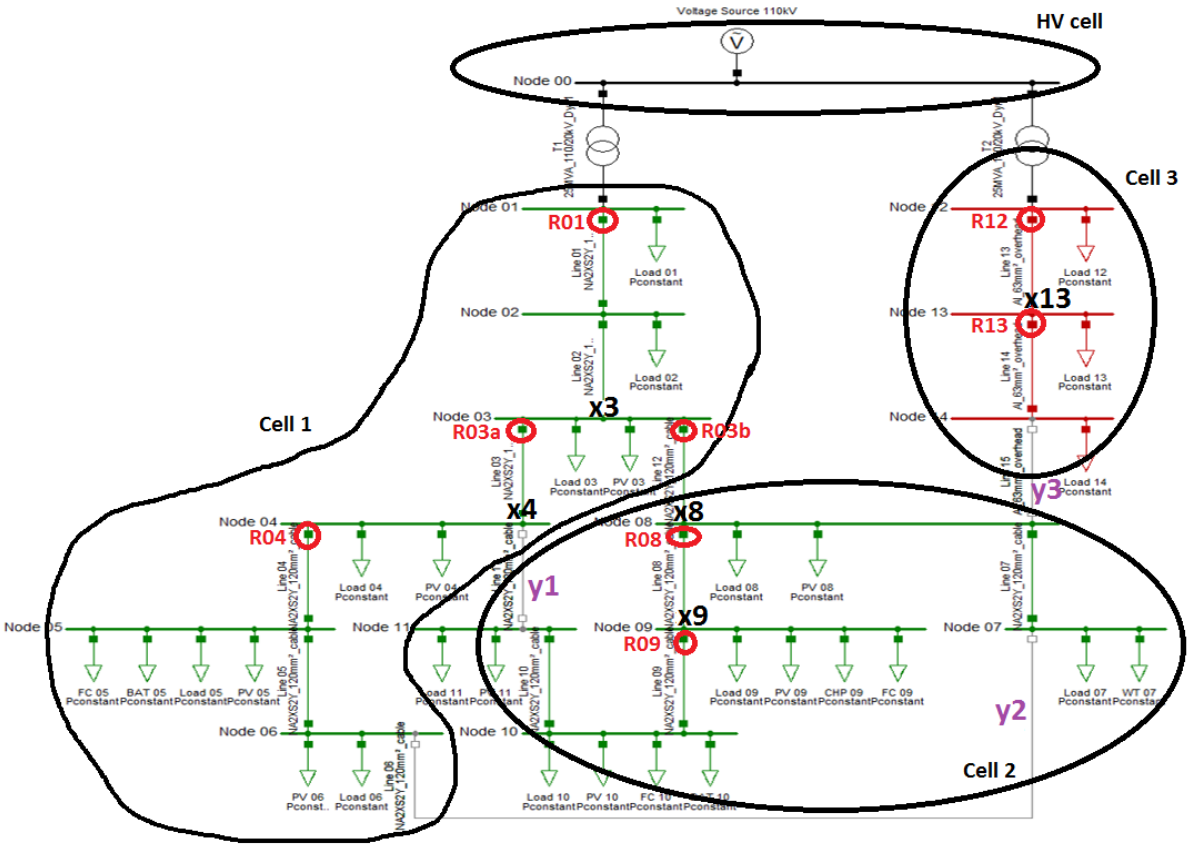

Figure 6-6: CIGRE MV test network and the location of OCRs

The reference network given in Figure 6-6 consists of three cells (excluding the HV cell). Cells 1 and 2 are supplied from the same transformer (i.e., Cell 2 depends on Cell 1) while Cell 3 is independently supplied by a different transformer (i.e. Cell 3 is separated from other cells by a normally open (NO) point). Thus, for the given topological structure, OCRs in Cell 1 and Cell 2 must be considered together in the calculation of set-points, but set-points for OCRs at Cell 3 can be calculated independently. The approach applied in this WoC structure is based on sharing information between cells for the optimal network protection. In this way, the calculation of OCRs

will be executed in each Cell individually by considering the back-up protection and relay coordination only between Cells 1 and 2. Therefore, dividing the network into cells provides an efficient network protection by decreasing the complexity with simple algorithms.

The reference network includes eight OCRs located in specific parts of the network. The placement of OCRs are determined considering the network characteristic and structure. Despite the fact that placing OCRs at the beginning of each line is the best way to protect the network, the number of OCRs is reduced due to economic feasibility (i.e. prices of OCRs are considerably high) and complexity (i.e. the coordination of OCRs becomes more challenging as the number of OCRs increases). Therefore, eight OCRs (modelled based on the Siemens 7SJ64 device) are placed in the specific locations in the network. Each OCR has a current transformer (CT) that is selected based on the maximum current flow through OCRs and IEC 60076-1 standard (R10 series). Although it is the standard applied on power transformers, measurement transformers are mostly designed considering similar ratings.

6.3.2 Algorithm Operation

The adaptive overcurrent protection algorithm presented in Figure 6-7 is triggered after a short circuit (SC) fault or a DER status change occurring in the network. A DER status change triggers the algorithm and the algorithm directly calculates new relay parameters in order to provide secure relay coordination due to the change in the fault currents. For a SC fault, the nearest OCR detects the fault and the corresponding circuit breaker (CB) operates to clear the fault. At the same time, the OCR that detects the fault triggers the adaptive overcurrent protection algorithm. The algorithm detects the fault zone and determines if it is possible to re-energize unaffected parts of the network or not. If it is not possible, new relay parameters are directly calculated without considering any topological change. If it is possible to re-energize the network, the algorithm isolates the fault zone by sending open commands to controllable breakers (x3, x4, x8, x9, and x13) placed at pre-determined areas necessary for isolating faults. Then, NO points (y1, y2, and y3) are re-arranged to supply customers at unaffected areas. After necessary re-arrangements are fulfilled, the adaptive algorithm calculates new relay settings and sends them to OCRs. The OCR detecting the SC current triggers the adaptive overcurrent algorithm, new relay settings are calculated if necessary. The calculation of OCR settings is a central process and must be performed at the operation centre of a responsible cell. Here, the responsible cell must get a confirmation signal from other cells and changing the cell structure must not affect balancing and voltage control operations.

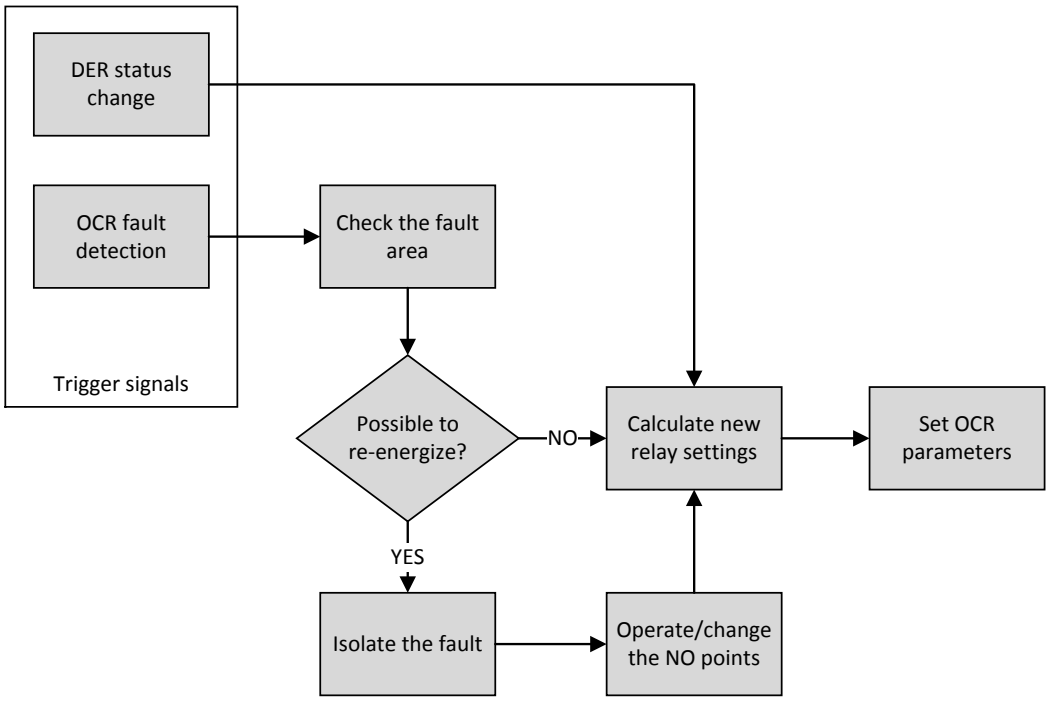

Figure 6-7: The main algorithm

The calculation of new relay settings, based on standard inverse time current characteristic Inverse Definite Minimum Time (IDMT) [8], is carried out as described in the following steps assuming that there are three series OCRs in the network (OCR1 (located furthest from the main transformer), OCR2, and OCR3). This part describes the general calculation procedure, which is given for three series relays from Cell 1. The procedure can be applied similarly for Cell 2 (with four series relays) and Cell 3 (with two series relays).

1. The execution of load flow in order to determine nominal currents (*In*) for each OCR. In practice, each cell system operator periodically collects the required data for OPF calculation in Post Primary Voltage Control (PPVC) use case. Thus, the same data can be imported into adaptive algorithm to perform load flow and SC fault calculations.
2. The calculation of maximum currents (Imax = In * 1.3) for each OCR
3. The calculation of PCs for each OCR
4. The execution of a SC fault calculation considering the maximum fault current (*If*) that the furthest OCR (OCR1) detects
5. The calculation of the value *Ir* (where *Ir* = *If* / *Imax*) for OCR1
6. Setting the TMS[5] of OCR1 to 0.05 (initial TMS settings as suggested in [9])
7. The calculation of OCR1 fault clearance time (OCR1 opening time) considering the IDMT relay characteristic (IEC 60255)
8. The calculation of fault clearance time for the backup OCR (OCR2 that is located upstream of OCR1) by adding a 0.3 s grading margin (tOCR2 = tOCR1 + 0.3 s)
9. The calculation of TMS for OCR2 considering the IDMT relay characteristic formula
10. Repeat steps 4-9, but for OCR2 and OCR3
11. Sending the calculated PC and TMS settings to all OCRs

[5] TMS is the parameter that calculates the relay opening time of an OCR. TMS is usually given in discrete steps starting from 0.05 (but this depends on the relay). Hence, TMS settings can be chosen as the lowest value to ensure a rapid fault clearance time for the first relay at the OCR grading chain.

The algorithm has been applied on the reference network with eight possible fault areas (fault zones), which requires to be simulated in separate scenarios. Table 6-2 demonstrates all possible fault scenarios generated from a topological change.

Scenario (S)	Fault Zone (FZ)	Fault detection relay	Topological change	Relay coordination (based on operation times/coordination)
Base	-	-	No change	• R01 >> R03b >> R08 >> R09 • R01 >> R03a >> R04 • R12 >> R13
S1	FZ1 (between R01 and x3)	R01	• x3 opens • y3 energized	• R12 >> R13 >> R08 >> R09 • R12 >> R13 >> R03a >> R04
S2	FZ2 (between R03a and x4)	R03a	• x4 opens • y2 energized	• R01 >> R03b >> R08 >> R09 • R12 >> R13
S3	FZ3 (between R03b and x8)	R03b	• x8 opens • y1 energized	• R01 >> R03a >> R04 • R12 >> R13 • R03b off • R08 & R09 not operates
S4	FZ4 (downstream of R04)	R04	Downstream of R04	• R01 >> R03b >> R08 >> R09 • R01 >> R03a • R12 >> R13
S5	FZ5 (between R08 and x9)	R08	• x9 opens • y1 energized	• R01 >> R03a >> R04 • R01 >> R03b • R12 >> R13
S6	FZ6 (downstream of R09)	R09	Downstream of R09	• R01 >> R03a >> R04 • R01 >> R03b >> R08 • R12 >> R13
S7	FZ7 (between R12 and x13)	R12	• x13 opens • y3 energized	• R01 >> R03b >> R08 >> R09 • R01 >> R03a >> R04
S8	FZ8 (downstream of R13)	R13	Downstream of R13	• R01 >> R03b >> R08 >> R09 • R01 >> R03a >> R04 • R12

Table 6-2: The required relay coordination and topology changes for each scenario

As indicated in Table 6-2, nine possible topological change scenarios may occur in the network. Furthermore, there are many possible DER status change scenarios that might require the calculation of new relay settings. Therefore, the algorithm has been developed using the DIgSILENT PowerFactory simulation tool with the DIgSILENT Programming Language (DPL) to analyze all scenarios effectively. For the purpose of simplicity, only some of selected scenarios are

explained in detail by presenting their valuable outcomes in the following subsections. In each scenario, current time characteristics for all OCRs are determined based on the IDMT curves calculated from the systematic algorithm described in this part.

6.3.3 Base Scenario (Current Network Topology)

The base scenario has been studied in order to investigate relay operating times and coordination for three-phase SC faults that occur on the reference network with and without distributed generation (DG). The base scenario is studied for SC faults occurring at Node 06, Node 11, and Node 14 (i.e., at the end of line 05, line 10, and line 14, respectively) separately (where all nodes are the furthest fault points for three separate relay coordination regions).

6.3.3.1 Fault at Node 06

For this fault location, R01, R03a, and R04 detect the fault, thus, the algorithm suggests a coordination between these OCRs. Simulation results, IDMT relay characteristic curves for three OCRs, are presented in Figure 6-8, Figure 6-9, and Figure 6-10.

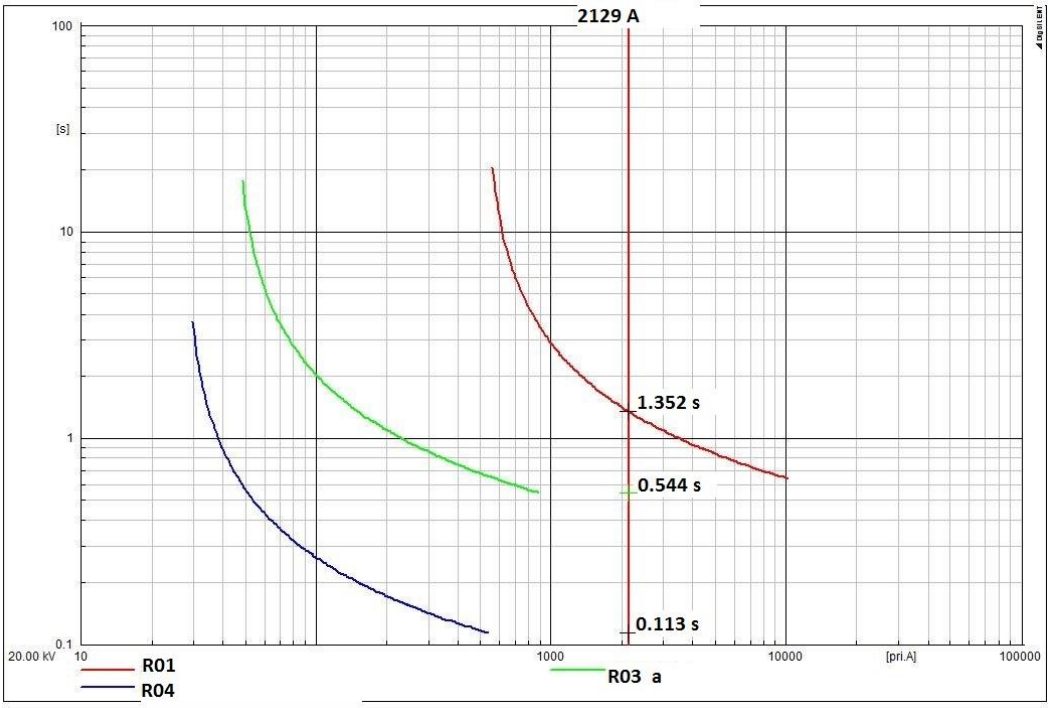

Figure 6-8: Fault response times of R01, R03a, and R04 (no DG – initial relay settings)

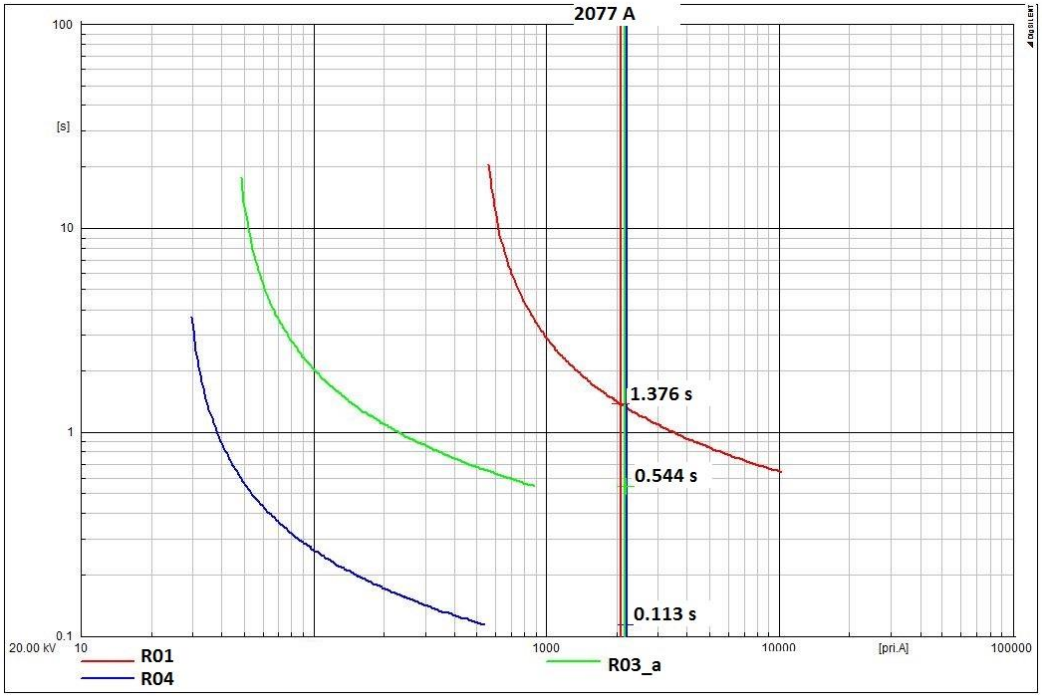

Figure 6-9: Fault response times of R01, R03a, and R04 (with DG - static settings)

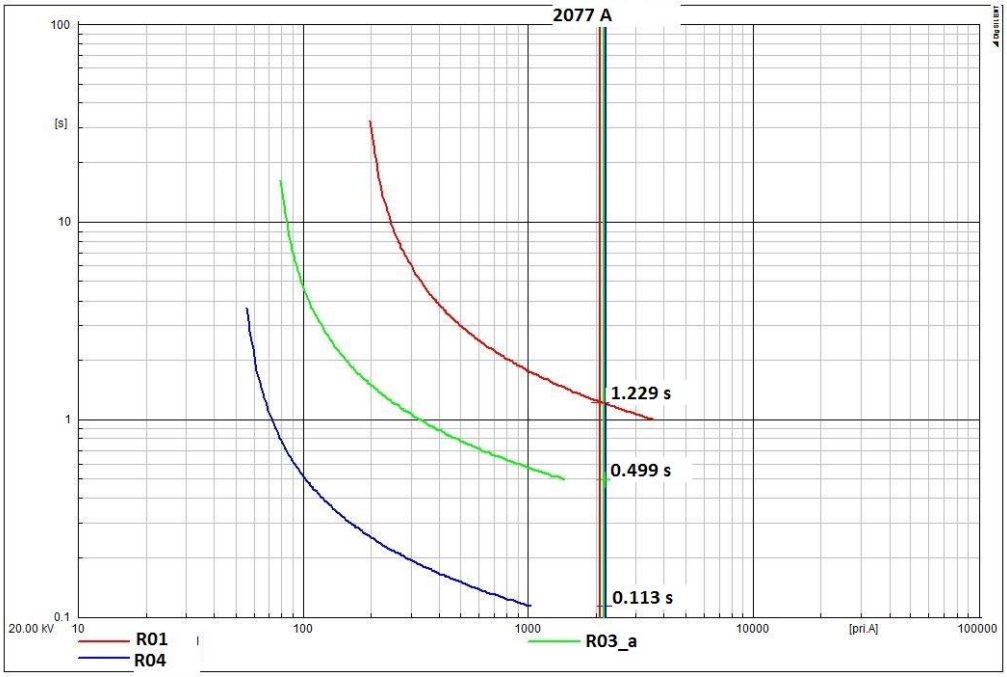

Figure 6-10: Fault response times of R01, R03a, and R04 (with DG - adaptive settings)

Figure 6-8, Figure 6-9, and Figure 6-10 illustrate that three OCRs (R01, R03a, and R04) are coordinated considering grading margins for providing effective back-up protection. Since R04 is the furthest OCR in this protection area, it responds to the fault as fast as possible. R03a, on the other hand, waits some time (it is highly desirable that R04 should operate before R03 for the faults that both relays detect) to provide efficient relay coordination. Normally, the coordination time of two series OCRs should be between approximately 0.3-0.5 seconds. The reason that R01 reacts to the fault longer than 1 second considers the coordination of other relay series (fault at Cell 2). The figures also indicate that changing OCR settings (adaptive relay settings) after a DER power injection provides around 0.1 second faster fault responses for back-up protection relays than keeping the old relay settings (i.e. for static relay settings).

6.3.3.2 Fault at Node 11

For this fault location, R01, R03b, R08, and R09 detect the fault, thus, the algorithm suggests a coordination between these four OCRs. Simulation results, IDMT relay characteristic curves for four OCRs, are presented in Figure 6-11, Figure 6-12, and Figure 6-13.

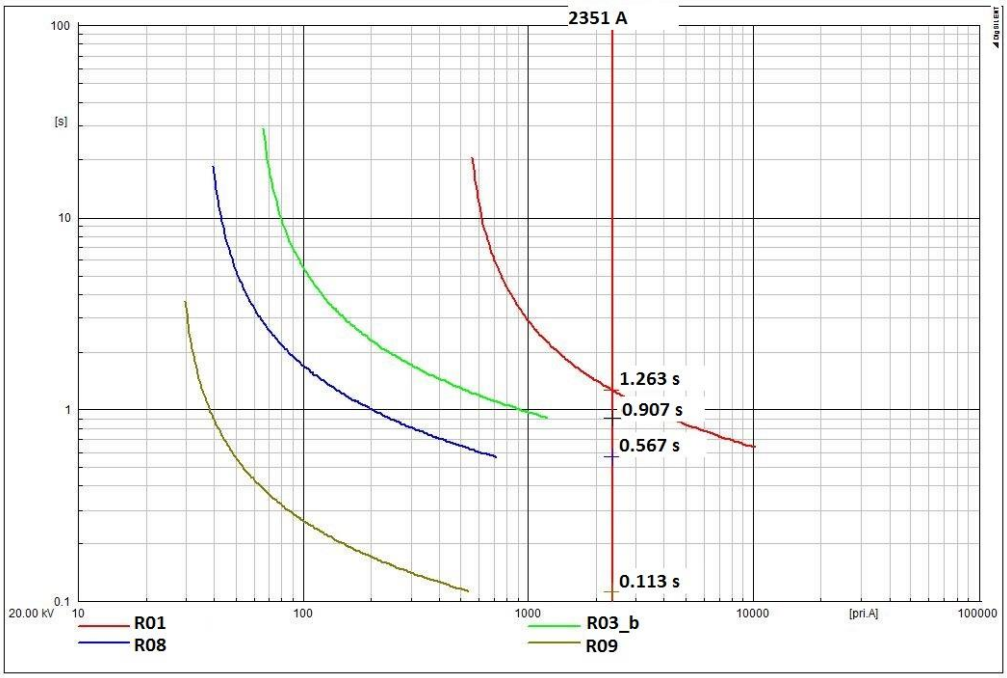

Figure 6-11: Fault response times of R01, R03b, R08, and R09 (no DG – initial relay settings)

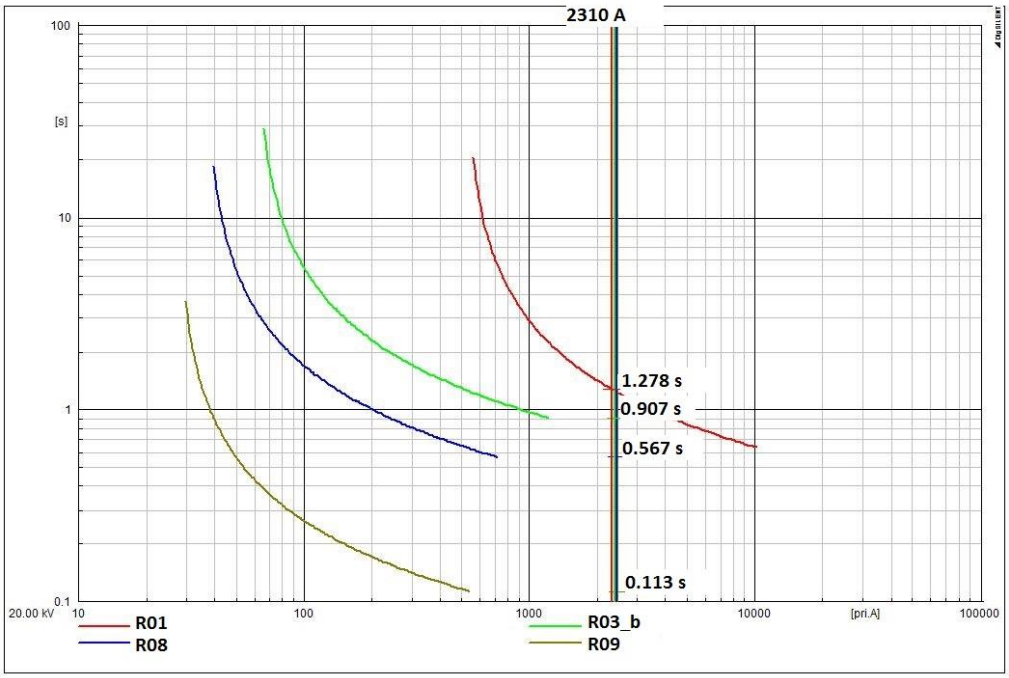

Figure 6-12: Fault response times of R01, R03b, R08, and R09 (with DG - static settings (initial ones))

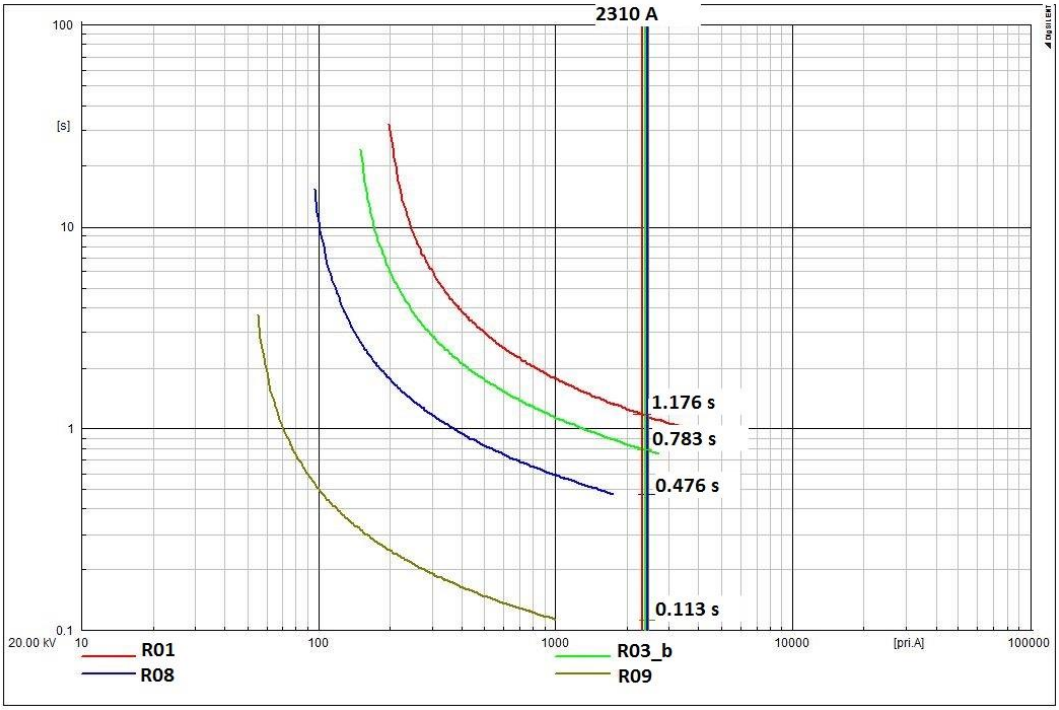

Figure 6-13: Fault response times of R01, R03b, R08, and R09 (with DG - adaptive settings (new calculation))

Figure 6-11, Figure 6-12, and Figure 6-13 indicate that four OCRs (R01, R03b, R08, and R09) are coordinated considering grading margins for providing effective back-up protection. Since R09 is the furthest OCR in this protection area, it responds to the fault as fast as possible. Then, all OCRs located at upper sides respond to the fault by considering the effective time margins. Similar to the fault at Node 06, changing OCR settings (adaptive relay settings) after a DER power injection provides faster fault responses for back-up protection relays than keeping old-relay settings (static relay settings).

For the base scenario, as an exception study, IDMT curve is combined with definite time (DT) curve for R01 in order to show the effectiveness of adaptive protection algorithm. In this way, R01 operates faster for the faults occurring upper side of R03a and R03b. Basically, the algorithm determines maximum fault currents that R03a and R03b capture, and then calculates DT settings for R01. Definite time characteristic requires a threshold current (the fault current) and an opening time value that is determined as low as possible since R01 is the only relay having a definite time setting (no coordination is necessary). Figure 6-14 and Figure 6-15 present that, by providing an effective DT setting, faults occurring between Node 3 and Node 1 can be cleared much faster than using only IDMT settings (around 0.6 second faster).

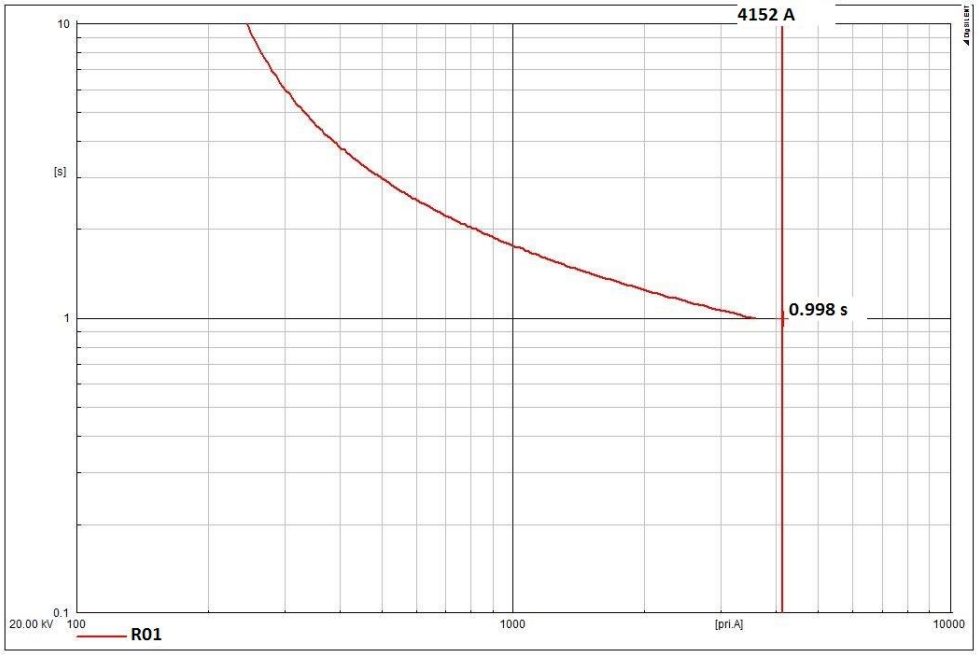

Figure 6-14: Fault response time of R01 with only IDMT curve

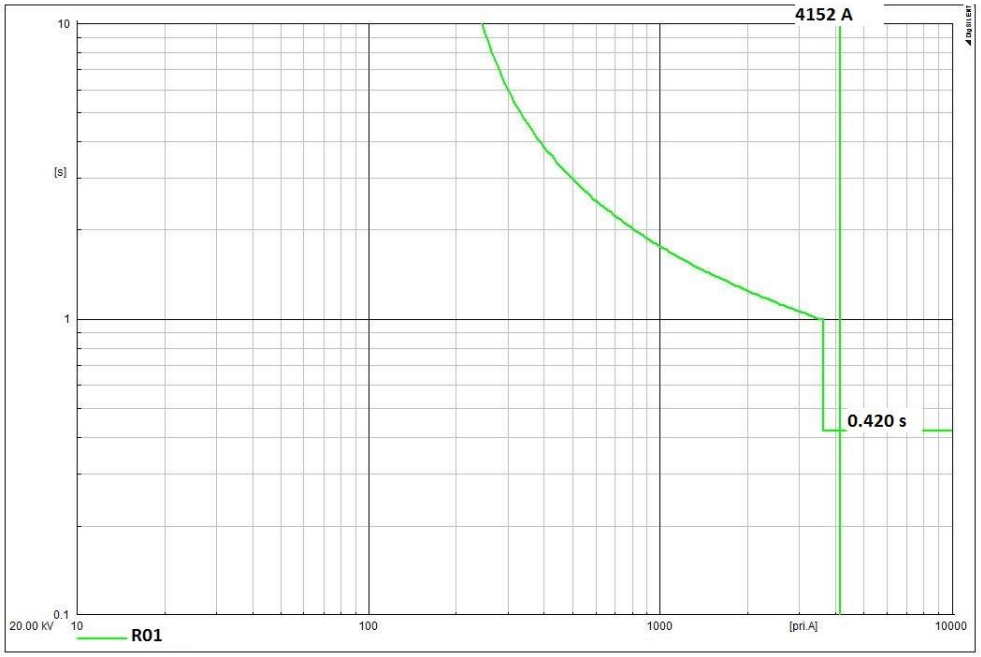

Figure 6-15: Fault response time of R01 with IDMT and DT curve

6.3.3.3 Fault at Node 14

For this fault location, only R12 and R13 are operating independently in Cell 3 region. Therefore, the algorithm coordinates only these two OCRs. Since simulation results are similar with the previous results, only Figure 6-16 is demonstrated showing the coordination of two relays.

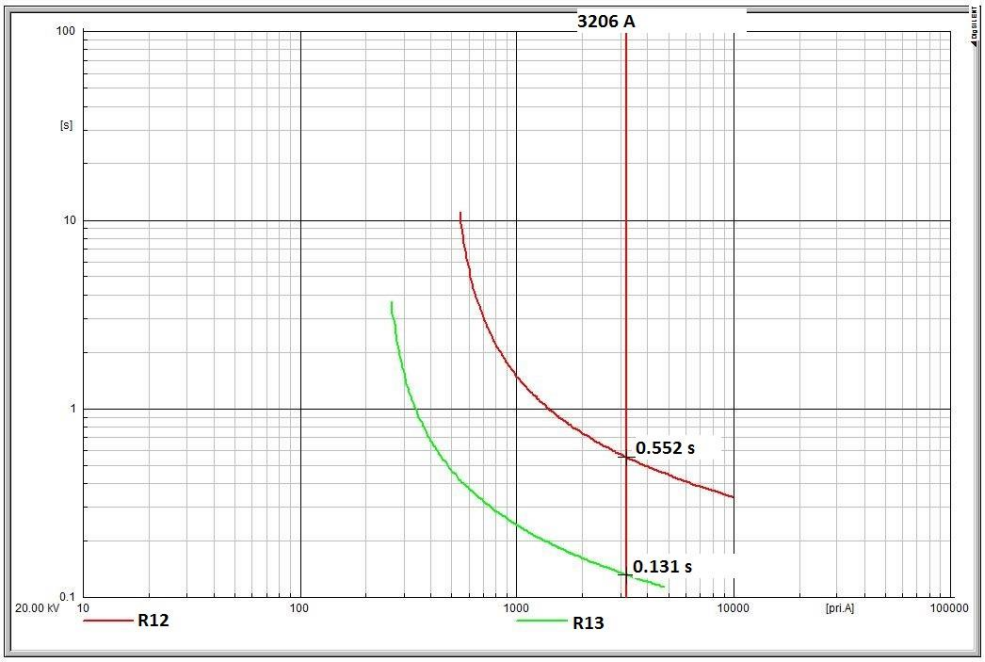

Figure 6-16: Fault response times of R12 and R13 (no DG – initial relay settings)

6.3.4 Scenario S1 (Fault at FZ1)

This scenario is the worst SC fault scenario that occurs on the base topology due to the number of effected customers. After R01 detects and clears the fault, all customers in Cell 1 and Cell 2 (except customers at Node 01) will suffer the power outage. Therefore, topology change on the protection area is highly required in order to supply customers without waiting to detect and clear the fault source. Since the topology is changed, the old relay coordination and parameter settings will fail to operate successfully, which requires to calculate new relay settings with new coordination. In this scenario, R01 (being at the fault zone) and R03b (do not detect the SC current due to its direction) are not included to the relay coordination. The remaining OCRs are coordinated considering the faults occurring at two cell areas (Cell 1 and Cell 2). In this direction, relay opening times are separately calculated for R03a and R08, then, relay settings for other two OCRs (R12 and R13) are calculated based on the OCR that having the highest opening time (R03a or R08). This scenario is studied for the SC fault at Node 05.

6.3.4.1 Fault at Node 05

Figure 6-17, Figure 6-18, and Figure 6-19 present IDMT curves for R12, R13, R03a, and R04 considering scenarios with and without DG generation.

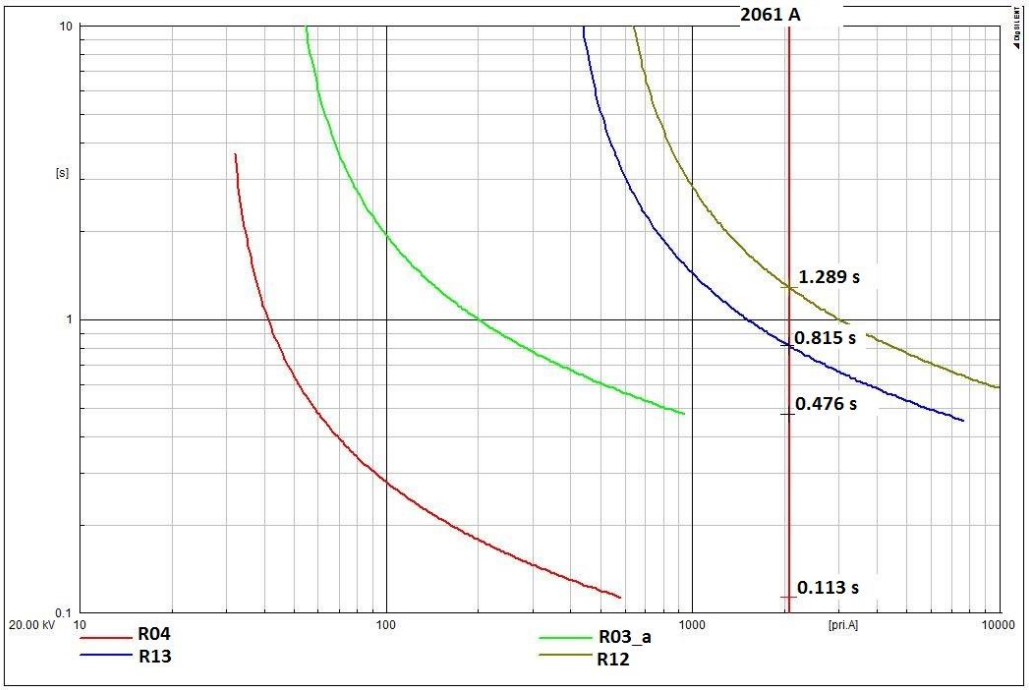

Figure 6-17: Fault response times of R12, R13, R03a, and R04 (no DG – initial relay settings)

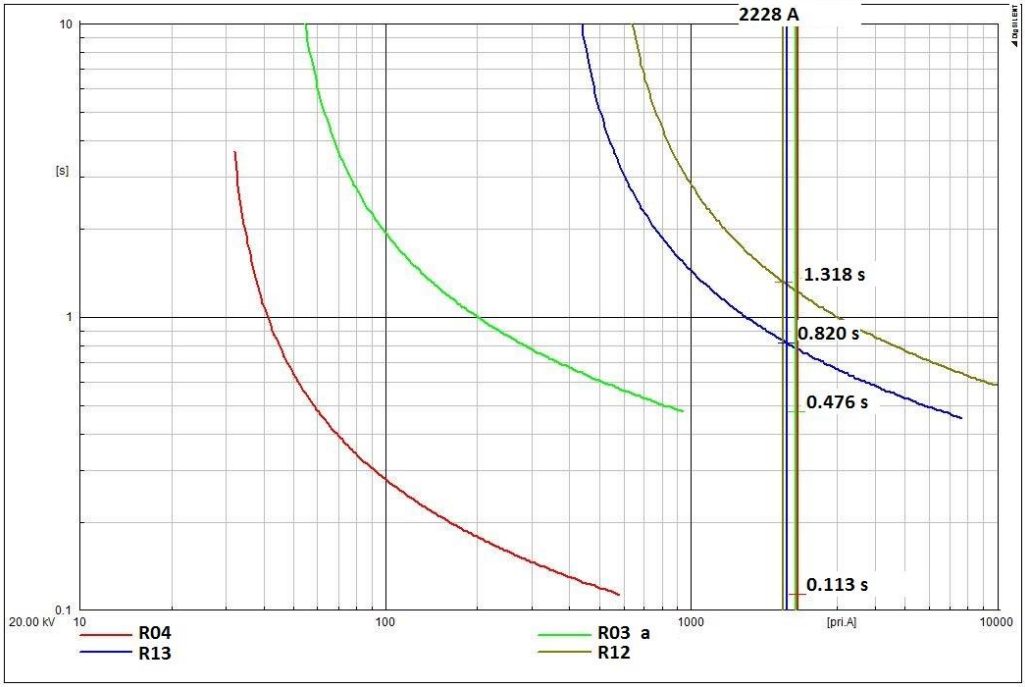

Figure 6-18: Fault response times of R12, R13, R03a, and R04 (with DG - static settings (initial ones))

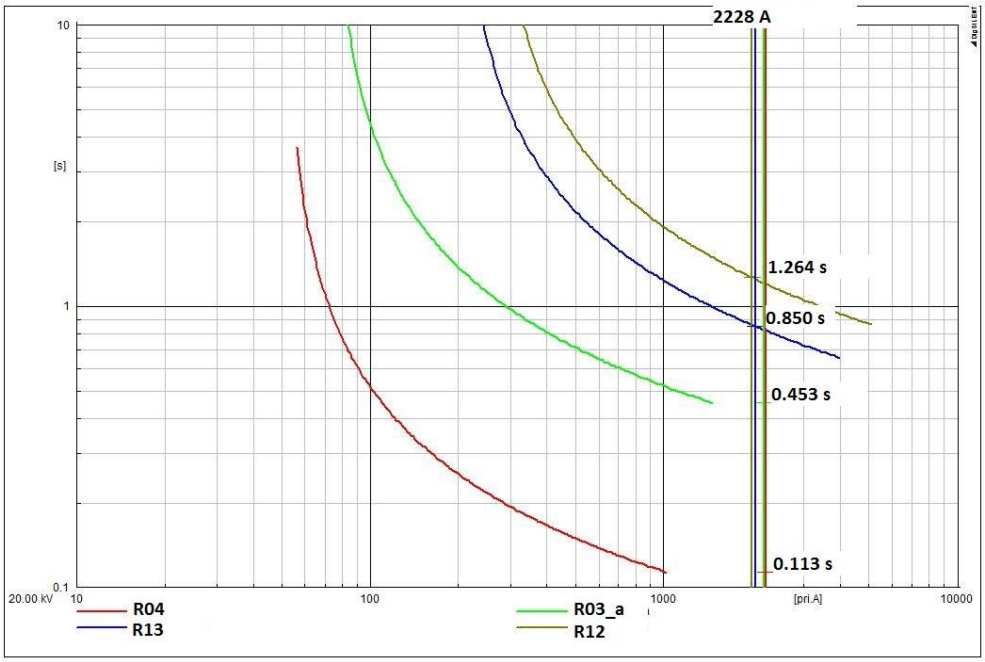

Figure 6-19: Fault response times of R12, R13, R03a, and R04 (with DG - adaptive settings (new calculation))

6.3.5 Scenario S7 (Fault at FZ7)

This scenario describes a fault that occurs at line 13 (in Cell 3) and is cleared by R12. After the fault detection, the algorithm sends an opening command to x13 in order to isolate the fault. Subsequently, the NO line y3 is put into use for supplying unaffected customers in Cell 3. In this scenario, since OCRs are still in the same coordination, it is not necessary to calculate new relay settings after changing the topology. However, DG status changes may still affect the optimal relay coordination, thus, new relay settings might be needed to be calculated.

The adaptive overcurrent protection performance for Scenarios 4 and 5 are stated in the following Section 6.4 by also evaluating PPVC response of the network within these scenarios.

6.4 PPVC Response of the Multi-Cell Test Network for Post Fault Scenarios

This section evaluates the interaction between Post Primary Voltage Control (PPVC) and adaptive overcurrent protection operation. The PPVC algorithm, basically, operates in two different modes (corrective and proactive) aiming to keep the voltages in network nodes in the safe band defined by regulations by properly controlling the available reactive power reserves. PPVC, while regulating voltage by management of reactive reserves, has no wide effects on adaptive overcurrent protection operations, since the SC fault currents and load flows do not dramatically change after PPVC corrective actions. Apart from that, considering post-fault scenarios that cause a topological change in one or more cells, new relay parameters are calculated according to the new network topology. It requires to observe the PPVC response of this new topology in order to ensure the transients caused as a consequence of the opening/closing of switches as well as the energization/de-energization of lines does not cause false trips according to the new settings calculated by the protection scheme. In order to validate the correct simultaneous operation of the PPVC in the presence of an adaptive current control scheme on multi-cell networks taking topological changes into account, two fault scenarios (S4 and S5) have been selected from Chapter 6.2. These two scenarios are intentionally selected for representing topology changes in an individual cell and in a multi-cell grid.

6.4.1 PPVC Use Case Simulations After SC Fault at Scenario 4

This scenario evaluates the PPVC response of a cell where a part of it is de-energized after a fault occurred at the cell (downstream of R04). In this scenario, cell boundaries do not change, only cell-1 structure changes because of the fault, and, as a consequence, the losses or the availability of some of its loads and sources located at the downstream of Node 04 (loads and sources at Nodes 05 and 06) are affected. Figure 6-20 presents the new topology at Cell-1 after a SC fault occurring at FZ4 (Fault Zone 4).

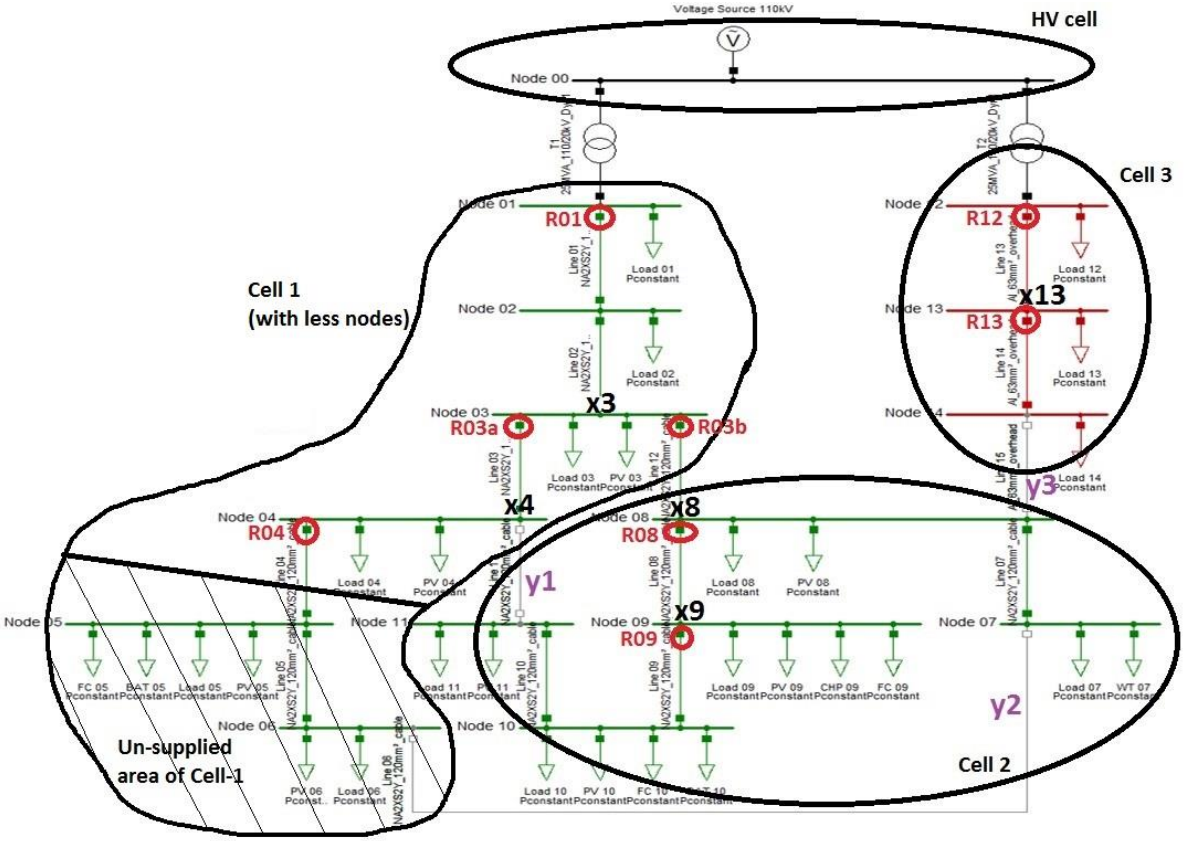

Figure 6-20: New topology of Cell-1 after a SC fault occurring at FZ4

Due to the changes in the grid topology, the adaptive algorithm will re-calculate trip thresholds to the new system conditions. Figure 6-21 presents that the tripping time of R03_a decreases from 0.5 s to 0.12 s with the new settings for a SC fault occurring at Line 03. It can be indicated that the adaptive algorithm clearly improves the performance of protection operations.

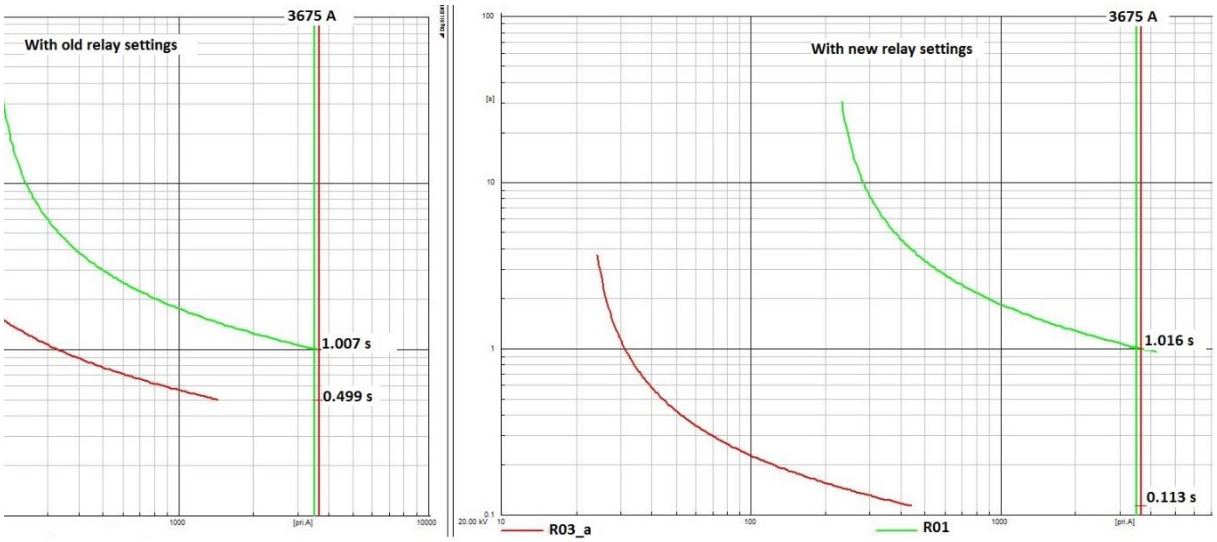

Figure 6-21: The tripping curves of R01 and R03_a with old and new settings for a SC fault at Line 03

Considering the PPVC operations, Figure 6-22 represents Scenario 4 in the simulation software where the fault detected by R04 isolating the region downstream. The fault has been simulated at t=3 min and it has been considered that the unsupplied area of Cell 1 cannot be re-energized in the consecutive minutes. After the event, new OPF set-points have been sent to the resources that restore their voltage levels accordingly to a new optimal point in around 75 s.

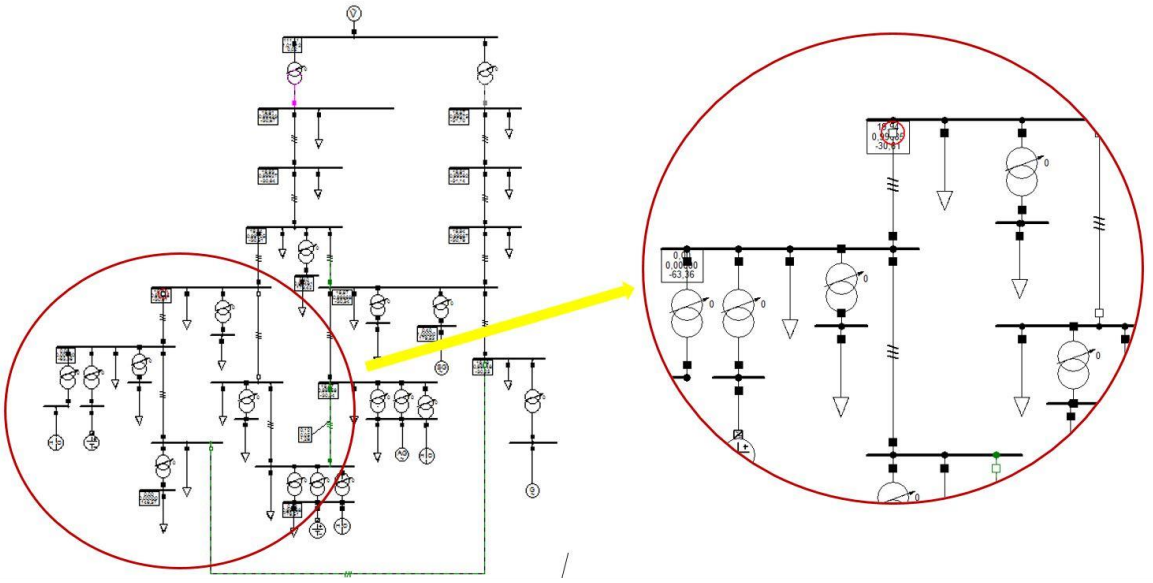

Figure 6-22: Simulation scheme of the WoC after the fault in FZ4

Simulation results of voltages at representative nodes are shown in Figure 6-23a while the currents flowing through the relays R03a, R03b, R08, R09, R12 and R13 are demonstrated in Figure 6-23b. It can be seen from the figures that after the topology change occurring at Cell 1, voltage profiles of representative nodes has successfully been stabilized after reflecting some transients, which has no wide effects on overcurrent protection settings.

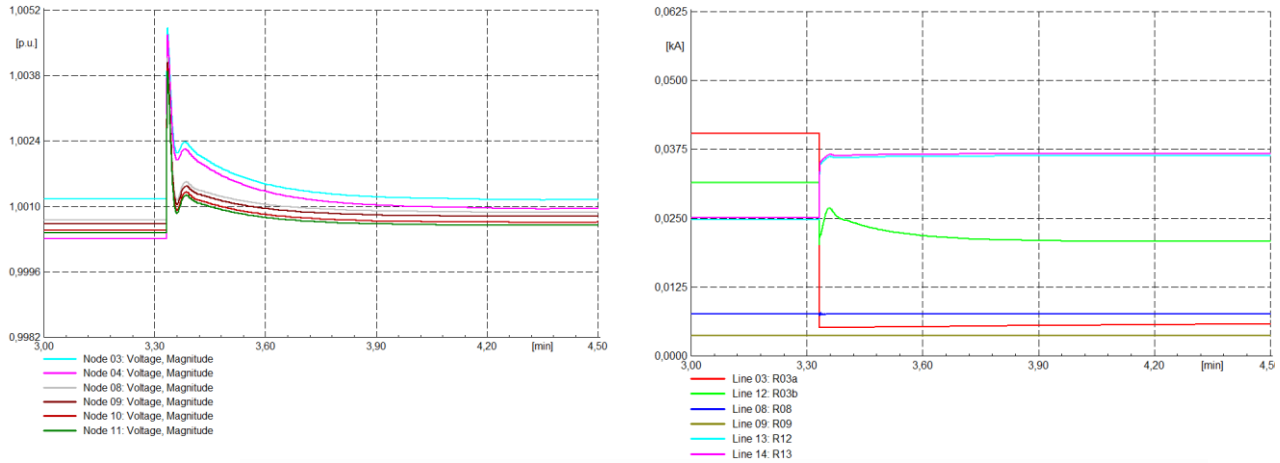

Figure 6-23: a) Voltages in representative nodes of the WoC. b) Currents measured in the coordinated relays.

Figure 6-21 and Figure 6-23 indicate that new relay parameters calculated by the adaptive algorithm increase the protection performance and PPVC operations have still be performed without any problem (i.e., OPF algorithm converges). Intense transients as a result of a topology change do not affect the operation of the adaptive control scheme because the time of the transient is very short and thus, according to the trip curves, the relays would not consider it as a fault and they would not act.

6.4.2 PPVC Use Case Simulation After SC Fault at Scenario 5

This scenario evaluates PPVC operations after topological changes occurred on two cells (Cell 1 and Cell 2) at the same time. After a fault occurs at Line 08 (i.e., at FZ5), the central algorithm will isolate the fault and calculate new relay settings for the new topology (it is assumed that cells can be adapted for increasing the reliability of the system). Then, un-supplied parts of Cell 2 are fed from Cell 1 by re-arranging NO points and breakers (i.e., *x9* opens and *y1* is energized). Figure 6-24 demonstrates the new topology of Cell 1 and Cell 2 after a SC fault occurring at FZ5.

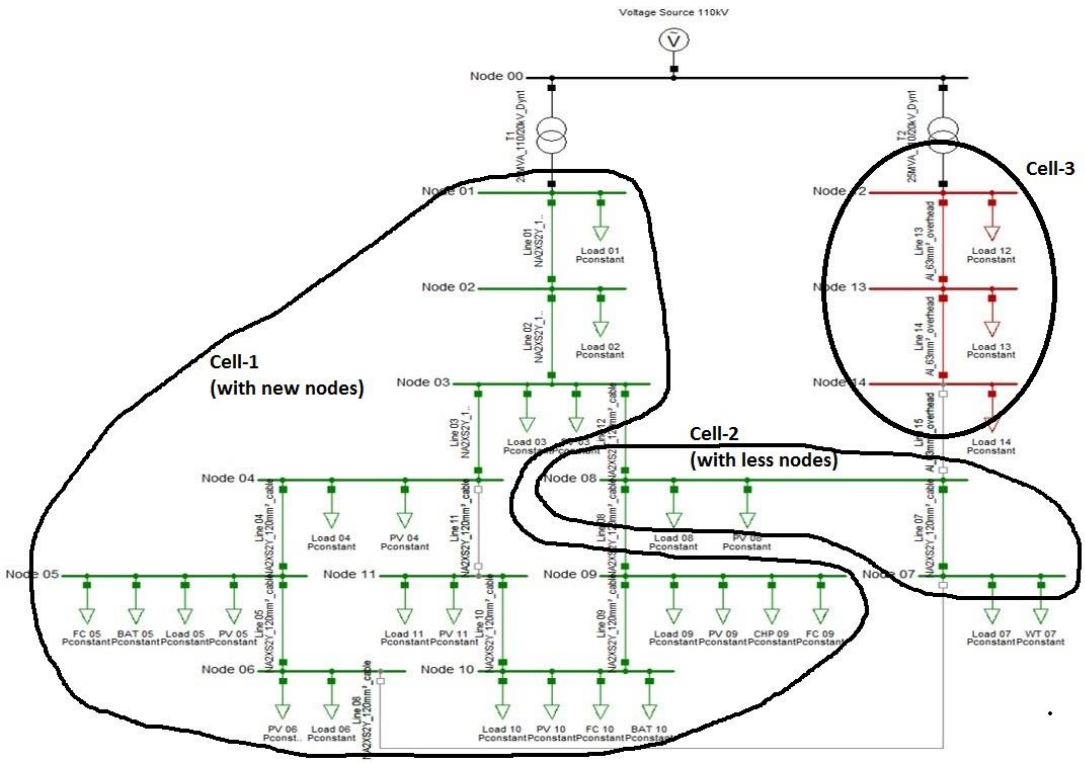

Figure 6-24: New topology of Cell-1 and Cell-2 after a SC fault at FZ5

Figure 6-25 and Figure 6-26 demonstrate relay tripping curves before and after new relay setting calculation for relays R01, R03_a and R03_b. As it seen from the figures, R01 provides a back-up protection for SC faults occurring at the downstream of R03_a (e.g., a fault at line 07) and for SC faults occurring at the downstream of R03_b (e.g., a fault at line 09). In both SC faults, calculating new relay parameters importantly increases the performance of overcurrent protection.

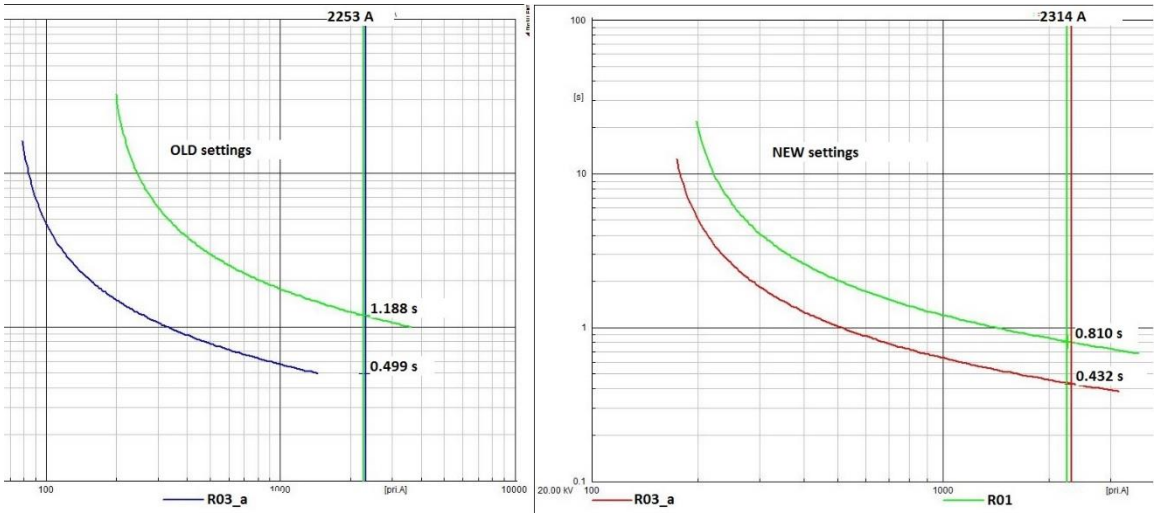

Figure 6-25: The tripping curves of R01 and R03_a with old and new settings for a SC fault at line 07

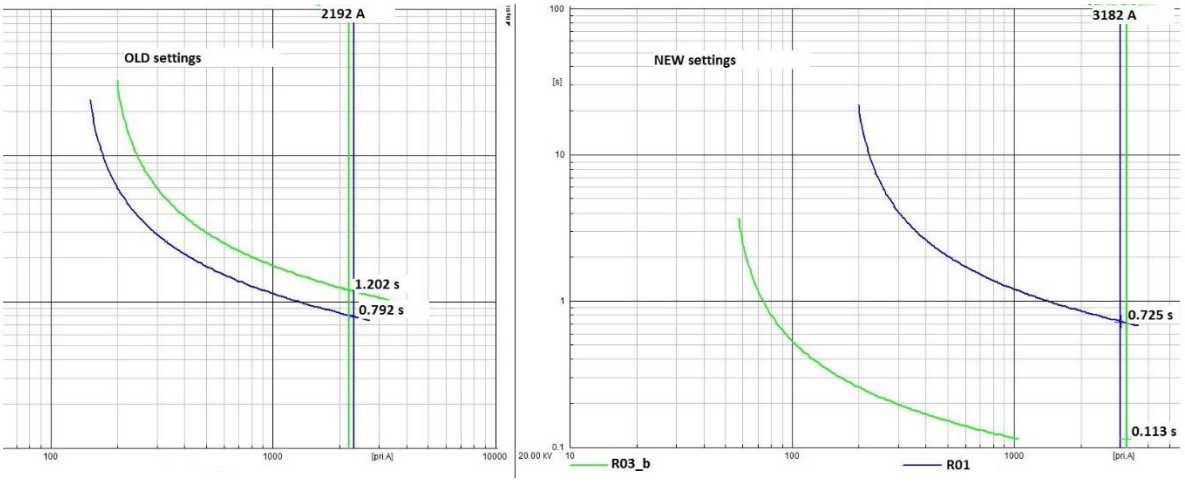

Figure 6-26: The tripping curves of R01 and R03_b with old and new settings for a SC fault at line 09

After adaptive overcurrent protection algorithm rearranges breakers and NO points, Nodes 09, 10, and 11 will be operated by Cell-1 instead of Cell-2. Therefore, PPVC response of Cell-1 and Cell-2 must be investigated with the new PPVC resources. In this direction, the following individual simulation has been performed (see Figure 6-27). In an analogous way to the work performed for Scenario 4 it has been accomplished also for Scenario 5.

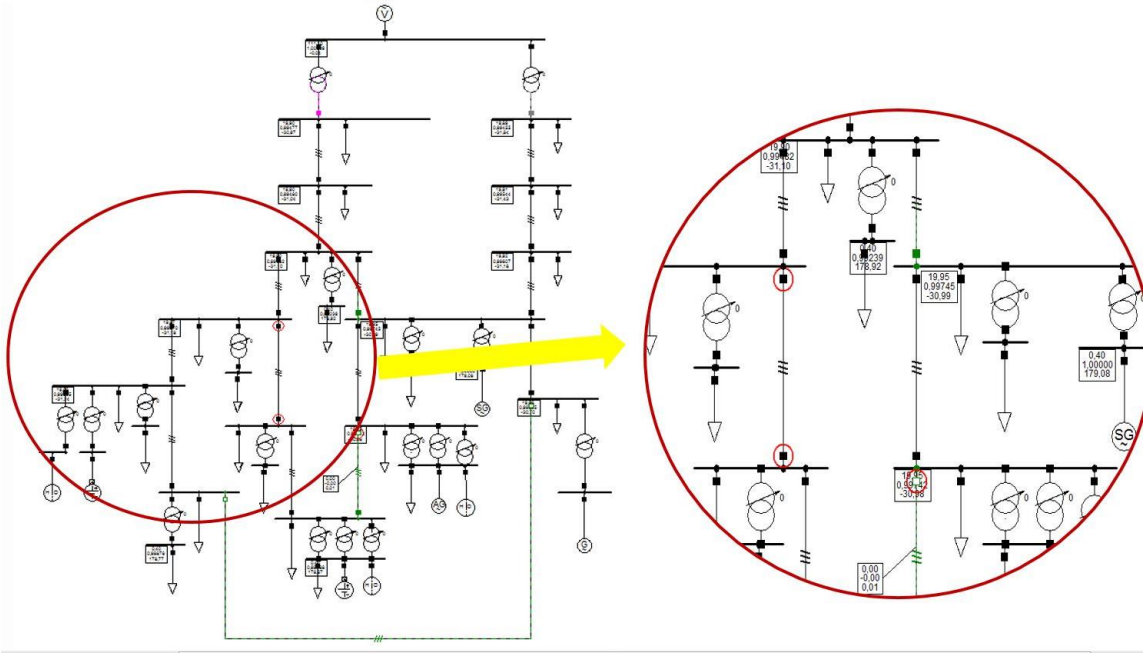

Figure 6-27: Simulation scheme of the WoC after the fault in FZ5

In Scenario 5, as a result of the fault between R08 and x9 simultaneously there is an opening of the switch located at the header of Line 09 and the energization of the Line 11, that was no active up to the moment. Voltage profile in representative nodes as well as currents in the relays are plotted in Figure 6-28.a and Figure 6-28.b.

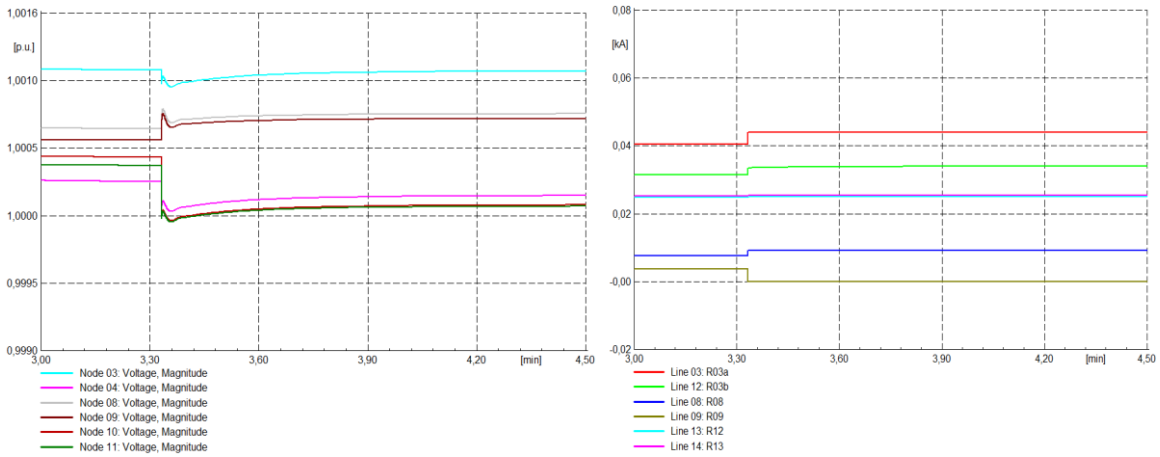

Figure 6-28: a) Voltages in representative nodes of the WoC; b) Currents measured in the coordinated relays

Considering the operation of the protection scheme, the values of the currents also in this second scenario remains below the new adaptive settings calculated and thus, the operation of the voltage control strategy does not have any impact over the thresholds, which could have caused false trips. Similarly, PPVC operations can handle to regulate voltages after the topology changes (i.e., OPF algorithm converges).

6.5 Summary of Results

Adaptive overcurrent protection systems update the set points (i.e., PC and TMS) of OCRs to fulfil the relay coordination for any network topology change as well as to provide fast responses to varying distributed generation. The adaptive algorithm developed in the scope of ELECTRA project

is studied for both a single cell network with DTM settings and a multi-cell network with IDTM settings.

The adaptive overcurrent protection ensures reliable network protection for high DER penetrations and islanding operations. For single cell networks, the relay tripping curves between islanding operations (lower relay settings) and normal operations (higher relay settings) can lead to false trips without implementing adaptive protection scheme. For multi-cell networks, the adaptive algorithm increases the network reliability in case of a SC fault due to the topology re-arrangement capability. In this way, some fault zones can be isolated, thus, supply to customers can be restored by reorganizing normally open points in the protected area. Besides, the adaptive algorithm improves relay opening times (0.1 sec faster relay responses are observed at almost each fault scenario and up to 0.4 sec faster responses in some scenarios) in case of a DER injection and prevents malfunctioning for relay coordination by providing sufficient grading margins. In this way, safety margin of network components can slightly be increased and some coordination problems occurred due to DER diffusion can be mitigated.

The combined simulations of adaptive overcurrent protection and PPVC have been performed on the multi-cell network with two specific fault scenarios in order to observe PPVC response after a topology change and investigate new relay set-point calculation for the protection scheme. In summary, PPVC and adaptive overcurrent protection actually behave as independent operations. On the other hand, adaptive algorithm may trigger PPVC operations in case of topology changes occurring for post-fault scenarios. In parallel, transient currents caused by PPVC operations remains in the safe margins and do not cause any relay tripping. The voltage and frequency stability operations (ELECTRA use cases) and adaptive overcurrent protection can successfully be carried out by the cell controller.

Finally yet importantly, the adaptive overcurrent protection scheme can be operated simpler with WoC network structures that ELECTRA project proposes. Considering the multi-cell WoC network, each cell controller can achieve OCR coordination in a simple manner (2 or 3 relay coordination for each cell). For larger networks (over 100 cells), the complexity of relay coordination with intense DER injections will significantly increase and the protection operation would be troublesome without dividing the network into cells. In summary, the adaptive overcurrent protection method can manage to protect the network in case of SC faults for WoC structures with a high DER generation and an islanding option.

7 Self-Organizing Protection for Cell-Based Power Systems

7.1 Overview of Method

The previous chapter discussed the automatic adaptation of protection settings after the occurrence of events or DER status change in the network: a further and complementary topic which is important to consider is communication between protection devices. This is a broad topic, which involves the use of Information and Communication Technology (ICT) in order to allow automated discovery and coordination of protection devices at run-time. With respect to the WoC concept developed in ELECTRA, these kind of algorithms involving communication between protection devices should take into account cases where the communicating devices are located within the same cell as well as cases where they are located within different cells.

A particularly representative use case for self-organizing protection applications, in the context of distribution networks (MV and LV), is logic selectivity: in its most basic form, the principle of operation, applied to a radial MV feeder, is shown in Figure 7-1.

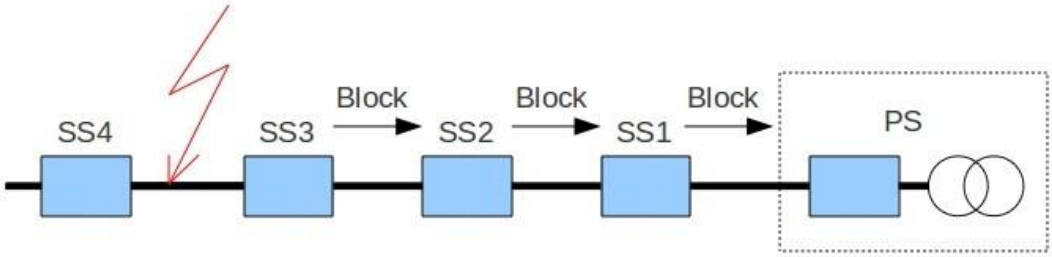

Figure 7-1: Logic selectivity, basic principle of operation

In Figure 7-1, the squares represent protection devices installed inside substations along a MV distribution feeder. The naming “SS” stands for “Secondary Substation”, while “PS” stands for “Primary Substation”. The basic principle of operation is the following: a protection device installed in a secondary (MV/LV) substation is configured to detect when the current flowing from primary (HV/MV) substation exceeds a maximum acceptable value, thus protecting the rest of the feeder “downstream” from the HV/MV substation. With respect to the figure, a fault is located between MV/LV substation SS3 and SS4, and is therefore detected by SS3, SS2, SS1 and PS. All these devices react to the fault detection by immediately sending a blocking signal to the preceding device, so that only the one which doesn’t receive the blocking signal within a specified timeout (SS3 in this case) will trip. After tripping, the protection device sends a trip command to the downstream device (SS4 in this case) to complete the fault isolation procedure.

Starting from this basic scheme, different variations have been proposed in recent years: for example, dealing with meshed network topologies [10] and directional overcurrent protections [11]. Also, in real implementations other details of the logic must be specified, for example the time duration of the blocking signal, since protection devices must not stay in the blocked state forever; in the above example, consider the case that SS4 fails to trip and the intervention of SS3 as backup is needed.

The main advantage of logic selectivity is that it allows to minimize the number of customers along a MV feeder which will be affected by a fault event, since all the users connected upstream to the faulty section will not be disconnected. The main drawbacks are:

- Protection set up must take into account communication time delays.

- Protection devices and circuit breakers should be duplicated along the line to minimise the load disconnected to isolate a fault.

From the above description, it is clear that its implementation requires communication between protection devices: more in detail, this use case can be implemented by means of IEC 61850 GOOSE (Generic Object Oriented Substation Events) communication, as illustrated, for example in [12]. This means, however, that GOOSE publish/subscribe configuration must be generated for each involved protection device, which can be difficult in case of large distribution networks. Moreover, this configuration should be updated every time a feeder topology changes because the devices that need to communicate may change. In the context of ELECTRA, the communicating devices might be located in different cells (consider the following network already used in Chapter 6 for example).

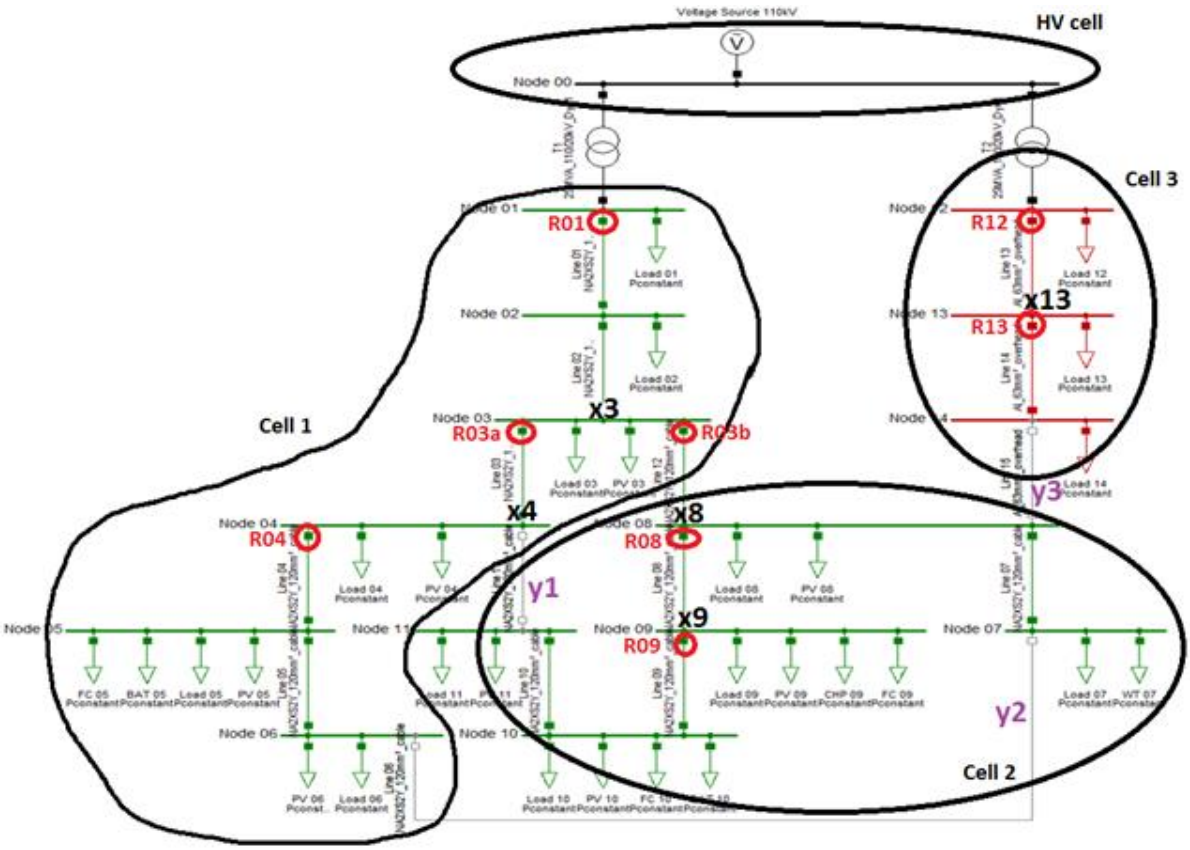

Figure 7-2: CIGRE MV test network from Chapter 6

An immediate problem arising from this scheme is network topology awareness: every node must always be sure to have the correct information about who is its 'predecessor' as well as its 'successor' along the feeder. Due to the tree structure of distribution networks, there are situations in which one node has more than two neighbours. This typically occurs in presence of branches of the network. Moreover, network topology may change in consequence to a fault or maintenance interventions, but also for optimization purposes (e.g. losses minimization).

In the context of the WoC concept, this actually implies that neighbouring cells have some form of knowledge about their network topology, in order to be able to properly coordinate during or following a fault event.

This is a strong argument in favour of the use of existing standardised protocols and data models: in particular IEC 61850 for protection communication and Common Information Model (CIM) for network topology representation.

The two standards may be used jointly: given a CIM based network representation, it is possible to automatically determine all the necessary publish/subscribe configurations, by means of a proper topology processing algorithm. This process involves a CIM model merging procedure from the individual network representations of each single cell, as illustrated in Figure 7-3.

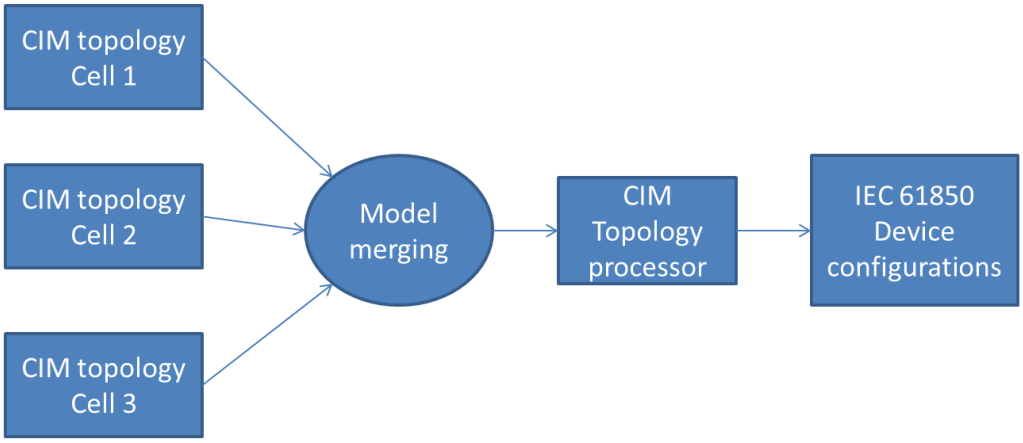

Figure 7-3: Principle of CIM and 61850-based handling of protection configuration

In order to better illustrate the configuration logic, the process should start from the CIM representation of the network shown in Figure 7-4, which has been obtained by the exporting functionalities of DigSilent PowerFactory. The disconnected lines are marked by dashed lines, and correspond to those of Figure 7-2 (Line 06, Line 11 and Line 15). The generators are modelled as negative loads.

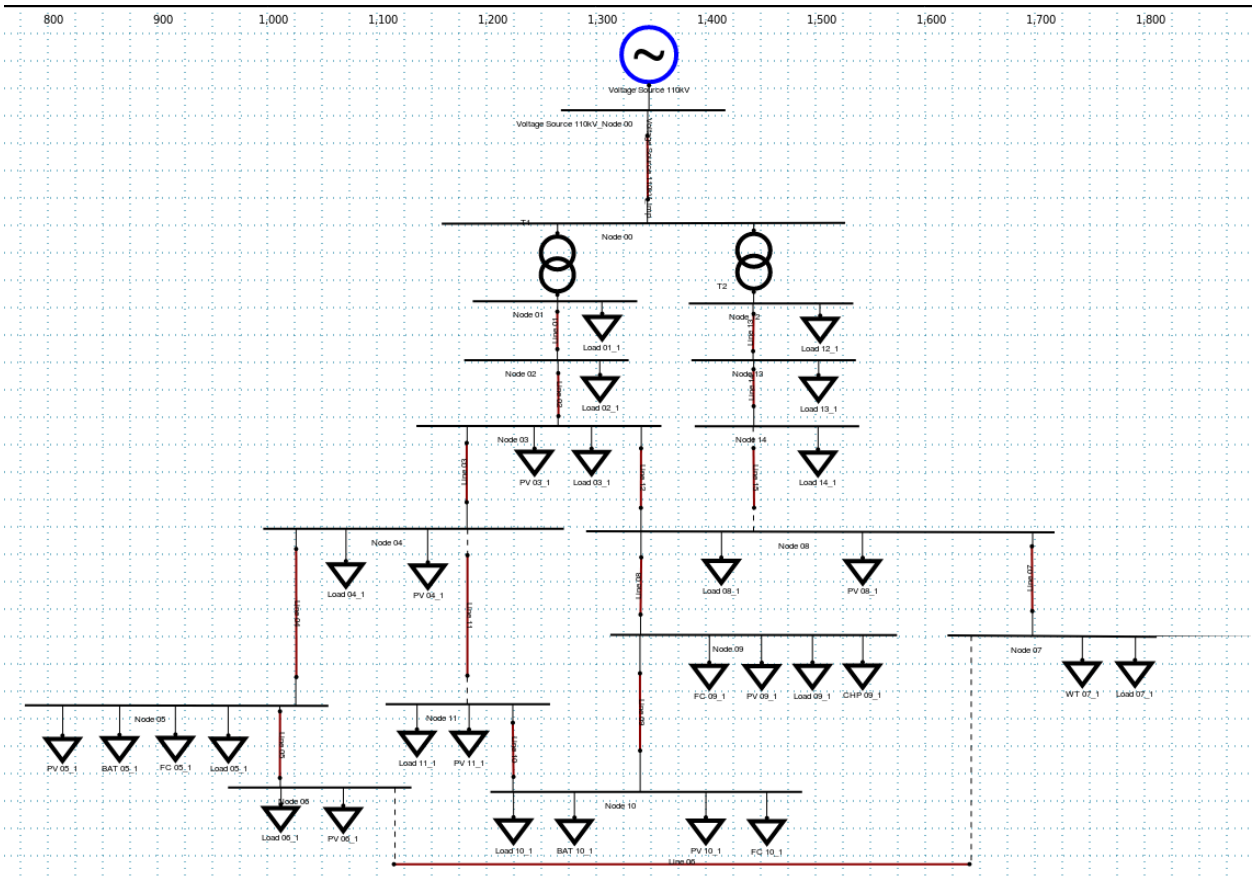

Figure 7-4: CIGRE MV network exported in CIM format from PowerFactory

Considering the same protection setup as Figure 7-2, it can be seen that information exchange between devices located in different cells is necessary, in particular between device R08 inside Cell 2 and device R03b inside Cell 1. Therefore, interoperability issues must be properly considered in order to allow the protection logic to function correctly. Note that, at the lowest communication levels, this also implies that the protection devices in different cells must be connected to the same network, or at least have some way of addressing each other (for example, some kind of VPN tunnel). This also may be an issue if cells are operated by different cell system operators, do not adopt the same standards for communications and data models, or use different (in most cases isolated) communication networks. Also, the latency of the communication between these devices must be compatible with the maximum allowable delay for the intervention of a protection in case of fault, and in case of VPN communication this must be properly taken into account.

The communication schema of the blocking signals which must be exchanged between protection devices is shown in Figure 7-5.

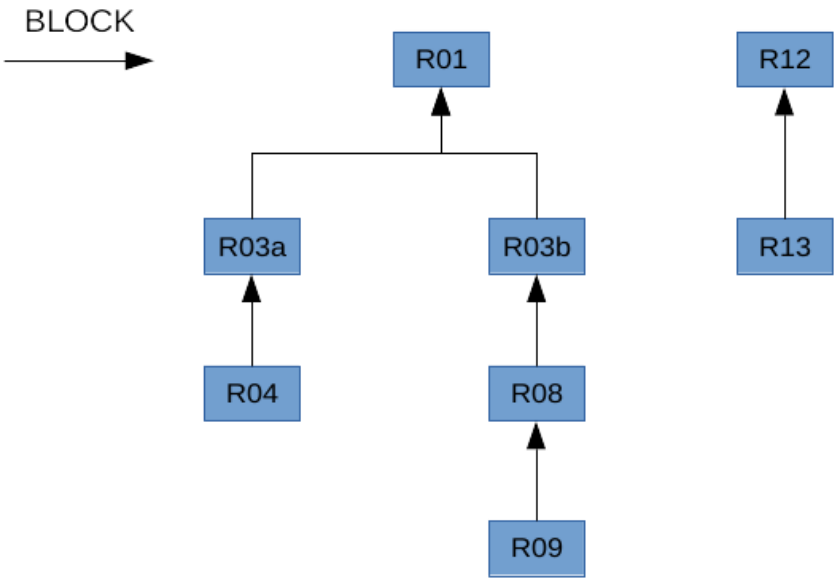

Figure 7-5: Communication flows for the network setup of Figure 7-2

This schema would change in case of network reconfiguration; consider for example the disconnection of Line 12 and the connection of Line 15: in this case protection coordination requires the information exchanges shown in Figure 7-6.

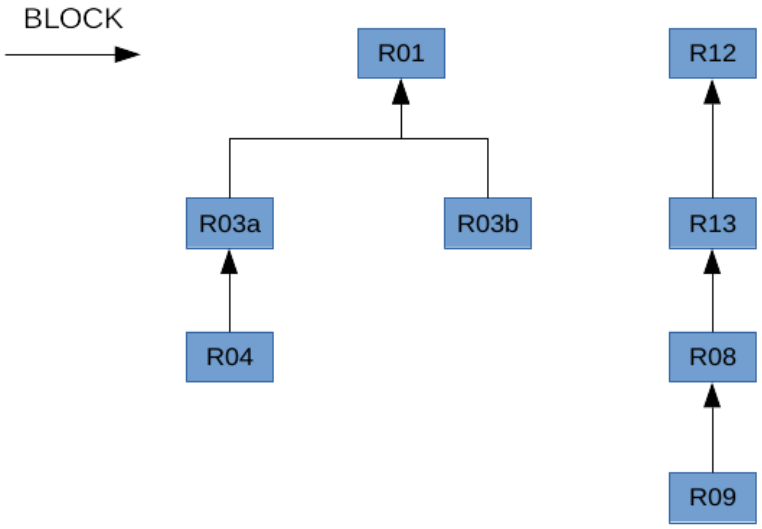

Figure 7-6: Communication flows for Figure 7-4 after network reconfiguration

In the case IEC 61850 communication is used for the exchange of the blocking signal, and in particular the Generic Object Oriented Substation Events (GOOSE) protocol, updated device configurations in terms of GOOSE subscriptions must be generated and exchanged between cells in correspondence with network reconfiguration events. For this reason, as already pointed out, the automatic and interoperable generation of such configurations would be an important tool for the implementation of such protection logic. Again, in case two cells are “owned” by different entities, the network topologies of each cell must be exchanged in an interoperable way in order to generate the proper IEC 61850 device configurations: for this reason the use of CIM network representations is a good candidate solution. The merging of the CIM network representations of each cell, in the case where they are “owned” by different cell operators, can be handled similarly to what is actually defined by ENTSO-E at European level for the merging of network

representation from different TSOs. In particular, a so-called Boundary Point can be inserted at the points of connection between different cells, in order to define them in a “Boundary CIM model” which is separate from all of the Cell’s specific model. The Boundary Point structure of the network considered in this chapter is illustrated in Figure 7-7.

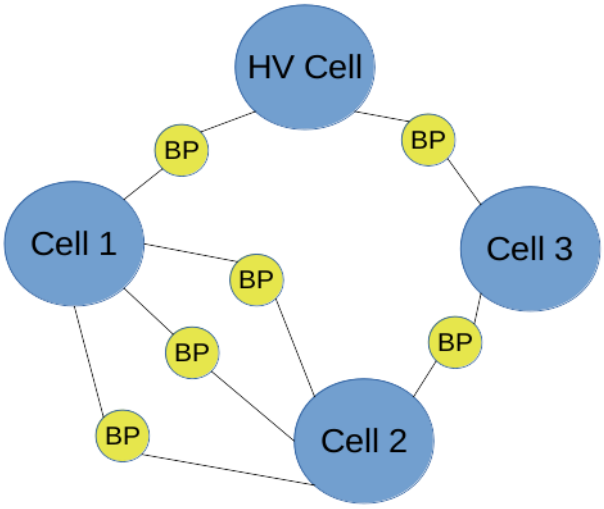

Figure 7-7: Boundary points between the cells of Figure 7-2

Each cell operator will then implement the following process in order to dynamically configure protection devices at run-time:

- Load the cell’s network topology model as well as those of the other cells. It must be noted that not only the neighbouring cells are needed since, for example, Cell 1 is not directly connected to Cell 3, but their network models must be merged anyway.
- Load the boundary sets descriptions.
- Merge the models, obtaining a unique network topology.
- Perform a topology processing of the merged network in order to determine the protection configurations.
- Generate the IEC 61850 device configurations for each device, in terms of GOOSE subscriptions.

7.2 Conclusions

The automated discovery and coordination of protection devices at run-time is usually a process, which depends on the topological structure of the underlying electrical network in a way that is independent of its logical subdivision into cells. For this reason, the widespread implementation of the WoC concept has an impact on such protection logic in terms of increased interoperability levels needed in order to allow the correct configuration of all the devices involved. For this reason, the use of the CIM model for network representation along with a model merging process similar to the one used at ENTSO-E level is needed. Also, from a communication point of view, the use of the IEC 61850 protocol for the communication between devices is very important for reaching interoperability. As pointed out, however, even if using IEC 61850 some implementation details must be clearly assessed in order to allow the implementation of such self-organizing logic, such as how the interconnection between ICT networks of different cell operators is organized and administered.

With respect to the range of topics discussed in the rest of this Deliverable, it is important to highlight that the focus of this chapter, i.e. the use of ICT in order to allow automated discovery and coordination of protection devices at run-time, is not strictly limited to protection functions but also involves all the supportive actions required for their correct operation under changing network conditions.

This dynamic configuration of protection devices enables efficient, scalable, and resilient protection coordination, which avoids centralised communications.

8 Coordination of Fault Ride Through Capability with Primary Voltage Control Use Case

8.1 Background and Relation to WoC

Fault ride through (FRT) or low voltage ride through (LVRT) is a basic capability of a wind generator and PV power converter to withstand disturbances leading to voltage dips in the network[6]. Both the shape of the envelope of the FRT characteristics and scope of its application are different in different TSOs and DSOs, however some similarities can be distinguished. The first part of the characteristic covers cases of close low-impedance short circuits causing severe voltage sags but with a relatively short clearance time; the remaining part, on the other hand, encompasses events of prolonged duration such as distant high-impedance faults.

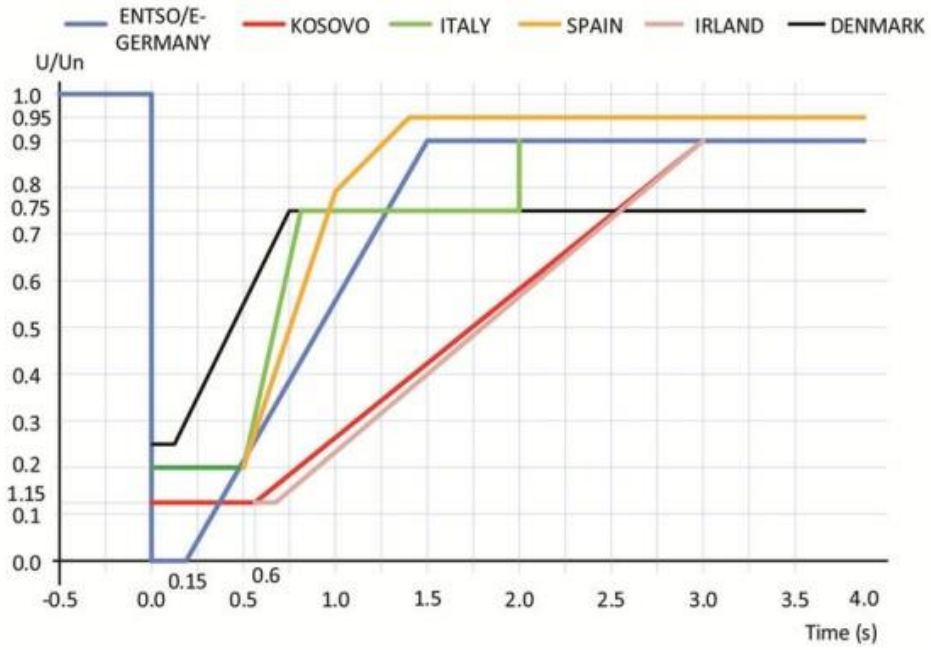

Figure 8-1: Fault ride through capability of wind turbines in National Grid Codes [13]

Currently all TSOs in Europe are in the process of standardization of the FRT characteristics performed as a part of establishing new network codes on requirements for grid connection of generators initiated by European Commission and carried out by the ENTSO-E. Each TSO is given specific freedom with respect to the level and duration of each part of the FRT characteristic in order to better fit it to the peculiarities of his own power system. However, due to the radical perspective of ELECTRA, which assumes high variability and intermittency of generation (mainly caused by high penetration of RES) and also high flexibility of demand, this approach may have to be modified in the future. Varying share of RES in total production portfolio will influence the level of short-circuit power, which in turn will affect the shape of a voltage sag should a grid fault occur. As a rule of thumb, it can be assumed that the lower the short circuit power, the lower and longer the voltage sag. In addition, voltage stability also might be affected by the lowered short circuit power.

These factors imply that in a highly variable future power system it might be necessary to change the shape of the FRT characteristics in order to be able to adapt to the changing grid conditions in

[6] Some FRT characteristics also entail overvoltage protection.

such a way that the wind turbine remains connected when necessary, but on the other hand can be disconnected by the FRT protection when this is needed.

Another important aspect of the behavior of the wind turbine power converter during the disturbance is that it is capable of supplying reactive current into the faulted network during the disturbance thus supporting grid voltage during this time. In many cases, it is achieved by means of voltage control and, as will be demonstrated, voltage controller parameters are of particular importance for this process. Within the ELECTRA WoC architecture, during normal operation it is the Primary Voltage Control (PVC) that is responsible for controlling voltage to a set-point provided by the Post Primary Voltage Control (PPVC). Even though FRT is conceptually a protection system whereas PVC is classified as a control system, the bandwidth (or time horizon) of the operation of the two systems is comparable, therefore there is a need for proper coordination of the parameters of the two, or in case where they are implemented within a single system, a proper adjustment of the important parameters.

8.2 Model Description and Assumptions of the Study

The study has been performed on a simple model consisting of a wind farm connected to an infinite bus by a chain of lines and transformers (see Figure 8-2). A positive sequence model has been prepared and used in simulations of electro-mechanic transients. For the infinite bus, a standard “gencls” model has been used, whereas the wind farm is represented by “regc_a” and “reec_a” models (Figure 8-3 and Figure 8-4), which are the second generation of full-converter models for wind and photovoltaic resources. In order to capture only the relevant phenomena, factors such as drive train model and power plant controller model were neglected.

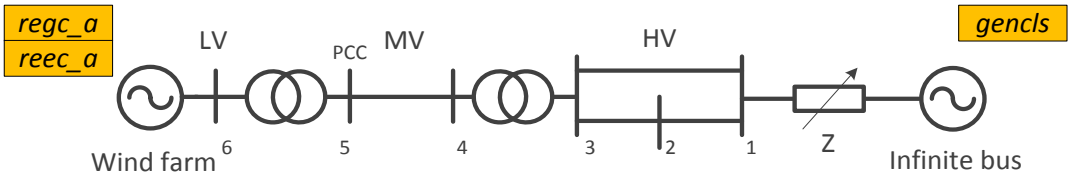

Figure 8-2: Single line diagram of the test model

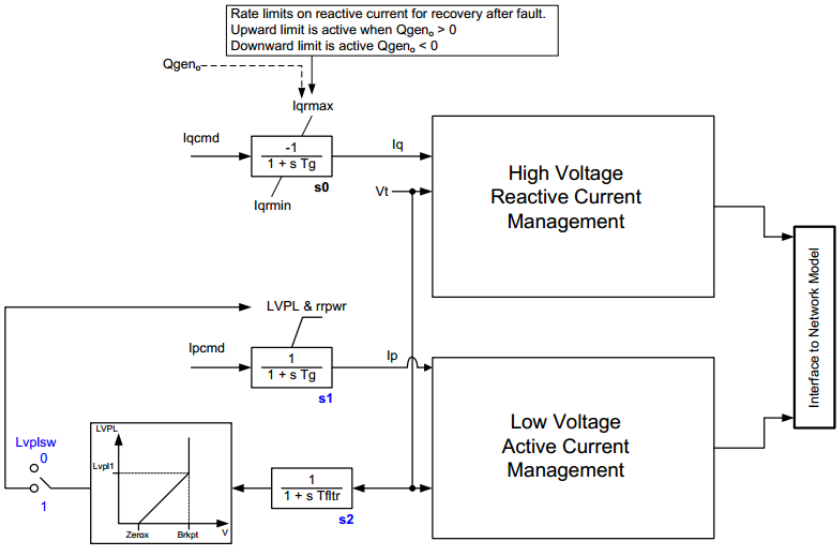

Figure 8-3: Generator/converter model (regc_a)

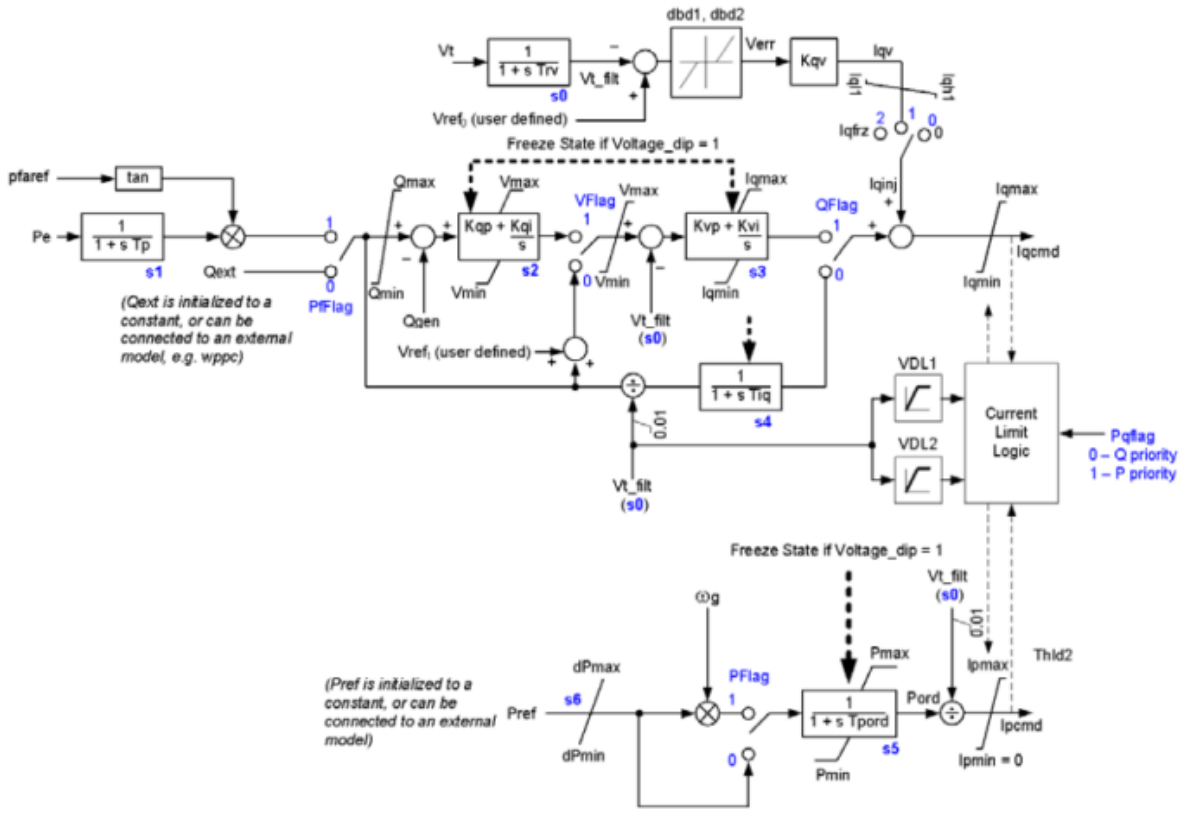

Figure 8-4: Renewable energy electrical control model (reec_a)

It is assumed that the wind farm operates in voltage control mode (PVC active) and keeps voltage at 1.00 pu which requires a small amount of positive reactive power to be supplied. At time t=1.0 s, a short circuit at bus 2 is applied and after 200 ms it is cleared by opening circuit breakers (CBs) at bus 3 and 1. Clearing the fault by opening CBs implies that after the fault the short-circuit impedance as measured at bus 3 increases. This is Scenario 1 of the study. Scenario 2 also considers an arbitrary change of short-circuit power of the network due to e.g. disconnection of a nearby synchronous generation or grid reconfiguration as a result of optimal power flow (OPF). In both scenarios, focus is put on how external conditions influence the performance on the PVC during and after the fault in the grid.

8.3 Scenario 1: Change of Short-Circuit Power After a Disturbance

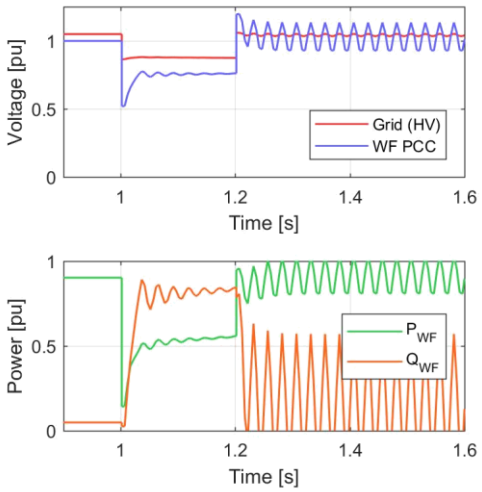

Step 1: Initial parameters

- Initially the model is stable and accurate.
- During the short-circuit, the wind farm produces a large amount of reactive current due to a high gain in the PI controller of the PVC.
- The response is oscillatory but the damping is enough to suppress the oscillations within 200 ms.
- After the clearance of the short-circuit and disconnection of lines, undamped oscillations appear and remain for significant time.

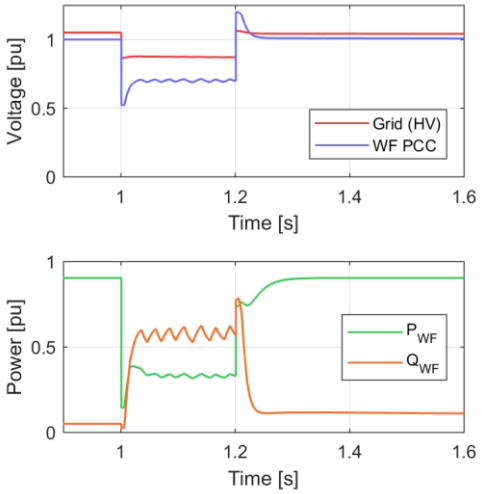

Step 2: Gain reduction

- The gain of the voltage controller (kvp) is reduced in order to avoid oscillations in low short-circuit power conditions.
- The response is stable and well damped, but the reactive power support is significantly less in this case.

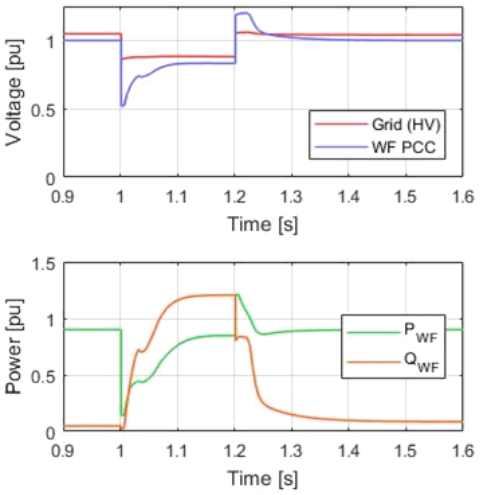

Step 3: Final parameterization

- In order to improve reactive power support capability the proportional gain is increased again slightly and the gain of the integral part of the PI controller (kvi) is also recalculated.
- The final response is acceptable.
- Note that supported recovery of voltage allows for active power supply even during the short-circuit.

8.4 Scenario 2: Change of Short-Circuit Power Due to Operations in Supplying Network

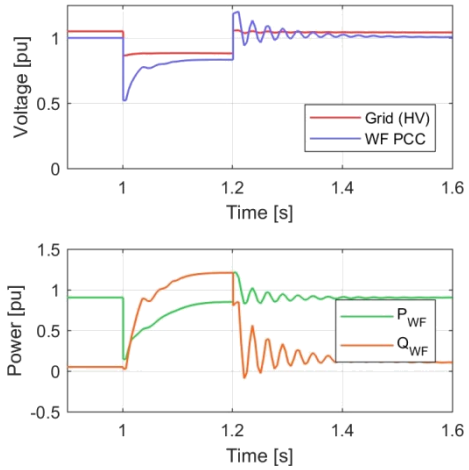

Step 1: Initial parameters

- In different conditions than in Scenario 1 (reduced short circuit power by 50%), the model is stable and accurate supporting grid voltage during the short-circuit.
- After the fault is cleared the controller reacts in an oscillatory manner, but the damping is positive and the oscillations disappear in less than 300 ms.

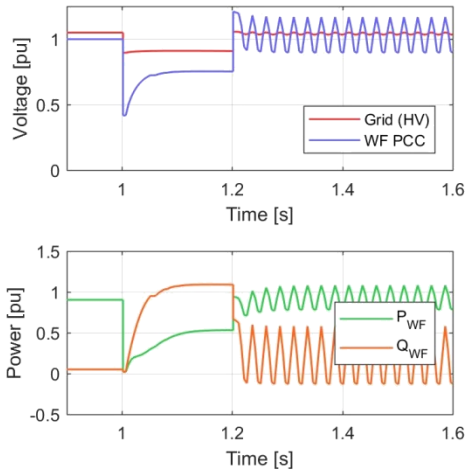

Step 2: Short-circuit power decrease

- The short-circuit power is decreased in the model (approximately by half) due to e.g. synchronous generator tripping or line disconnection.
- If a fault is repeated in lower short-circuit power conditions, then the controller with the same settings as in step 1 will perform worse: even though during the short-circuit it acts to deliver reactive power, its response after fault clearance is highly oscillatory with close to zero damping.

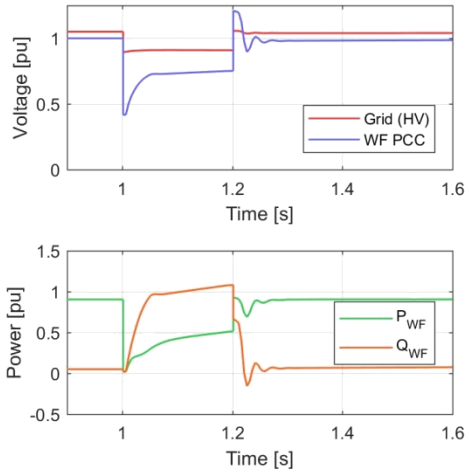

Step 3: Final parameterization

- In order to remove the oscillations, new controller parameters are calculated. Proportional gain is reduced by half and integral gain is decreased by a factor of 10.
- Considerable reduction of short-circuit power firstly by grid operations and secondly by line tripping required a significant recalculation of the controller settings.
- The final response is acceptable both in terms of during and post-fault recovery.

8.5 Verification and concluding remarks

The two resulting sets of parameters are used in full FRT simulation, in which a voltage sag of a typical shape is applied. For illustration purposes, the disturbance is applied at bus 1. Relevant plots are presented in Figure 8-5.

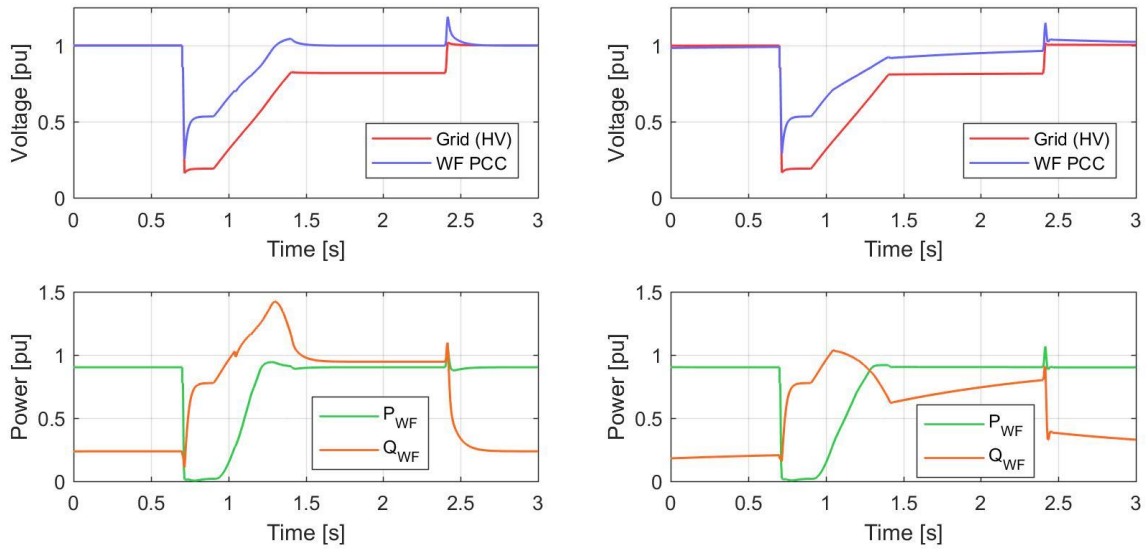

Figure 8-5: FRT simulation with settings from Scenario 1 (left figure) and Scenario 2 (right figure)

In both cases, the response reveals high level of support of the wind farm to the grid during both phases of the fault. Wind farm delivers high amount of reactive power which effectively increases voltage at PCC and in the MV and HV network buses. In the first case the voltage is restored faster than in the second, but due to higher gains there is a risk of overshoot and overvoltage should the grid voltage suddenly be restored.

It can be concluded that if PVC shall be deployed on a RES with FRT capability, then:

- Parameters of the two controllers, i.e. the PVC parameters and FRT settings, should be coordinated or one controller should perform both functions; as it was demonstrated PVC parameters are of crucial importance both in steady state operation and during (and after) disturbances.
- In order to support that the grid, impedance estimation functionality of the PVC can be utilized to adapt parameters to the current operating state of the grid by using estimated values of the grid impedance and thus requires an analytical approach to find new parameters of the controller. High gain is beneficial for reactive power generation during a short-circuit, but if the strength of the grid is reduced during or after the fault (e.g. due to line tripping) then it might be necessary to reduce the gain.
- Coordination and/or calculation of the new settings can also be achieved on the PPVC layer (at CTL-2) and communicating the new values into the flexible resource (at CTL-0). It is assumed that PPVC has a good knowledge of the state of the cell due to estimator operation and that the current grid impedance value can be calculated.

The coordination between FRT (or in general PVC) settings and inertia/balance controllers is not necessary as it is mainly the reactive power that is affected by the PVC.

9 Efficient and Resilient Wide Area Protection using PMUs within the WoC Architecture

9.1 Overview

Fast-acting response to power system events is becoming critical to ensuring power system stability in real-time [14], [15]. Wide area Phasor Measurement Unit (PMU) monitoring schemes are being utilised to enable new system functions, such as fast-acting frequency control in low- and variable-inertia systems [3] and distributed control paradigms [16]. The use of data from PMUs will therefore underpin the real-time operation of future power systems, particularly for the WoC architecture, which requires an unprecedented level of distributed measurement and control.

This chapter outlines the key architecture, characteristics, and capabilities of PMU-based monitoring, protection, and control schemes, including robustly applying measurements for novel wide area protection methods and determining real-time latency. This work highlights what could be achieved, in terms of protection, assuming a very high level of observability in future power systems.

9.2 Background

Wide Area Monitoring, Protection, and Control, which typically involves the use of Synchrophasor measurement data for power system applications, has gathered significant interest, including recent investigations by CIGRE [17] and IEEE Power System Relaying and Control (PSRC) committee [18]. These applications are diverse and include: state estimation, coordinated frequency response, real-time transfer capability, phase angle monitoring, real-time oscillation damping, system restoration, and coordinated protection. This chapter focuses on the area of coordinated protection, in the context of the ELECTRA project and the WoC future power system architecture.

Synchrophasor data must be robust to be trusted for use in real-time control and protection applications [19]. Therefore the quality of Synchrophasor measurements from PMUs, including timing accuracy, has also been a key topic of research, particularly in the EU [20] and the USA [21], [22]. Research work has highlighted the challenges associated with: measurement quality, which is very important for distribution system applications of PMUs [22][7], PMU “data quality” [21], PMU timing accuracy [23], real-time supervisory assessment of multiple PMU data streams [24], and latency [15] (Section 9.6 presents a novel method to accurately characterise latency). The importance of rigorous testing of PMU-based systems is strongly emphasised in [25] and analysis of the large-scale PMU data quality issues is given in [26].

Utilities are already using PMU data as tools for visualisation and stability monitoring [27]–[29], but closed-loop control, i.e. where PMU data automatically and directly influence power system operation, are presently undergoing validation [3], [30]. Furthermore, the North American SynchoPhasor Initiative (NASPI) presently recommends *avoiding* the use of PMU data for system-critical operations – unless timing accuracy and resiliency have been fully validated [23].

Issues relating to cybersecurity are also not implemented in the work described in this chapter. However, previous work has shown that real-time authentication and encryption can be applied to

[7] As noted in [123], fault location in distribution systems may require voltage angle measurements which are approximately two orders of magnitude more accurate than for transmission systems i.e. with a maximum phase error in the range 0.01-0.1°.

protection applications with negligible impact on latency [31]. Furthermore, the IEC 61850-90-5 standard includes provisions specifically for authentication and encryption of PMU data.

9.3 Approaches to Wide Area Protection using PMUs

The term “wide area protection” often refers to special provisions to respond to large disturbances during severe or multiple contingencies [32]. However, in the context of this report, the term is used to refer to methods which are alternatives (or backups) to conventional protection schemes (e.g. differential, distance, and overcurrent protection), but which exploit information from multiple locations in a coordinated manner. In most cases, the wide area scheme is intended to be implemented as a fast-acting backup scheme (relative to conventional backup systems) due to the communications latency which must be accommodated, rather than replacing primary protection [33].

The relevant fault detection and location[8] methods in the literature can be categorised and summarised as follows:

1. **Extensions of the principle of current differential protection**. The method in [33] collects multiple PMU measurements and performs differential protection for each applicable zone, per phase. Expanded zones are established which can operate due to loss of inner zone PMU data or other issues. As described in [34], expanded zones can also block operation of an inner zone due to issues such as transformer saturation; this provides resilience to erroneous or lost measurements. The main benefits of the scheme are faster-acting backup operation, and avoiding the need to perform extensive, challenging validation of distance protection schemes. A similar method is presented in [35] for shipboard applications, where extended protection zones are created to provide backup operation and avoid false trips. Another method is presented in [36] based on the sum of the zero- and/or positive-sequence currents entering a protection zone (which is bounded by PMU measurements).
2. **Centralised protection concepts**, which are typically designed for application within a substation [37], [38], could be applied over a wide area [39]. In summary, this approach involves the integration of multiple protection and control functions within a single system, typically using multiple synchronised measurements, in order to better detect fault conditions, improve protection reliability, and improve efficiency. However, this approach may not be scalable to very large systems, and there is a perceived lack of resilience compared to a paradigm using distributed protection devices (although, centralised protection systems can be designed with redundancy provisions). The concept has been extended to the virtualisation of IEDs [40].
3. **Pattern-matching, neural networks, and other machine learning or rule-based methods** to detect and locate grid disturbances [41]–[46].
4. **Expert systems** using, for example, “action factors” to combat uncertainty in order to identify the fault location [47], [48].
5. **Superimposed components** [49]–[51], which typically involves the difference between measurements during a fault and the pre-fault measurements. A similar approach involving autocorrelation of a current waveform for use in directional relays is described in [52]. Similarly, [44] proposes using the difference between steady-state voltage and the minimum voltage during a disturbance to identify the bus closest to a fault. The fault detection algorithm in [53] is based on the difference between measured voltage and

[8] “Fault location” in this context refers to identifying the faulted circuit to trip, rather than estimating the distance to the fault such as in [124], [125], and [126], and the work in Chapter 10.

frequency values and the nominal values, and fault location is based on the circuit with the largest normalised current magnitude.

6. **Fault passage indicators** in distribution systems can be used to locate a faulted circuit section [54], [55] based on a simple indication of current flow. Reference [56] presents a method for MV and LV systems using directional fault indicators which communicate with a control centre. Reference [57] presents an efficient method for fault location in distribution systems.
7. **Voltage magnitude-based protection**, such as [58] and [59]. Reference [60] uses positive sequence voltage magnitude values to locate the bus closest to the fault, and positive sequence current angle differences to locate the faulted line. A similar method is presented in [61] where fault detection is based on negative- or zero-sequence voltage or current criteria, and which is enhanced by a method to improve the confidence of trips by combining information from conventional protection systems. A similar method of fault detection, using the angle difference for a two-terminal system, is described in [62], and a further related method is given in [63] (along with a fault detection method based on the ratio of symmetrical components). Another method of fault location using the change in voltage measurements is given in [64].
8. **Distributed photonic sensor systems** offer a novel approach to integrate multiple voltage and current sensors over a wide area within a single optical fibre [65]. A central interrogator unit is able to process all measurements and deliver waveform data or Synchrophasor data from each monitoring location. The sensors are passive, i.e. a power supply and GPS or other time synchronisation method is not required at each monitoring location. Other parameters, such as temperature, can also be monitored.
9. **Cloud-based** power system services and "management" is described in [66] and [67]. The use of a bespoke real-time database of large-scale PMU data for event detection and fault location is described in [22], however, it is not clear if the system could be used for protection applications where low latency is required.
10. **Model-based techniques**, such as the use of a genetic algorithm to match multiple measurements to a simulated fault location and impedance [68]. Similar methods, for transmission and distribution systems, are described in [69]. Another approach is given in [70] using a real-time state estimation process. A further method is presented in [71], but with an impractical computational time approaching 100 ms. Reference [46] discusses a "physics-based" method to identify dynamic events from transmission system PMUs. These approaches all require power system impedances and other data.
11. **Hybrid approaches** which dynamically select the most appropriate fault location method [69]; however this is not suitable for real-time operation for protection applications.

9.4 Proposed WoC Wide Area Protection Architecture

9.4.1 Influencing Architectural Approaches

Further to the literature referenced in Section 9.3, the following research is of particular relevance to enabling a real-time measurements architecture for the WoC:

1. The concepts of multiple layers of Phasor Data Concentrators (PDCs) and "SuperPDCs" is widely documented in the literature [72]. A discussion of the trade-offs between a distributed (hierarchical) and a centralised Synchrophasor architecture is given in [73] and IEC 61850-90-12 [74]. A peer-to-peer inter-substation communications architecture to enable flexible and adaptive applications over a wide area is presented in [66], [75]. Decentralised discovery of data and services is described in [76], and the use of Common Information Model (CIM) data to discover relevant system-wide PMU data sources is

described in [77]. Reference [78] also describes a decentralised alternative the SuperPDC architecture to avoid a single point of failure. However, redundancy can be applied to the "conventional" SuperPDC architecture as illustrated in [19].

2. The NASPI Network, or NASPInet, has been designed to provide a continent-wide PMU data architecture [79], [80]. This involves local "clusters" of PMUs and a PDC, with a large-scale "data bus" which is intended to enable efficient sharing of data between clusters. However, it is not clear if this approach is suitable for the low latency requirement of protection applications.
3. Multi-area power system state estimation using PMU data, where each area performs state estimation independently, but with central coordination [81].
4. Triangulation of the location of large disturbances using multiple frequency measurements [82]. A "detrending" method is presented in [67], but it is not suitable for real-time operation.
5. Agent-based division of protection functionality [83].
6. Reference [63] proposes division of the system into areas (with further sub-zones) for protection, although just for radial distribution feeders.
7. Reference [84] describes a generic platform for creating wide area protection functions using data from up to 20 PMUs, and also describes a peer-to-peer PMU approach.
8. A method which integrates protection with post-fault control, particularly for distribution systems with high levels of DG, is presented in [53]. Similarly, [34] includes a post-fault process to balance load and generation on shipboard systems.
9. "Multi-layer" differential protection, which enables trips to be confirmed by using "outer" layer measurement, or provides backup zones for communications failures [35].

9.4.2 Discussion of WoC Wide Area Protection Requirements

The following protection requirements are important to the characteristics of the WoC concept:

1. The use of a cell provides a convenient boundary for each instance of a wide area protection scheme. There are practical requirements which may govern the size of a cell, in terms of effectively implementing wide area protection:
    a. Management of data volume i.e. ensuring that the quantity of measurement data involved does not lead to excessive computational time within a cell. For this reason, it may be required to operate separate wide area protection PDC structures for transmission and distribution levels, particularly due transmission systems having stricter protection requirements.
    b. Management of data latency i.e. ensuring that the size of a cell is optimised to limit communications delays, which would reduce the timeliness of wide area protection. For example, reference [85] specifically proposes the regionalisation of wide area protection schemes to minimise communications latency. A discussion of the impact of area size (i.e. cell size) on communications infrastructure for WAMS applications is provided in [86].
2. The links between cells, i.e. tie-lines, must be protected. Therefore, "overlapping" of cell-wide area protection zones is desirable, otherwise cell tie-lines would not benefit this supervisory backup. This would require some sharing of PMU data between cells.
3. It may be desirable to link a wide area protection scheme, which has supervisory knowledge of an entire cell, with frequency containment control (FCC) or fast-acting balancing restoration control (BRC). For example, fast-acting BRC requires each cell to know the location of the underlying disturbance (either within or outside the cell) and the wide area protection system, which is responsible for locating faults, could therefore inform the BRC controller.

4. State-of-the-art PDCs include provisions for enhanced security [87] and minimising latency [88], which are important characteristics for wide area protection applications.
5. For protection purposes, it is important that a PDC does not merge or "average" multiple PMU measurements into a single measurement; it is best for a protection scheme to have direct, granular access to measurements from each node to help discriminate fault location.

The following assumptions underpin the wide area protection architecture presented in Section 9.4.3:

1. PMU measurements are ubiquitous, at both HV and MV. A relatively high level of observability may also be available at LV, but this is out of the scope of this chapter. Therefore, a wide area protection scheme should leverage this observability.
2. It is assumed that sufficient PMU measurements are available to maintain an accurate knowledge of the power system topology [15]. A method for achieving fault location with reduced PMU measurements is described in [89]. It is also assumed that a high-performance communications network is available to distribute Synchrophasor data; however, the impact of latency is explicitly considered in Section 9.6.
3. This chapter does not consider the necessary communications technologies and topologies in detail, although a discussion on suitable approaches for protection is given in [90]. The use of multicast communications, which is supported by both the IEEE C37.118.2 and IEC 61850-90-5 Synchrophasor communications standards, could enable the efficient use of PMU data for multiple applications.

9.4.3 Proposed Architecture

Based on the requirements in Section 9.4.2, this subsection illustrates the proposed wide area protection architecture. It may be tempting to map the concepts of a hierarchical or multi-layer PDC architectures [32], [72], [91] directly to the CTL hierarchy within ELECTRA WoC concept. However, for protection applications, this structure is not appropriate because fault location requires granular measurements to be most effective, and these measurement should be delivered with as low latency as possible. Therefore, the proposed architecture is "flat", and separate wide area protection systems should be applied at CTL1 and CTL2, with the critical transmission system primary assets typically existing at CTL2. For CTL1, which will broadly contain distribution voltage levels, it is assumed that each cell would be protected by one or more separate instances of the wide protection scheme due to the less stringent requirements for protection operation, compared with transmission systems; this is not illustrated further for brevity.

Two variants of the proposed architecture are presented:

1. **Separation of cells**, with a special case for tie-lines (Figure 9-1). Tie-lines may be protected using conventional methods such as current differential protection. This variant reduces the area over which the wide area protection operates (potentially reducing the impact of communications delays), but the tie-lines do not benefit from the enhancements offered by wide protection (i.e. faster acting backup). This approach also may be appropriate for DC tie-lines which may not fit with the wide area protection operating principle, which may be designed for AC networks.
2. **"Overlapping" of cell boundaries** to include tie-lines within the wide area protection scheme (Figure 9-2). This requires slightly more measurements to be communicated to the cell PDCs, but ensures that the tie-lines are included within the wide area protection scheme. Note that Figure 9-2 shows each tie-line being included in the wide area protection scheme for both neighbouring cells; alternatively, a single cell could manage each tie-line.

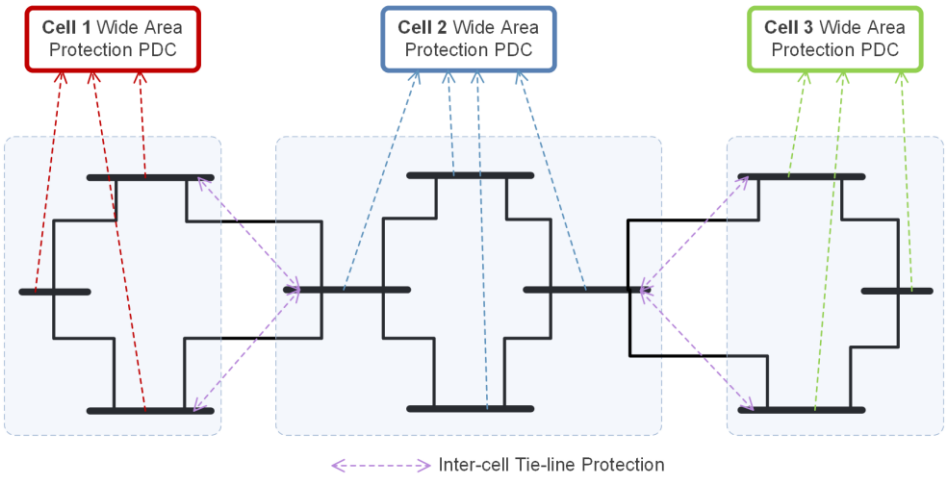

Figure 9-1: Wide area protection architecture – without cell overlap

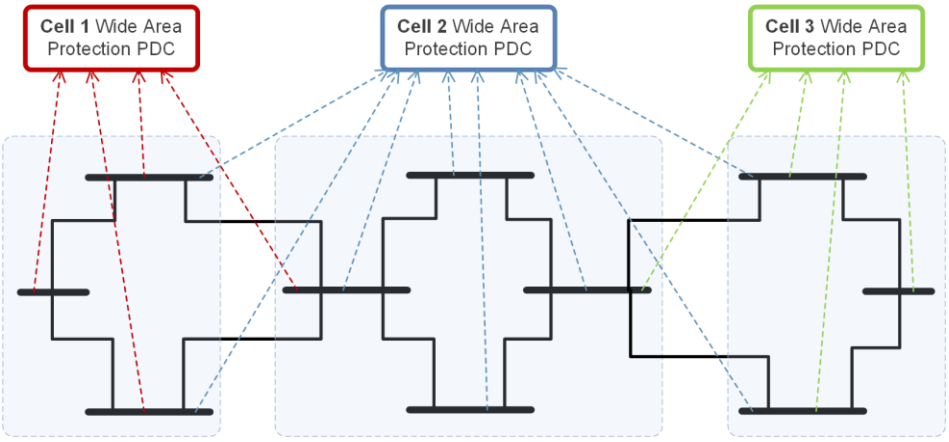

Figure 9-2: Wide area protection architecture – with cell overlap

The following section describes in detail how the proposed wide area protection architecture can be implemented, which could be applied to either of the two variants.

9.5 Demonstration and Comparison of Novel Wide Area Protection Methods

9.5.1 Testbed Power System Model

Figure 9-3 illustrates the test network used to validate potential wide area protection algorithms. This is part of a 400 kV transmission system within a single cell (i.e. other neighbouring cells are not shown). The effect of dividing the network into cells is that each algorithm instance will operate on a smaller network topology. This network has been chosen because it represents a meshed topology (unlike the CIGRE MV model) which can be challenging to protect using conventional backup methods, and avoids catering for multiple voltage levels (as present in the Pan-European model) which adds unnecessary complexity.

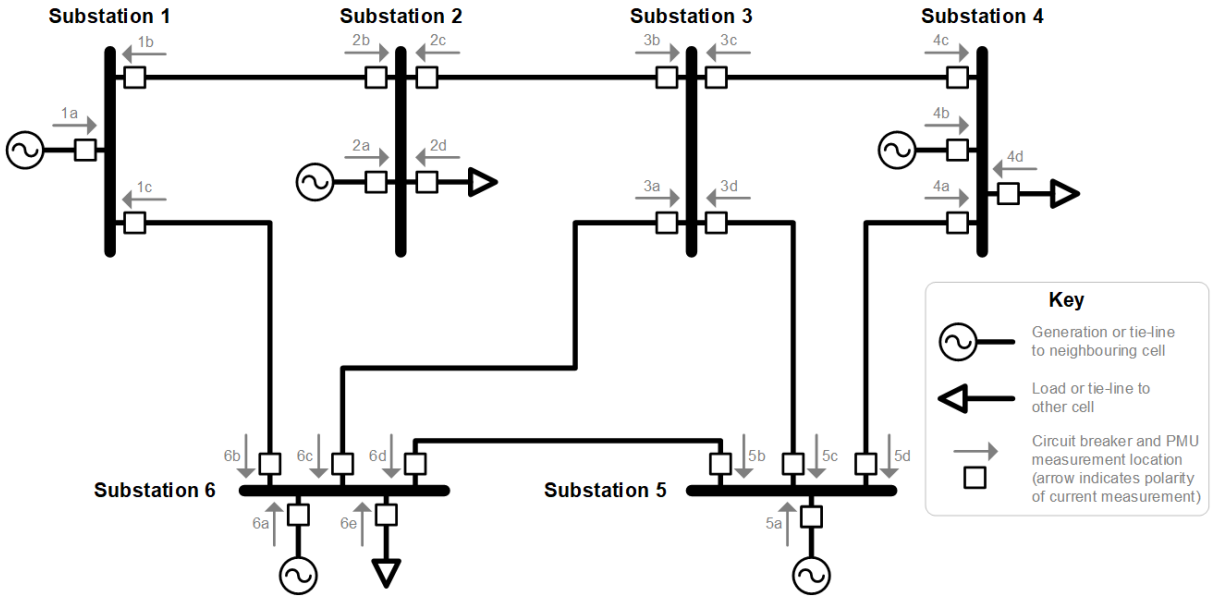

Figure 9-3: Wide area protection test network (content of one cell)

Figure 9-3 represents a snapshot of the system state, but it is assumed that the power flows to or from any load or generator (or tie-line) may change over time. It is also assumed that each feeder in each substation is equipped with a circuit breaker and a PMU, and that each cell can communicate with a PDC, which is designed for low-latency wide area protection applications, as illustrated in Figure 9-4. Each PMU provides positive sequence voltage and current measurements and the status of the circuit breaker for the feeder.

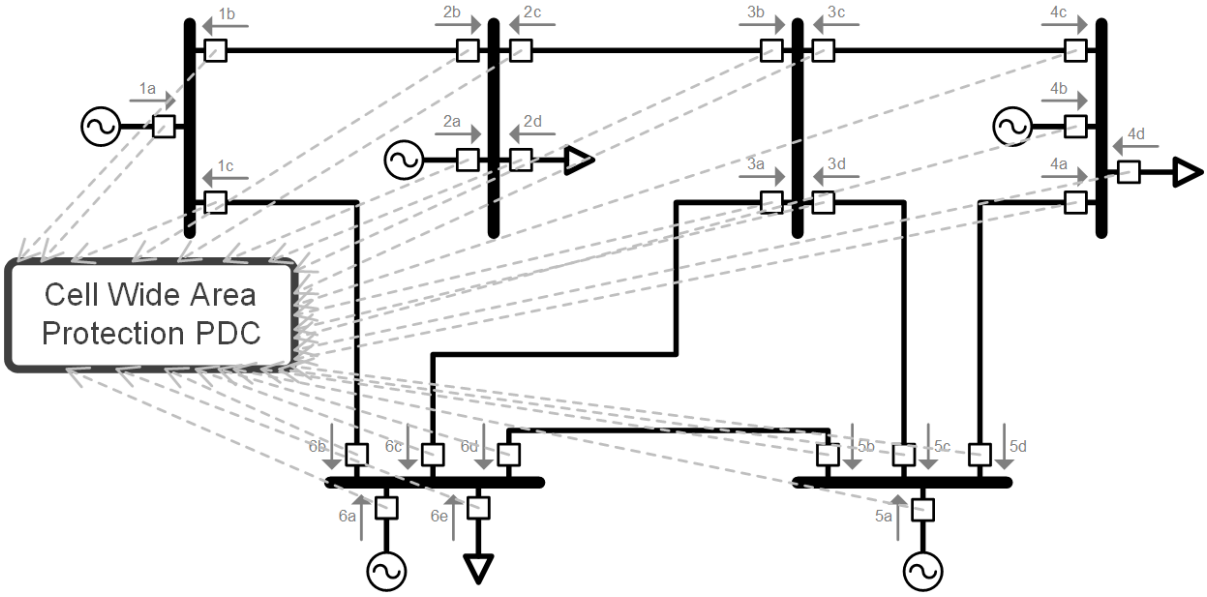

Figure 9-4: Wide area protection PDC

9.5.2 Power System Topology Representation

The use of graph theory and an incidence matrix to capture power system topology is widely discussed in the literature: [34], [57], [92]–[94]. The system in Figure 9-3 can be represented as nodes (buses or lines) interconnected by measurement locations (i.e. circuit breakers with PMUs). The polarity of each PMU's current sensors is important, relative to a voltage measurement, and this is specified by the direction of arrows for each PMU location in Figure 9-3. A matrix can be constructed which defines the power system topology i.e. interconnections of nodes and

measurement locations. For example, considering just Substation 1, with bus B1 and lines L1 and L2 as shown in Figure 9-5, the incidence matrix is:

$$\boldsymbol{PMUs}\begin{matrix}\\ 1a\\ 1b\\ 1c\\ \vdots\end{matrix}\begin{matrix}\boldsymbol{Nodes}\\ B1 \quad L1 \quad L2\end{matrix}\begin{bmatrix}1 & 0 & 0 & \cdots\\ 1 & -1 & 0 & \cdots\\ 1 & 0 & -1 & \cdots\\ \vdots & \vdots & \vdots & \ddots\end{bmatrix} \tag{1}$$

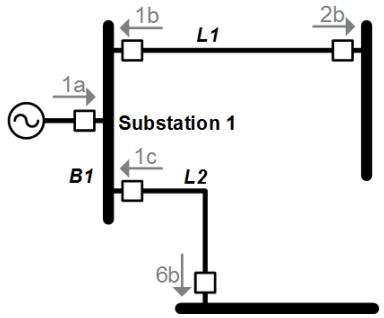

Figure 9-5: Substation 1 bus and lines

A convention has been used where “1” denotes “forward” nominal power flow into the node, “-1” for “reverse” power flow, and “0” for no connection. As noted in [70], it is trivial to update the power system topology incidence matrix in real-time using Boolean circuit breaker status values which are included in the PMU data. It is also feasible that the physical topology could be known automatically, based on a machine-readable format such as the CIM, as described in Section 7.

The full topology matrix defines the coefficient matrix of Kirchhoff’s current equations [95]. For example, each column in the matrix defines the zonal measurements required for current differential protection of the node (whether a bus or line). These protection zones are illustrated in Figure 9-6.

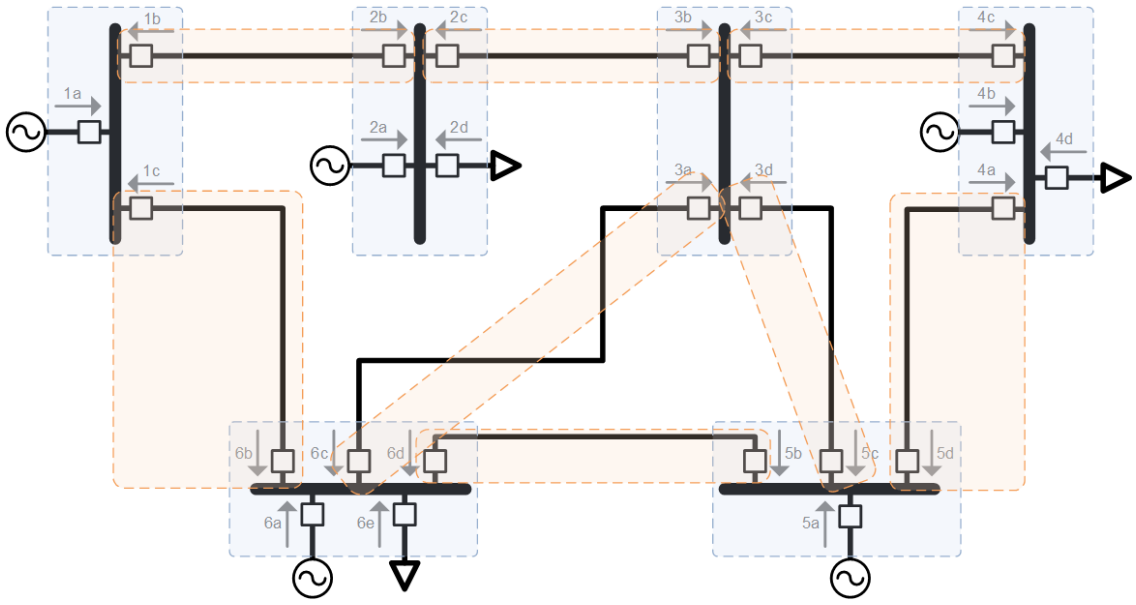

Figure 9-6: Bus and line primary protection zone

Wide area protection must also be resilient to partial loss of data e.g. due to failure of a PMU or a communications link [61]. This can be mitigated by automatically merging the two zones linked by the missing measurement. Figure 9-7 illustrates an example of one backup zone assuming data

from PMU 1a was missing. In such scenarios, it may be appropriate to delay trips for backup zones (for example, to allow a backup communications path to be established) to avoid unnecessarily tripping a transmission system bus during a transient loss of information.

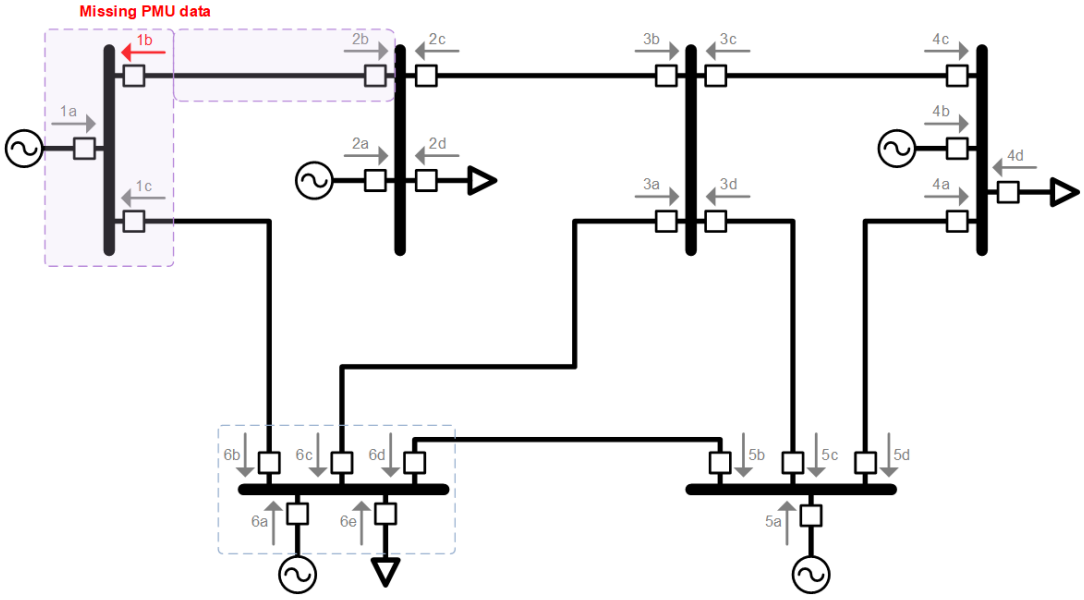

Figure 9-7: Backup zone example

9.5.3 Theory of Novel Wide Area Protection Algorithms

The use of an incidence matrix is important for the efficient and convenient implementation of wide area protection. This is because a vector (i.e. $1 \times M$ matrix, where M is the number of PMUs) of suitable measurement data can simply be multiplied by the topology incidence matrix. This results in a $M \times 1$ matrix, which contains the "residual sum" for each node, which can be used to identify fault location. Therefore, the residual, R, can be calculated from measurements, M, and topology, T, as follows:

$$R = M \times T \quad (2)$$

Due to the fact that T is likely to be very sparse, the execution time of the computation time of R is negligible (particularly compared to communications delays). The input vector of measurements, M, can be defined in several ways, and the following algorithms are investigated further in this chapter:

1. Change in real[9] positive sequence current.
2. Change in real power.
3. Transient energy [51] i.e. the accumulation of real power following fault inception.

For each algorithm, following fault detection (which is ignored for simplicity, but could be based on the same principle as for fault location or other indicators), the largest value (or largest absolute value) in R will indicate the faulted node. The reason for extracting the real component of the PMU measurements (which include both the real and imaginary components for voltage and current) for each algorithm is that faults are assumed to be resistive (i.e. not inductive) which would result in only "real" current flow into the faulted node. Each algorithm is also inspired by the concept of superimposed components, because the change in measurements following fault inception is important. This approach is elegant and very computationally efficient, therefore enabling low latency and scalability to many measurement locations.

[9] Where "real" can be interpreted as the portion of current which is in phase with the voltage.

9.5.4 Real-Time Laboratory Implementation and Validation

The power system model in Figure 9-3 has been implemented on a Real Time Digital Simulator (RTDS). A GTNET card has been used to generate actual data for 24 PMUs i.e. one for each measurement location in the power system model. Due to hardware constraints, the PMUs are restricted to providing positive sequence voltage and current measurements at a maximum reporting rate of 50 Hz. The User Datagram Protocol (UDP) protocol is used rather than Transmission Control Protocol (TCP), because it is well established as being most appropriate for real-time applications. It should also be noted that a separate PMU connection must be used for each measurement location. However, another approach would be for a single PMU to aggregate the bus voltage and all feeder current measurements for a substation into a single data stream.

A PDC has been created in C, using the “libuv” library for managing UDP communications and other events. The role of the PDC is to connect to each PMU, manage these connections over time, and execute all the wide area protection algorithms when a set of time-aligned measurements arrives (or a timer expires for a partial data set). The PDC sends a GOOSE message (using the open source “rapid61850” library [96], [97]) to the RTDS based on the fault location result calculated by each algorithm. The PDC therefore provides a platform for testing and comparing the performance of multiple prototype wide area protection and control algorithms. In all cases, two identical consecutive fault location results are required before the algorithm issues a trip.

Figure 9-8 illustrates the laboratory testing configuration at the Dynamic Power Systems Laboratory at the University of Strathclyde. The RTDS simulation model and “Runtime” for control and visualisation is shown in Figure 9-9.

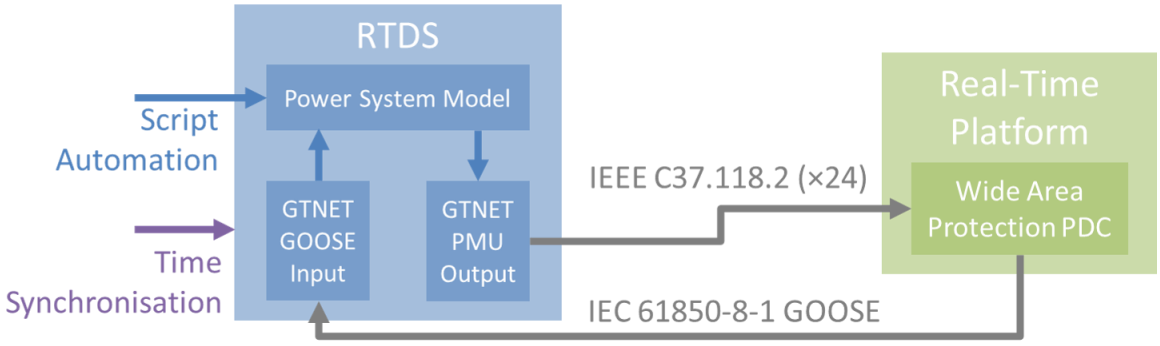

Figure 9-8: RTDS and PDC laboratory configuration

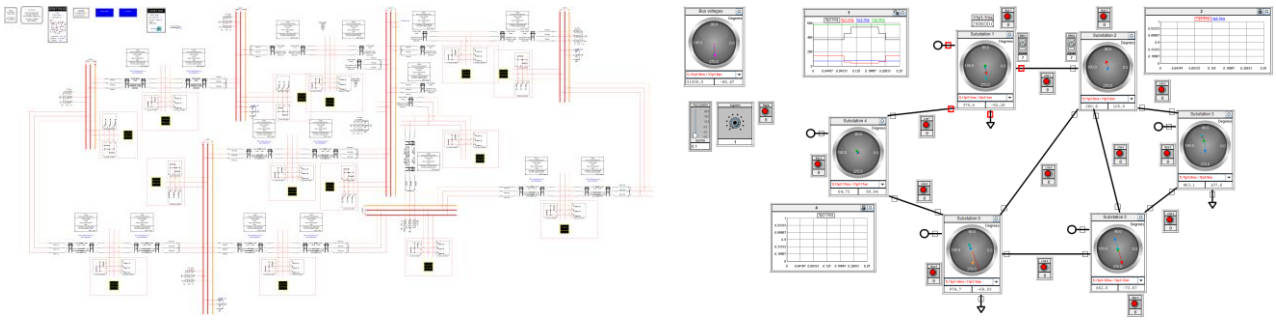

Figure 9-9: RTDS model Draft and Runtime

9.5.5 Real-Time Simulation Results

A script has been created to automatically and systematically test a wide variety of fault conditions. The script controls the RTDS and varies: fault location (i.e. every bus and line), fault position (the

distance along the line, for line faults), fault impedance (values between 0.01 Ω and 100 Ω), fault type (single-phase, phase-to-phase, or three-phase), and the point on wave of fault inception. This generates a total of 900 different fault scenarios, and the response for each algorithm is recorded. This can be repeated with missing PMU data for multiple locations, and for simulated line outages.

The three proposed algorithms have been compared with the fault location method in [60], which also uses an elegant operating principle and is relatively simple to implement. However, it was important to improve upon this algorithm by calculating the change in voltage magnitude following fault inception, rather than using the instantaneous voltage; otherwise the method may incorrectly identify the faulted bus in some cases.

Table 9-1 summarises the results from executing the RTDS script.

Algorithm	Description	Correct fault location	Notes
1	Change in real positive sequence current	99.4%	Fails for some high-impedance single-phase faults
2	Change in real power	77.6%	Fails for some low- and medium-impedance faults
3	Transient energy	100.0%	Correctly identifies all fault locations
4	Voltage magnitude and current angle difference (modified algorithm from [60])	99.8%	Fails for some high-impedance single-phase faults

Table 9-1: Fault location test results

Algorithms 1 and 4 are susceptible to incorrectly identify the fault location for high-impedance single-phase faults. This is due to the use of positive sequence current measurements, and would likely be resolved by using per-phase measurements (as well as providing faulted phase discrimination).

Algorithm 2 is ineffective for low- and medium-impedance faults, but operates correctly for high-impedance faults. This is because faults with a relatively low impedance will dissipate relatively low real power, which will be difficult to distinguish between other power flows.

Algorithm 3 consistently operates correctly, regardless of the fault scenario, and without requiring per-phase measurements.

9.5.6 Summary of Proposed Wide Area Protection Framework

This sub-section has demonstrated a cell-wide approach to wide area protection whilst testing multiple potential algorithms. In summary, the main characteristics of the novel wide area protection method are:

- Suitable for radial and complex meshed systems.
- Designed as a backup for transmission systems due to the inherent measurement and communications delays, but could be primary protection for distribution systems.
- With an appropriate choice of protection algorithm, the method does not require knowledge of system impedances or other parameters. It is immune to factors such as fault impedance, fault type, and the fault point on wave.
- The method does not require protection settings, although some thresholds can be specified.

- Adapting to topology changes is trivial. This includes supporting the formation and reconnection of islanded parts of the power system.
- The method is well suited to automatically adapt to the loss of measurements e.g. due to a communications failure.
- The fault location process is computationally efficient and elegant.
- The protection method is centralised, but only at the cell level. This means that the approach can scale to large power systems, using the WoC concept.

Further research could investigate the following additional enhancements:

- Fully demonstrate operation with missing measurements.
- Demonstrate applicability to distribution systems with highly distributed flexible generation and demand.
- Implementation of communications delays and perform analysis of the impact on trip time.
- Establish how the new fault location methods could be used to enable fault detection, and how this affects protection operation time.
- Utilise per-phase PMU measurements for better fidelity and faulted phase discrimination.
- Test higher PMU reporting rates, e.g. 200 Hz, and investigate the impact on trip time and protection stability.
- Application to cells with multiple voltage levels.
- Operation during multiple or “evolving” faults.
- Further testing of varying load and generation conditions.
- Validate immunity to power swings and phase angle disturbances as highlighted in [98].
- Establish adaptive behaviour i.e. dynamic selection of protection algorithm based on some logic (e.g. current magnitude).

9.6 Accurate PMU Latency Measurement Characterisation

9.6.1 Overview of Method

In real-time protection and control applications involving PMUs, it is essential that measurement and communications latency is minimised, and it is therefore important that latency can be correctly characterised. One of the requirements for PMU performance, as defined in the IEEE C37.118.1a Synchrophasor standard [99], is “reporting latency”. The reporting latency is the time difference between the time of transmission of the first bit of a PMU report message and the timestamp contained in the report. This means that a device with an Ethernet interface which supports hardware timestamping (according to IEEE 1588 [100]), and the accompanying software stack, can be used to very precisely measure reporting latency of a PMU, according to this definition. Figure 9-10 illustrates this method for accurately measuring PMU reporting latency. The software required to implement this is open source and is available at [101].

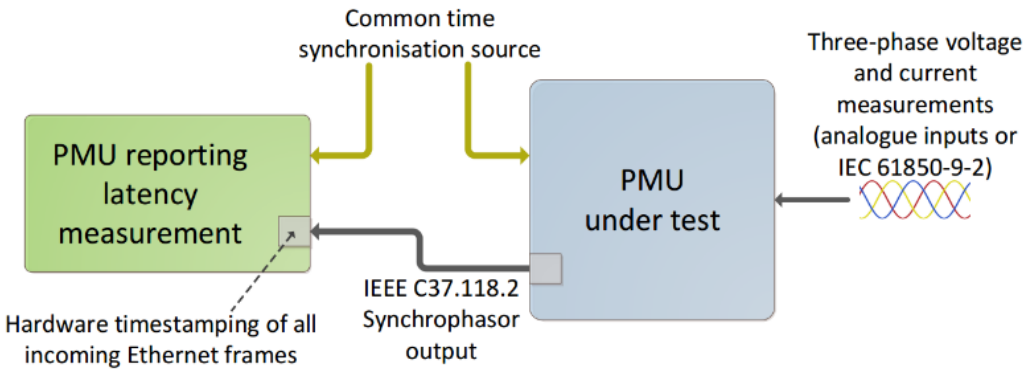

Figure 9-10: Overview of PMU reporting latency measurement method

9.6.2 Application to Wide Area Networks

This approach can also be extended to measuring the total latency perceived when communicating PMU data over wide area networks (WANs) i.e. between substations (but within a cell). Results of measured latency, for an assumed wide area communications network with a mean delay of 11 ms and standard deviation of 2 ms, are given in Figure 9-11. The latency data has been acquired using real laboratory measurement data from P class PMUs whilst using real-time communications network emulation (using the method presented in [102]), resulting in a mean total latency of 32.7 ms (i.e. PMU reporting latency plus communications latency). This information is important for understanding dynamic system behaviour, and for realistically accommodating communications delays within complex power system simulations, as described in the following subsection.

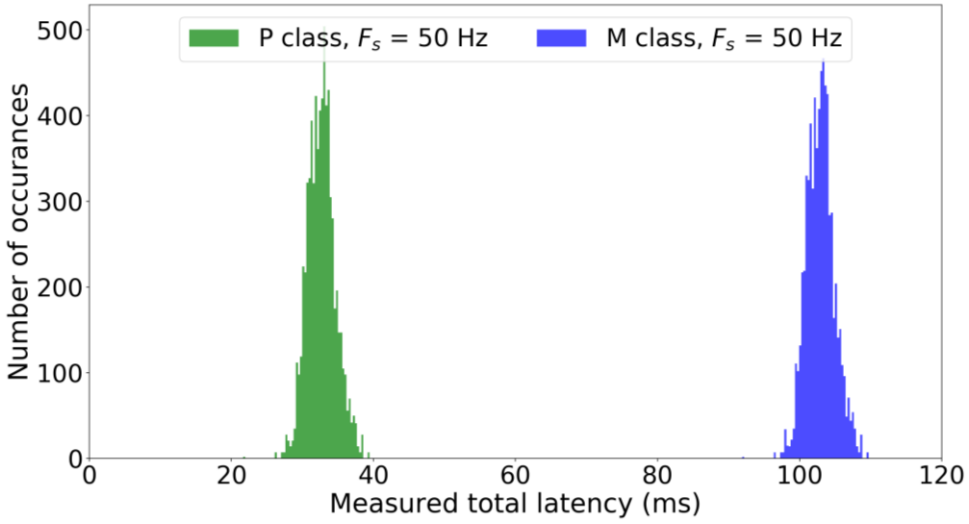

Figure 9-11: PMU WAN latency results

9.6.3 Enhancing the Realism of Large-Scale Power System Simulations

This section demonstrates the practical use of the latency characterization data acquired, as given in Section 9.6.2, to significantly improve the realism of power system simulation studies, whilst also enabling simpler simulation models to be used (and avoiding a complex analytical approach). Figure 9-12 illustrates a hypothetical PMU-based differential protection scheme, where PMU data are transferred over a WAN. Each protection Intelligent Electronic Device (IED) receives local and remote current phasors which are compared according to a typical line differential protection algorithm for a 400 kV transmission system [31]. The objective is to realistically characterise the protection operation (trip) time of this system following a simulated fault, catering for as many factors as possible.

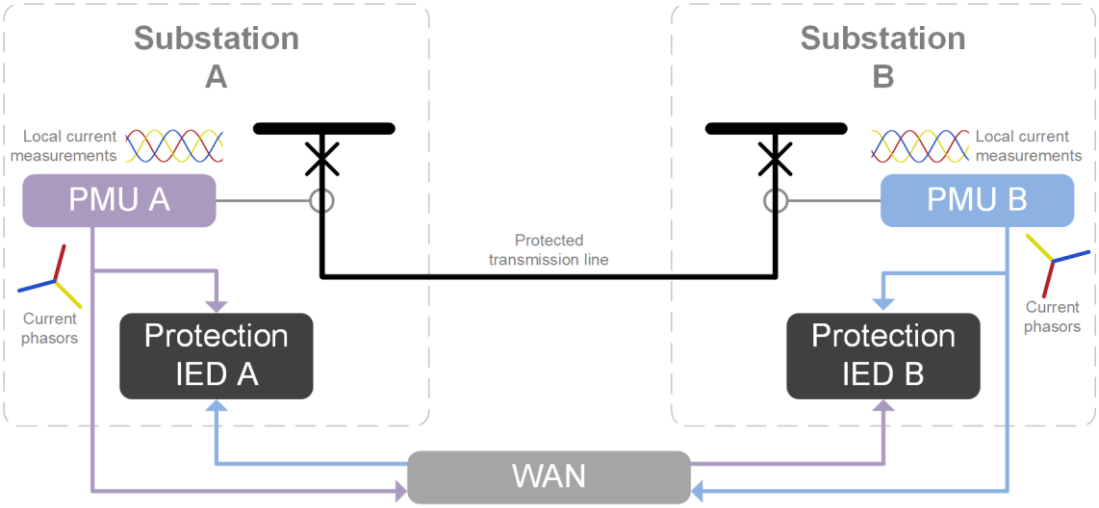

Figure 9-12: Simulated PMU-based differential protection scheme

The power system model and protection IED logic have been implemented in MATLAB Simulink. The use of a phasor-based power system simulation, rather than a detailed transient simulation [103], greatly simplifies the model, reduces execution time, and avoids the need to explicitly implement a PMU algorithm because the simulation intrinsically generates current phasors at each time-step. However, using the simulation phasor data directly for protection or other real-time applications is very unrealistic because it does not incorporate the latency associated with the measurement window of the PMU (i.e. the reporting latency), the reporting rate of the PMU, or communications delays. Therefore, an additional logic block has been added to the simulation to cater for the following:

1. Down-sample the simulation time-step (1 ms) to map to appropriate PMU reporting rates (e.g. 100 or 200 reports per second). This emulates the periodic, packetized nature of the PMU data stream.
2. For the PMU data transferred over the WAN, the data is queued with a random delay to represent the measurement and communications latency (using the data presented in Section 9.6.2). To maintain the original order of data within the queue, the delay applied to a given set of phasors is forced to be greater than that for data already in the queue; this also represents the level of service which can be achieved using modern packet-based WANs [104]. It should be noted that a mean of 11 ms to represent the WAN is significantly larger than would be expected in practice for such a protection scheme for transmission systems, but is less than empirical delays of approximately 40-50 ms from an actual wide area monitoring system, due to relatively low bandwidth links which are shared for other applications [105].
3. Pass the PMU data to the remote Protection IED after the simulation time reaches the computed delay time.

The delay for the local PMU measurements to reach the Protection IED is much smaller than the delay of the remote measurements, and is therefore ignored. The protection algorithm compares local and remote current phasors with the same timestamp, and must “trigger” for three consecutive measurements before a trip is issued. Figure 9-13 illustrates the results for the trip time of the protection scheme, for PMU reporting rates of 100 Hz and 200 Hz, following the initiation of a simulated three-phase short-circuit fault within the protected zone. Due to the stochastic nature of the latency characterisation, the entire simulation is executed for 1000 iterations to provide a distribution of the trip time. The distributions illustrate the combined effects of the PMU reporting period, the random delay to represent the measurement and communications

latency, and the requirement for three trip confirmations. The distributions are skewed, compared to a normal distribution, due to packet order being maintained.

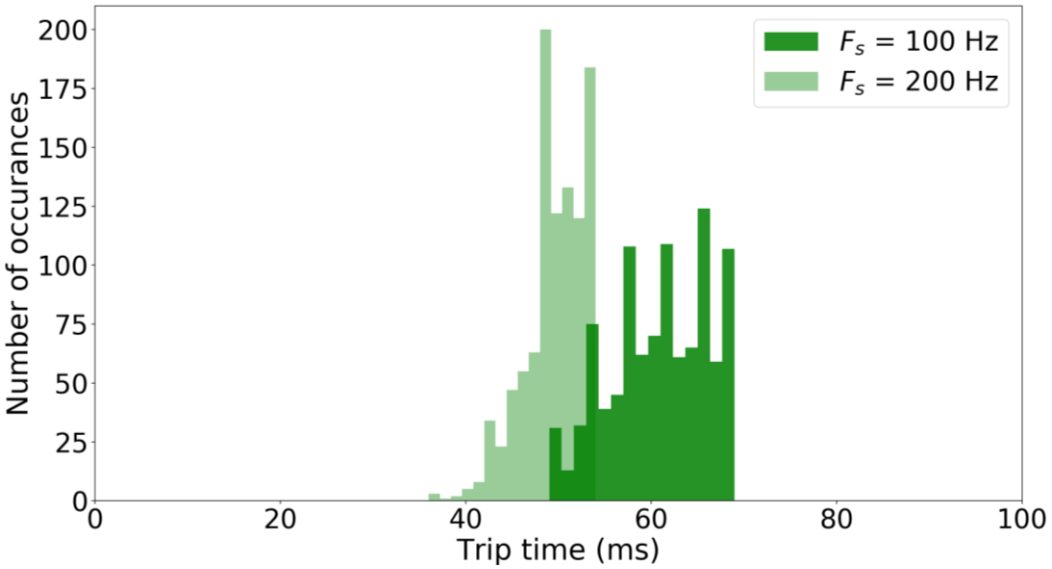

Figure 9-13: Trip time distributions using P class PMU-based protection scheme

Without the emulation of measurement and communications (but still catering for the PMU reporting rate), the simulation would yield a constant trip time of 59 ms (F_s = 100 Hz) or 44 ms (F_s = 200 Hz). Using static parameters may be acceptable for some applications, but for protection schemes it is important to understand the worst-case behaviour. This example therefore demonstrates how the PMU latency measurement method introduced in Section 9.6.1 can be used to create more realistic simulations – informed by actual data – whilst also reducing simulation complexity because phasor-based models can be used. This enables the rapid prototyping and validation of novel control and protection schemes which require authentic representation of power system, measurement, and communications domains.

9.7 Conclusions

This chapter has defined the measurement architecture for wide area protection in the WoC paradigm. A new approach for leveraging the wealth of measurements in future power systems to provide correct and timely supervisory protection functionality has been demonstrated. The key characteristics of the proposed wide area protection approach, in terms for future power systems, are:

1. Resiliency to missing measurements.
2. Adaptability to varying system conditions, such as changes in topology, changes in generation and demand, and changes in inter-cell tie-line flows.
3. Scalability to many measurement locations due to efficient computational design.

This approach therefore has the potential to create a new class of supervisory protection methods.

Timely measurements are critical for addressing many challenges associated with power system operation, such as the increasing requirement for fast-acting reserves to stabilise frequency following a significant system disturbance. This chapter has presented a new method to very accurately and conveniently characterise the latency performance of PMU measurements. The open source software is readily available at [101] for use in further research and development activities. The timing accuracy achieved is typically <500 ns—significantly more accurate and more cost-effective than the method presented in [106] (with accuracy of approximately 600-900 µs). It has also been shown how the proposed method can be used to measure end-to-end latency of

PMU applications in representative wide-area communications networks, and how this information is valuable to improve the realism of cross-domain simulation studies – which is increasingly important for future power systems.

10 Impacts of Short Circuit Faults and Self-Healing Concept on Post Primary Voltage Control Use Case

10.1 Overview

The automated measurement, monitoring, control and communications capabilities of Intelligent Electronic Devices (IED) provide information needed to implement the self-healing concept. This means automated fault identification and location, fault isolation and power restoration. As a result, power outages can be shortened and system reliability improves significantly. IEDs, among other fault indicators, provide preliminary information of fault type, phase and location in the network, but they alone cannot provide the accurate fault position in all cases, because the fault indicators are normally placed in network nodes (i.e. branch points of feeders or pole-mounted substations). Accurate fault location needs calculation methods based on the measurement on substation and network nodes. It is possible to calculate an estimate for the position of a fault. If the faulted feeder has several branches, there are also several possible fault locations. In this case, the remotely-read fault current indicators can complement the fault location process. In applying the self-healing concept, fault location is the most critical task. If accurate knowledge of the fault position is available, the fault isolation and power restoration to the healthy part of the network will be based on conventional opening and closing of network switches (disconnectors and circuit breakers). Due to this fact, the focus of the following investigations is in the location of short circuit faults.

Fault location in the WoC concept network is very challenging, because a significant quantity of distributed generation is connected at the MV and LV levels. Therefore, a novel technique for short circuit fault location in distribution networks is presented in this chapter. The technique computes the fault distance as reactance, based on the measurement of busbar voltages and feeding primary substation currents. The key factor is the compensation of the load currents superposed on the fault current. This leads to high accuracy, which is improved compared to existing methods, and to reduced measurement requirements (i.e. in the conventional networks only one or two measuring device are needed, depending on the number of primary transformers at the substation). In the WoC concept network, the current and voltage measurements are needed from the substation and/or IEDs in the network nodes.

This chapter outlines first the characteristics of the CIGRE model used for simulations of fault location. The fault distance calculation algorithm and simulation results of its accuracy are presented. Impacts of short circuit fault and fault distance calculation on the ELECTRA Post Primary Voltage Control (PPVC) use case are analysed by simulations.

10.2 Characteristics of CIGRE MV Model

The CIGRE MV grid [3] was modelled using MATLAB Simulink, see Figure 5-1. The overall accuracy of the model is close to the given reference results supplied with the model description. Results have been compared to a PowerFactory model to strengthen the trust in the model. This is displayed in Figure 10–1.

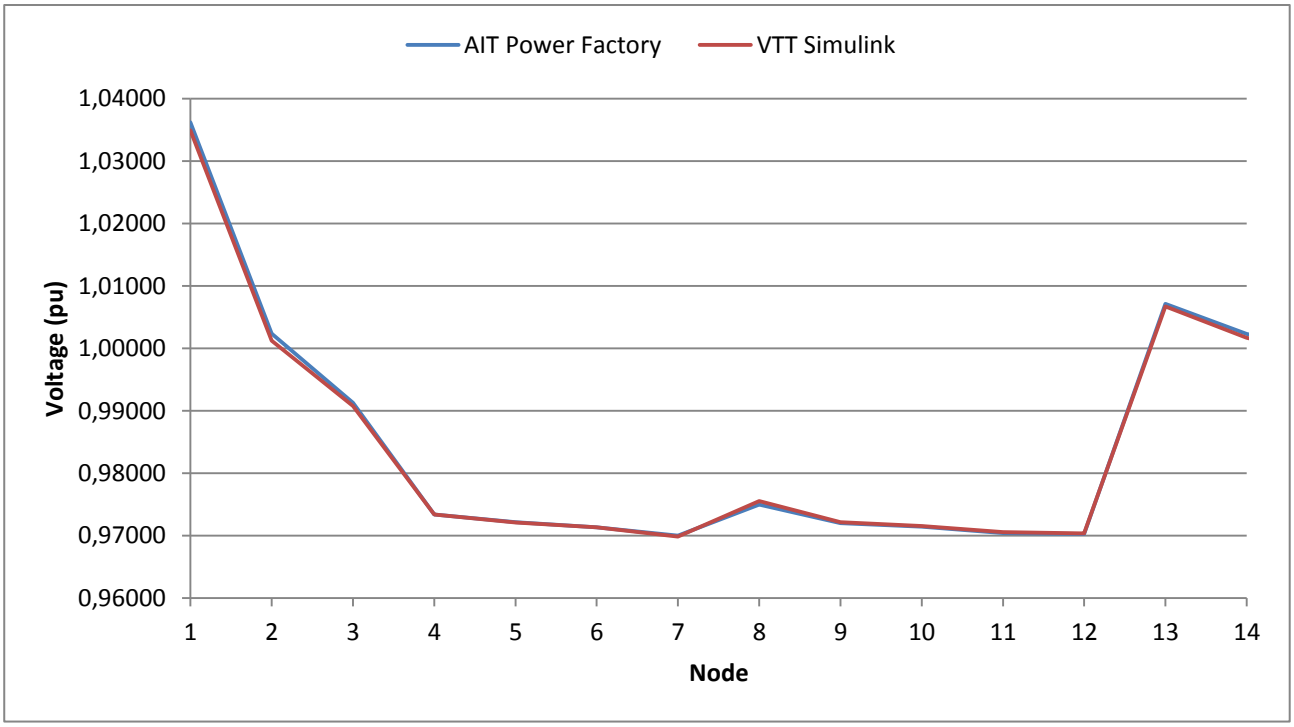

Figure 10–1: Comparison of base simulation case results between Power Factory and Simulink models

The simulation in the Figure 10–1had the load flow values in the nodes displayed in Table 10-1**.**

Node	P (MW)	Q (MVAr)
Node01	19.83900	4.75120
Node02	0.00000	0.00000
Node03	0.50170	0.22538
Node04	0.43165	0.10818
Node05	0.72750	0.18233
Node06	0.54805	0.13735
Node07	0.07650	0.04741
Node08	0.58685	0.14708
Node09	0.57375	0.35558
Node10	0.54330	0.17241
Node11	0.32980	0.08266
Node12	20.01000	4.81000
Node13	0.03400	0.02107
Node14	0.54005	0.27271

Table 10-1: Active and reactive power values in the test

10.3 Fault Distance Calculation Algorithm

The main error source of the reactance-based relays used for fault location is the reactive fault current superposed on the measured fault current. This error is stronger the larger the load of the feeder. However, in this case the measurements are in the primary transformer enclosure, the load current is usually very high, and conventional reactance relay applications are not possible. The configuration of this principle is displayed in Figure 10–2.

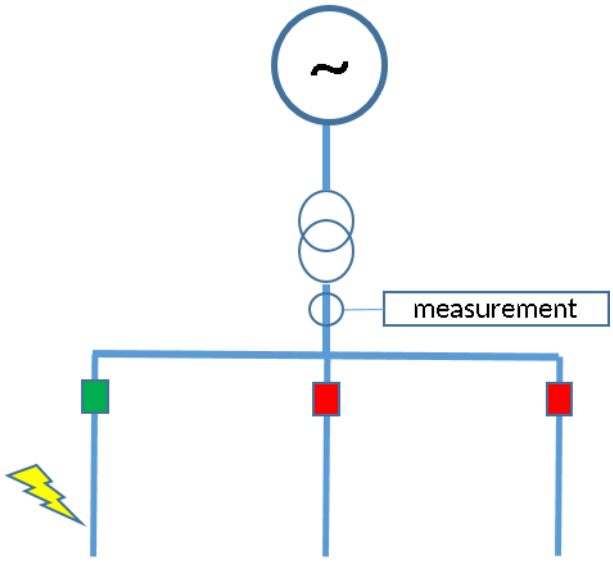

Figure 10–2: Principle picture of grid with the method

The measurement is at the transformer and relays are at each individual line[10]. The faulted line is found by relay activation and distance estimated by the algorithm.

To mitigate the problem of error due to load current, a new fault location algorithm has been developed. The aim is to estimate the load currents from the measured quantities before, during and after the fault, and to make the compensation for the load current superposed on the fault current (written for the case of phases S and T):

$$I_{L2} = I_{sj} - f_{I\_cor\_re} \cdot U_{L23} \cdot f_{I\_re} \cdot I_s - f_{I\_cor\_jl} \cdot U_{L23} \cdot f_{I\_jl} \cdot I_s \quad (3)$$

$$I_{L3} = I_{tj} - f_{I\_cor\_re} \cdot U_{L23} \cdot f_{I\_re} \cdot I_t - f_{I\_cor\_jl} \cdot U_{L23} \cdot f_{I\_jl} \cdot I_t \quad (4)$$

After the load current compensation, the fault distance is computed as reactance as follows:

$$X = \mathrm{Im}\left(\frac{\underline{U}_{sj} - \underline{U}_{tj}}{\underline{I}_{L2} - \underline{I}_{L3}}\right) \quad (5)$$

In the above equations:

- $f_{I_{re}} = \frac{I_{1\_a}}{I_1}$ is the p.u. share of normal state load current flowing in the parallel, sound lines
- f_{I_jl}=*(I1-I1a)/I1* is the p.u. share of normal state load current flowing in the faulty line
- U_{L23}=*($U_{sj} - U_{Tj}$)/(U_s-U_T)* is the p.u. voltage in substation busbar during the fault compared to the voltage before the fault occurred
- $f_{I_cor_re}$is the correction parameter for the compensation of load current flowing into the parallel sound lines during the fault (it depends on load distribution along the lines)
- $f_{I\_cor\_jl}$ is the correction parameter for the compensation of load current flowing into the faulty line during the fault (it depends on the load distribution along the faulty line)
- I_s and I_T are the S- and T-phase currents before the fault

[10] The algorithm is possible also to implement using relays at each feeder. In that case, the calculation algorithm and load current compensation method described in this chapter should be changed. However, if the measurement is in the relay in the transformer feeder, only one relay is needed where the measurement and the calculation algorithm is implemented. Therefore, this is a relatively cheap method to implement in the legacy substation because only one modern relay is needed in order to apply the accurate fault location method.

- I_1 and I_{1_a} are the positive sequence current components before and after the fault has been disconnected
- I_{s_j} and I_{T_j} are the S- and T-phase currents during the fault
- U_s and U_T are the S- and T-phase voltages before the fault
- U_{sj} and U_{Tj} are the S- and T-phase voltages during the fault

The same algorithm is used for both two and three phase faults. In the latter case, Equations (3) and (4) are applied to the two phases with the highest current. This arrangement minimises the effect of the possible power arc, since in the phases with highest current, the fault resistance must be at its smallest.

The algorithm works using the measurements obtained from the primary substation infeeding compartment and/or IEDs in the network nodes. The problem with the superposed load current is that its magnitude is changed dynamically with the voltage change during the fault. For the load behaviour, the following theoretical models have been developed in [107]. These models can be used for load current compensation: $P/P_j=(U/U_j)^{Pu}$ and $Q/Q_j=(U/U_j)^{Qu}$, where U and U_j are voltage before and during the fault, P and P_j are the corresponding power and Q and Q_j corresponding reactive power, respectively, and P_u and Q_u are the parameters that model the voltage dependency magnitude. The parameters P_u and Q_u vary with load type and time. According to the measurements made in distribution networks, the values are within the range P_u = 1.5 … 2.0. and Q_u = 2.0 … 6.0. The key point is to make the compensation separately for the load current of the parallel healthy (unfaulted) lines and for the load current flowing during the fault in the faulted line. For defining the correction parameters ($f_{I\_cor\_re}$ and $f_{I\_cor\_jl}$) the voltage used for load current estimation is in the case of parallel lines the voltage measured in the substation busbar. In the case of estimating the load current in the faulted line, a lower voltage value has been assumed. Typically this is, when the load current is assumed to be equally divided along the line, about 50% of the voltage in the busbar.

In a nutshell, the algorithm is implemented as follows:

1. The relay at the infeed measurement location records phase currents and phase voltages on a continuous basis. Line voltage is used as a phase angle reference.
2. The fault distance computation is initiated by the tripping of a feeder circuit breaker due to a fault.
3. The phase currents and phase voltages are registered in three steps: before the fault, during the fault and after the faulty feeder circuit breaker was opened.
4. The quantities during the fault are computed as three cycle mean values with the corresponding statistical deviations. These values are computed in a moving time window over several sample sets. The sample set with the smallest deviation is taken as a basis for fault distance estimation.
5. The two phases with the biggest fault current are selected.
6. The load currents during the fault are compensated for using Equations (3) and (4).
7. The faulty line length reactance is computed using the model of Equation (5).
8. The computation result is compared to the line reactances and it is possible to be shown within the network map of the distribution management system (DMS).

Since the method is able to give only the distance from the substation to the fault or from node point to fault (as a reactance value), usually several possible fault locations are obtained, in the different line branches. The actual fault location applied in self-healing concept must be found among these candidate locations by complementing the distance estimations with information from distributed fault indicators.

10.3.1 Distance Calculation Results

The fault distance calculation error remains quite small until the transformer acts nonlinear near the nominal capacity of the transformer. This is presented in Figure 10–3.

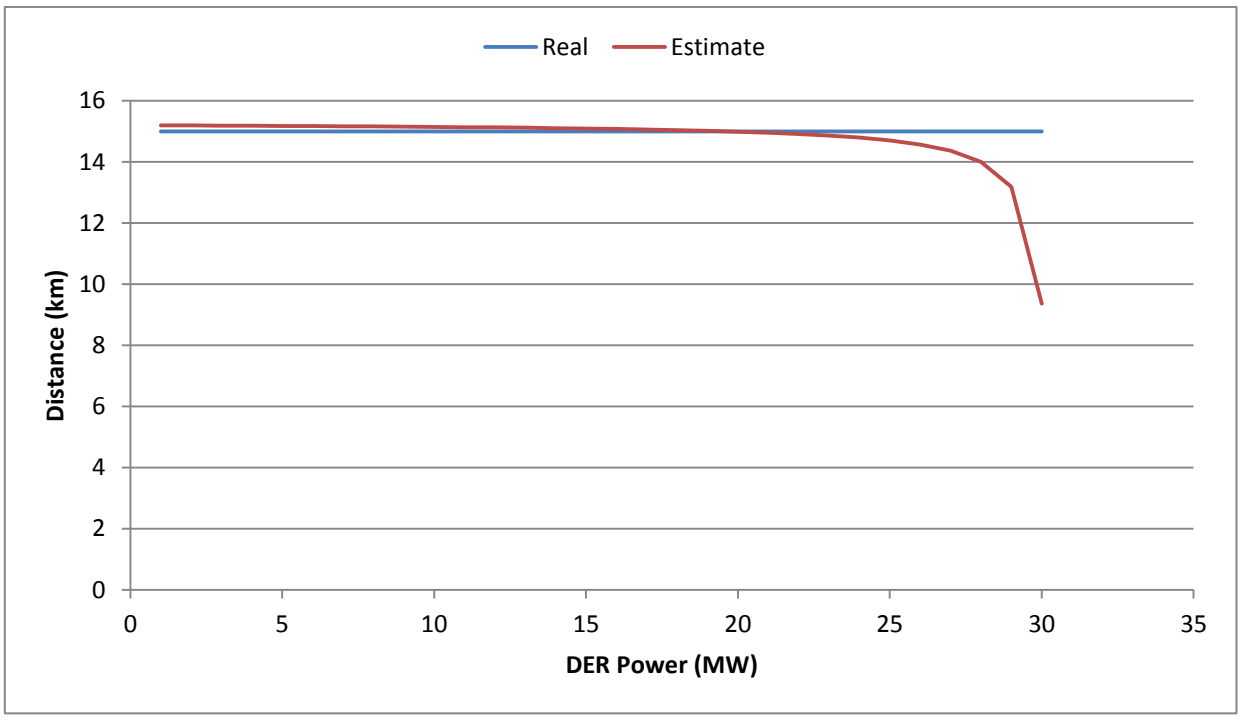

Figure 10–3: Calculation results with respect to DER production in feeder before the fault location

Calculation accuracy holds until 25 MW generation. This is, however, maximum power that the feeder transformer can take so in this case the algorithm works well even with the maximum feasible DER.

The actual fault distance has smaller effect on accuracy than DER if the system is calibrated to the grid model (i.e. measurements from the grid have been used to verify the model). This is presented in Figure 10–4.

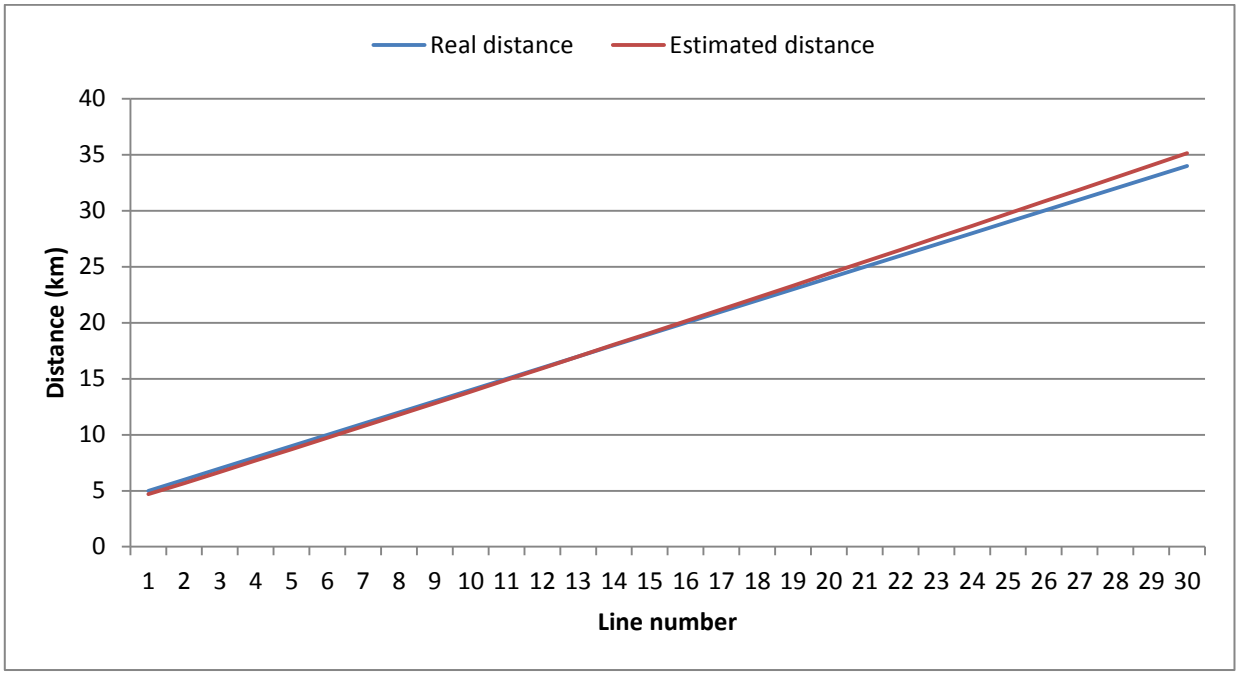

Figure 10–4: Estimation accuracy in simulation respect to distance of the fault

10.4 Fault Distance Calculation with Post Primary Voltage Control

The idea behind this study is to investigate how fault simulation and distance calculation method affects operation of the PPVC use case[11]. For this reason use case simulations within the ELECTRA project are combined to identify possible problems unseen in individual studies.

10.4.1 Post Primary Voltage Control Description

PPVC is a method of optimal voltage control for future electrical grids considering the WoC concept [108], [109]. The main point is to utilize DER as an active component in voltage control using reactive power injection. The DER units have differing degrees of reactive power capacity and this depends on active power production. For solar panels with PV inverters, this means less reactive power capacity the stronger the sun shines. Control settings are calculated with an optimal power flow algorithm, which is an external component from the main simulation model, which has been created in MATLAB/Simulink. This section describes the result for combined simulation of fault case with distance calculation.

10.4.2 Optimal Power Flow Algorithm

Load flow and optimization models have been utilised using Pandapower, which is built using PYPOWER (which is the MATPOWER tool converted to Python). MATLAB/Simulink is emulating the actual grid (transient model) opposed to Pandapower (optimum powerflow), which represents the grid model. Pandapower is used in optimisation of the control and control signals of which are given to the Simulink model. Components and principal data directions are presented in Figure 10–5.

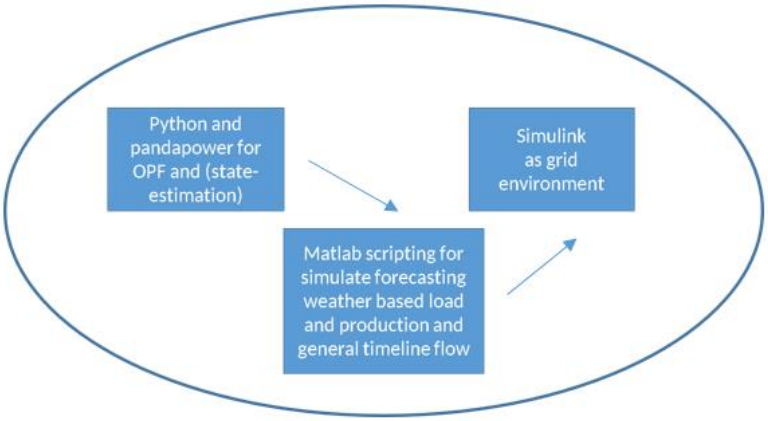

Figure 10–5: Components in simulation environment

Forecasting is determined based on the weather forecast data used in load and generation forecast as simple functions. Simulations were conducted using an arbitrary dataset but meteorological data for Europe can be acquired free of charge from Finnish Meteorological Institute's website [110]. The interior point method is applied with PIPS (a Python package) [111].

Optimal power follow problem can be described by:

$$min \sum_{i \epsilon gen,extgrid} \boldsymbol{P_i} \cdot \boldsymbol{f_i}(\boldsymbol{P_i}) \qquad (6)$$

[11] Note that the inverse is not a concern i.e. PPVC operation does not affect the distance calculation.

Which means minimum of the sum of all generation in the system (external grid and generators), subject to the following:

- loadflow equations
- branch constraints
- bus constraints
- operational power constraints
- Where,
    - gen=generators
    - extgrid=external grid

A detailed explanation of the algorithm is available at Pandapower documentation [112].

Since the OPF function is not capable of controlling tap changers, a loop of trial error type for the method is built on the top of OPF function. In principal, the program code is structured as follows:

```
"For loop" (array of tapchanger positions to try)
            OPF-function(tap changer value)
            Append result to array()
End
Select the best result from the array.
```

In this way, the OPF is evaluated for all feasible positions of the tap changers. The solution with the lowest active power losses is selected as the final result.

10.4.3 PPVC with Fault Simulation Results

If there is a fault and part of the grid is disconnected, the optimization results of remaining cells give incorrect results to varying degree (i.e. losses are higher). Voltage results are displayed in Figure 10–6.

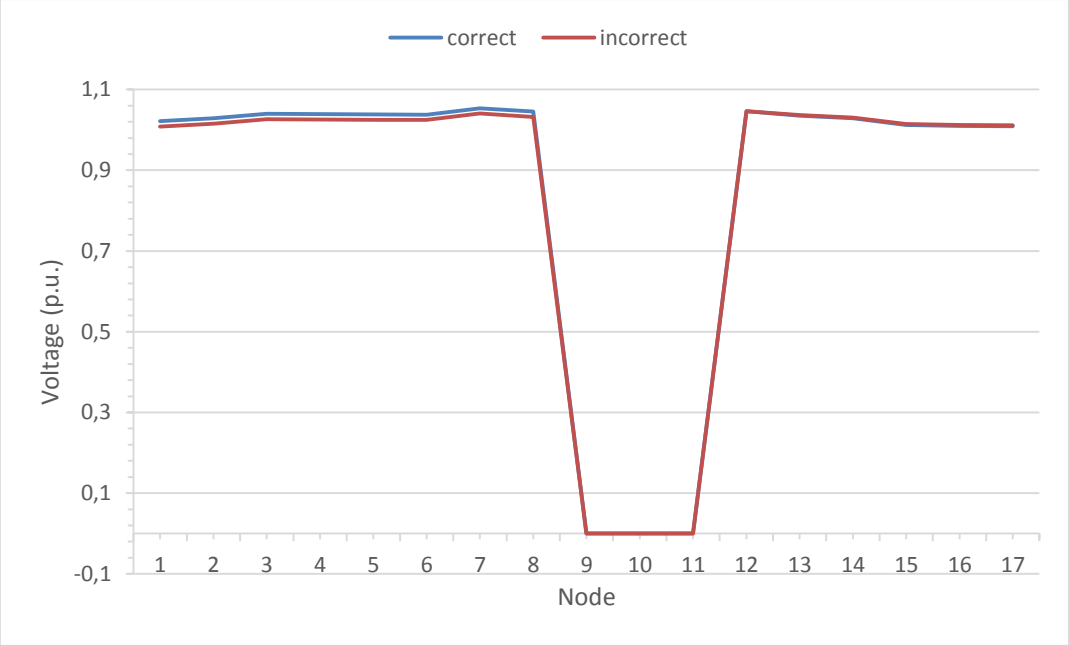

Figure 10–6: Voltage results with fault area separated

In Figure 10–6, the separated area and nodes are from 9 to 11. These nodes are marked as zero voltage. The blue line in the figure is the correct grid simulation meaning that grid model is updated and calculated again with new data. Voltage is lower than assumed if the grid model is not updated for the new situation. Nodes from 12 to 17 are on a separate feeder and the calculation result is unaffected. Losses are also higher but losses are irrelevant in fault situation where safe operation is the first priority. PPVC itself has no impact on the fault location. PPVC will be affected if the grid configuration following fault separation is not changed. This should be taken into account even in the cell method, if the calculation cells are not same as areas that can be disconnected. This means the grid model needs to reflect the new changed situation in grid configuration. If the grid model is updated after a part is disconnected, PPVC will work just as well as before the fault.

11 Fault Detection and Classification for the WoC Concept

11.1 Introduction

System operators need to deal with high impedance fault detection (HIF) in electricity grids that can lead to serious safety hazard or fire. These faults are usually produced as a consequence of a conductor getting into contact with a tree, falling to ground or, in general, when any conductor enters into contact with a high impedance surface. However, HIF detection has been a traditionally persistent problem to address, because the overcurrent values produced are typically not large enough to be detectable by normal overcurrent protection schemes.

An important characteristic of the voltage and current waveforms as a consequence of HIFs is they are highly non-linear and intermittent as a result of the electrical arcs produced. As these faults are difficult to detect, there are no exact records by the utilities, which could provide a real estimation value of the percentage of HIF existing in the electrical grids. This detection of HIF is a problem that has been explored in the recent years and many methods have been considered to solve it [113]–[116]. Despite this, a highly trustable and definitive method to detect these faults is still missing. Trying to take advantage of the harmonic characteristics of the waveforms, conventional methods to detect HIF have been based on the direct measurement of voltage and current waveforms, the latter decomposition in the harmonic spectra and the evaluation of certain harmonic components (or combination of several harmonics). However, it is difficult to find the critical harmonics that simplify the detection process clearly distinguishing between the fault and no fault conditions and thus, the analysis based on the frequency domain can lead to false trips of the protection systems. The progresses in the signal processing techniques have allowed the use of novel approaches for the detection of the HIFs. Recently, the exploration of the use of Fuzzy Logic (FL) and Artificial Intelligence methods, such as the use of Artificial Neural Networks (ANN) have been explored. Even both FL and ANN have demonstrated to be effective in the detection of the fault type the time needed for training the algorithms is high. Considering the expected reconfiguration capabilities expected for the WoC, this poses a serious drawback.

In order to overcome all these issues in other detection techniques, the wavelet transform (WT) has been raised as a powerful tool to detect and classify the faults in a fast way in distribution grids. The WT has the advantage to represent the faulted signal in both the time and frequency domains, extending the capabilities of Fourier transforms, that can detect the different peaks in the frequencies of a signal but not the time where these peaks where reached. If taking into consideration, as previously mentioned, that HIFs are highly non-linear with intermittencies and arcs, a very important part of the information would be lost if simply considering a frequency-domain analysis. The application of the WT could be assimilated to the process to sequentially apply filters in order to detect the frequencies of the signal. Even the possibility to detect also low impedance faults (LIF) is also feasible with WT, its detection is not so interesting because LIFs are more easily detectable by the normal overcurrent relays than HIFs.

11.2 Methodology

When applying the WT for the detection of HIFs, the signal needs to be analysed in order to detect the useful information contained within it. Due to this, it can be considered, in general, that the application of the WT to a signal can be split into three main subprocesses [117]:

1. Denoising
2. Signal decomposition
3. Information extraction

Denoising is a preprocessing step required to eliminate the distortion that could have been produced in the signal as a consequence of network switching events, events in nearby grid nodes, etc. In general, distortions they are not linked to the fault itself.

The decomposition is done to get the approximation (A_j) and detailed coefficients (D_j). The detailed coefficients are those low-scale, high-frequency components of the signal produced by filtering the signal with a high-pass filters. The other way round, the approximation coefficients would come up as a result of filtering the signal with low-pass filters. Thus, the signal can be decomposed into several signals, as shown in Figure 11-1.

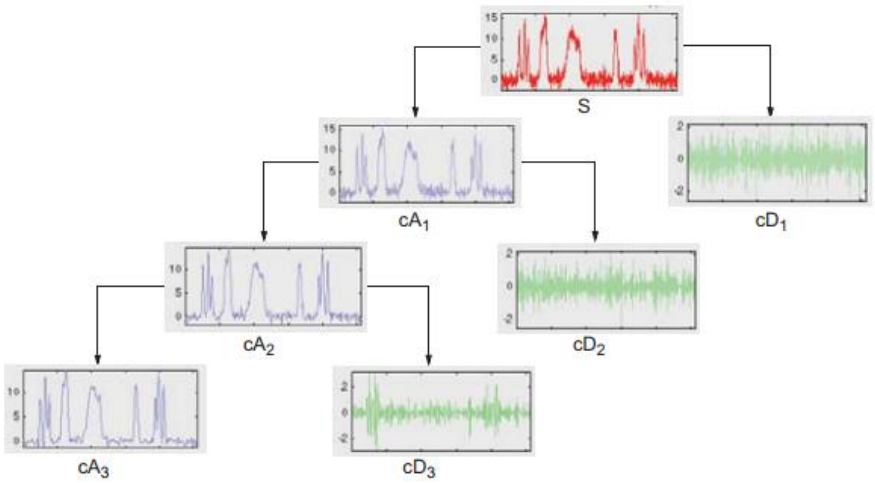

Figure 11-1: Wavelet decomposition [118]

This way, given a discrete signal x(n), it can be written as the sum of waveforms that result from the subsequent application of high frequency and low frequency filters by using the discrete wavelet transform as shown in Equation (7):

$$x(n) = A_J(n) + \sum_{j=1}^{J} D_j(n) \quad (7)$$

where the frequency band of the information contained in the signal components, detailed and approximate coefficients, are calculated for a certain time instant k at a scale j, as displayed in Equation (8) and Equation (9). The sampling frequency of the original signal is f_s.

$$D_j(k) = \left[2^{-(j+1)} f_s, 2^{-j} f_s\right] \qquad j = 1,2 \dots m \quad (8)$$

$$A_j(k) = \left[0, 2^{-(j+1)} f_s\right] \quad (9)$$

The later stage comprises the information extraction from the wavelet decomposition. Many possibilities have also been explored in the use of certain magnitudes, such as the entropy or the energy of the wavelet decomposition in order to classify the fault. In [119] the classification of the fault type has been accomplished by using the percentage energy level at highest approximation level (Daubechies 5 level 4) together with the maximum threshold using remove near zero method of compressed signal has been employed [120]. The threshold is used to compare the coefficients received in the decomposition and discard all those that are below that certain threshold (denoise

the signal). The near-zero methods ensure all the coefficients that are not significant for analysing the information in the current of the faults are not considered. The retained energy represents the percentage of the original signal that remains after the denoising process. The method proposed in [120] is suitable for the detection of LIFs, but its employment in HIFs detection is unclear, since it needs a noticeable change in the current to reflect a change in the maximum threshold using remove near zero magnitude. Otherwise, the use of the ratio between the maximum threshold calculated in disturbed conditions over the maximum threshold in normal state as detecting magnitude can lead to false trips. The feasibility of this method for the fault detection in a single-cell, which has been considered of interest within ELECTRA. The test grid is the CIGRE MV grid modified with distributed energy resources (i.e. wind, PV, fuel cells, and batteries) that has been previously shown in Chapter 6). The results from the application of a single-line fault in phase A in Node 08 (R_f =10 Ω) are shown in Table 11-1 for demonstrative purpose. Node 08 has been selected as a representative node for the explanation of the methodology. The second column (normal operation) represents the reference pattern in a normal operating state with no fault that is used to detect the fault by comparison with it.

		Normal operation	Single-line ground fault
Retained energy (%)	I_A	99.94	99.93
	I_B	99.96	99.95
	I_C	99.98	99.94
Maximum threshold	I_A	2.40	2.76
	I_B	2.23	2.31
	I_C	2.15	2.20
Threshold ratio	I_A	1.00	**1.15**
	I_B	1.00	1.03
	I_C	1.00	1.02

Table 11-1: Results for the single-line ground fault in Node 08

It can be observed from the previous results in Table 11-1 that the threshold ratio (the relationship between the maximum threshold calculated in disturbed conditions over the maximum threshold in the no fault case in the current of phases B and C) is almost close to one while ratio regarding the current in Phase A increases. Even the ratio in phase A is different from the ratio in the other two phases, its value is not big enough to be considered as decisive and the application of the algorithm can produce false trips of the protections. The method was validated into a simple grid with a large synchronous generator but the method in a more complex grid, and thus, for the expected WoC is not useful, because the differences between disturbed and undisturbed conditions are not large enough to be used as discrimination criteria for setting the relay trip threshold.

Another application of the wavelet transform to identify the fault type in the CIGRE MV grid has already been explored in [121]. However, the grid tested is the original CIGRE model where there is a lack of distributed generation. The massive presence of distributed generation is constituent of the WoC so exploring other approaches for the detection of faults in grids with a high penetration ratio is essential. The WT decompositions are highly dependent on the grid topology and the conditions defining the normal operation of the power system (reference pattern). The application of the methodology in [121] has been demonstrated to be invalid for the modified grid of interest in

ELECTRA including high penetration ratio of distributed resources; this is because the use of the absolute value of all entropies makes complicated the establishment of the tripping threshold. The method considers the absolute entropy of the wavelet coefficients for both the phase currents and the currents in αβ0 framework (after the use of Clarke transformation). However, this methodology, even not valid as it is for the example of interest, can lead the way to the development of an ad-hoc methodology for detecting the faults in the WoC context. In this work, a specific method based in wavelet transform has been applied and tested over the modified European CIGRE MV grid with DERs. The absolute value of the entropy of the D_1 coefficient of the current of the phases and the zero sequence component of the current (I_0) have been selected as magnitudes of interest. The zero sequence current is essential to detect the unbalanced faults. As the wavelet transform can be considered as a sequential application of high pass filter to a signal, the detailed coefficients are those more representative of the high-frequency transient phenomena linked to the short-circuit events. In the application example selected for demonstrating the validity of the methodology within the WoC, the analysis method selected for the Wavelet decomposition has been the Daubechies 5 up to level 4 decomposition. The entropy of the signal is a useful magnitude for the measurement of the order/disorder of a signal and provides relevant information about the dynamics. From all the possible methods to calculate the entropy of a signal that can be found in the technical literature [122] the Shannon approach have been chosen. The non-normalized Shannon entropy can be calculated as shown in Equation (10):

$$H_j = -\sum_k E_{jk} \cdot \ln E_{jk} \quad \textbf{(10)}$$

where E_{jk} is the wavelet energy at different scales.

11.3 Simulation Results

In order to test and validate the proposed method for detecting and classifying faults, Single-line (AG/BG/CG), phase-to-phase (AB/BC/AC), phase-to-phase to ground (ABG,BCG,ACG) and three-phase (ABC/ABCG) HIF faults have been simulated in one representative node of the cell: Node 08 (R_f =10 Ω). Results have been evaluated with the use of the MATLAB Wavelet Toolbox. For any case, the comparison of the wavelet absolute entropy of the D_1 coefficient in the current of the phases and for the zero sequence current are compared with the reference values of the normal operation condition.

11.3.1 Normal Operation

As an example, the wavelet decomposition for the current in phase A (I_A) and the current I_0 is shown in Figure 11–2.

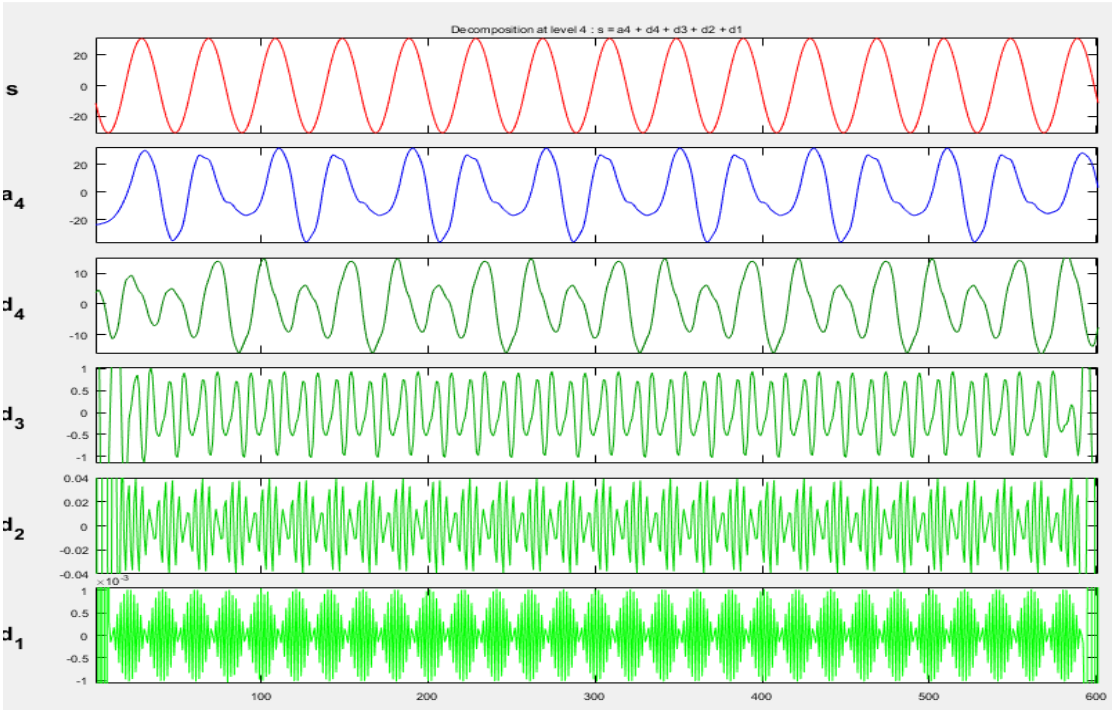

(a)

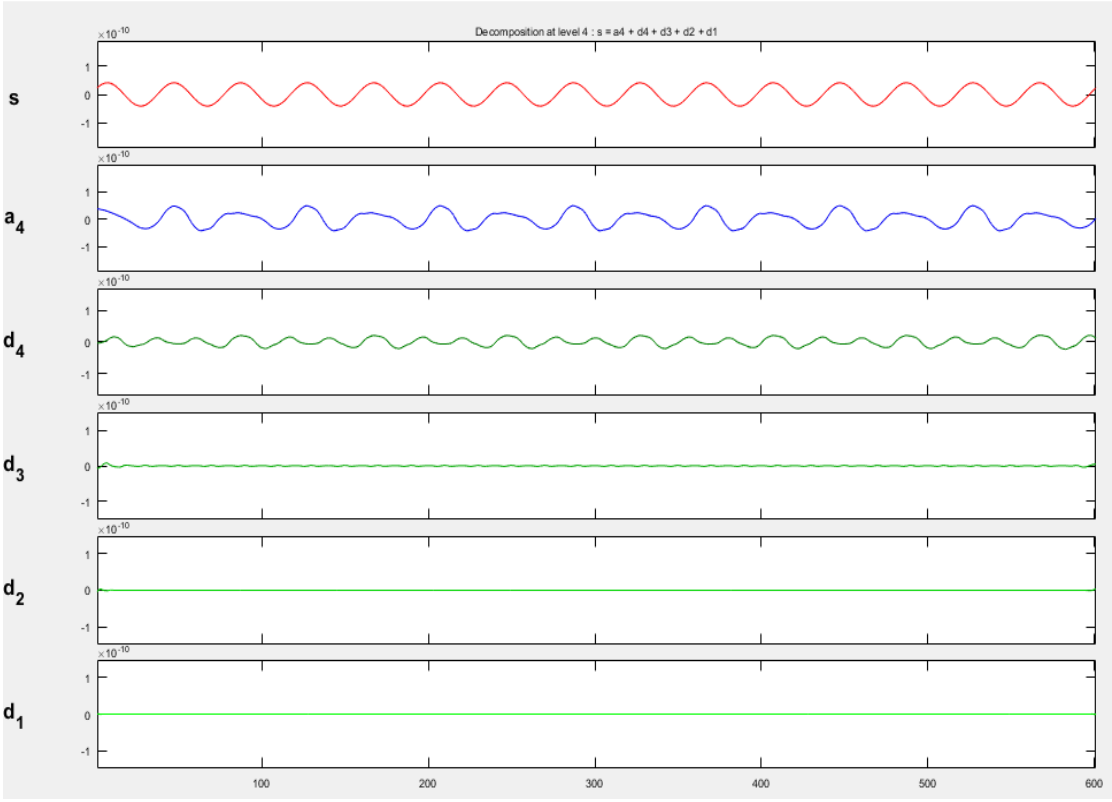

(b)

Figure 11–2: (a) Wavelet decomposition of current I_A. (b) Wavelet decomposition of zero sequence current I_0.

Even with a simple visual analysis, it can be observed that the values of D1 coefficients are low and thus, the absolute value of the entropy calculated in these conditions will also be low. The

summary of the calculations of the entropy in the normal operating conditions is shown in Table 11-2. These will constitute the reference values for the no-fault case.

Entropy	
I_A	1.540
I_B	0.144
I_C	1.326
I_0	0.000

Table 11-2: Absolute value of entropy of D1 coefficients for normal operation conditions

11.3.2 Line to Ground Faults

In Figure 11–3, the currents measured by the relay in Node 08 are plotted.

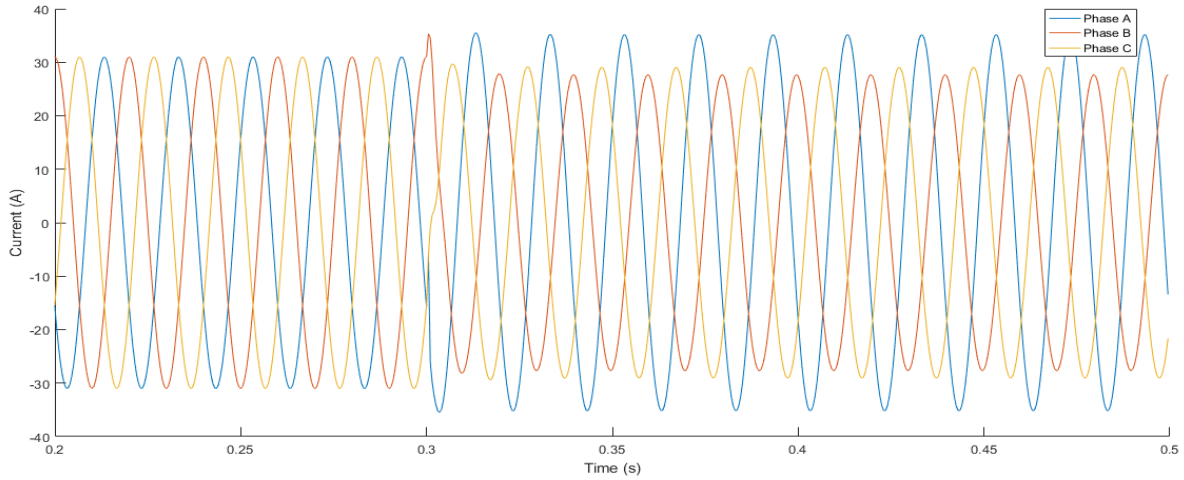

Figure 11–3: Currents measured in case of AG fault

As an example, it has been represented in Figure 11–3 it the Definite Time (DTM) relay curves for one of the alternatives of adaptive protection scheme for the WoC (see Chapter 6) for the same AG fault with high impedance in Node 08. The curve shows in the x-axis the value of the measured current and in y-axis the tripping time for the fault. It can be clearly seen that, according to the classical overcurrent curves, the overcurrent relays would not trip for the fault in an acceptable time, not even the relay closer to the fault (R08). In this case, the overcurrent value in the faulted phase is less than 20% greater than the rated current. This means that, according to the curves, the thermal-magnetic circuit breaker associated tripping time would be in the order of hundreds of seconds, endangering the safety of people close to the installation. However, the implementation of a backup protection functionality in the relay based on the proposed wavelet decomposition would have been able to detect the HIF, improving the capabilities of the protection scheme.

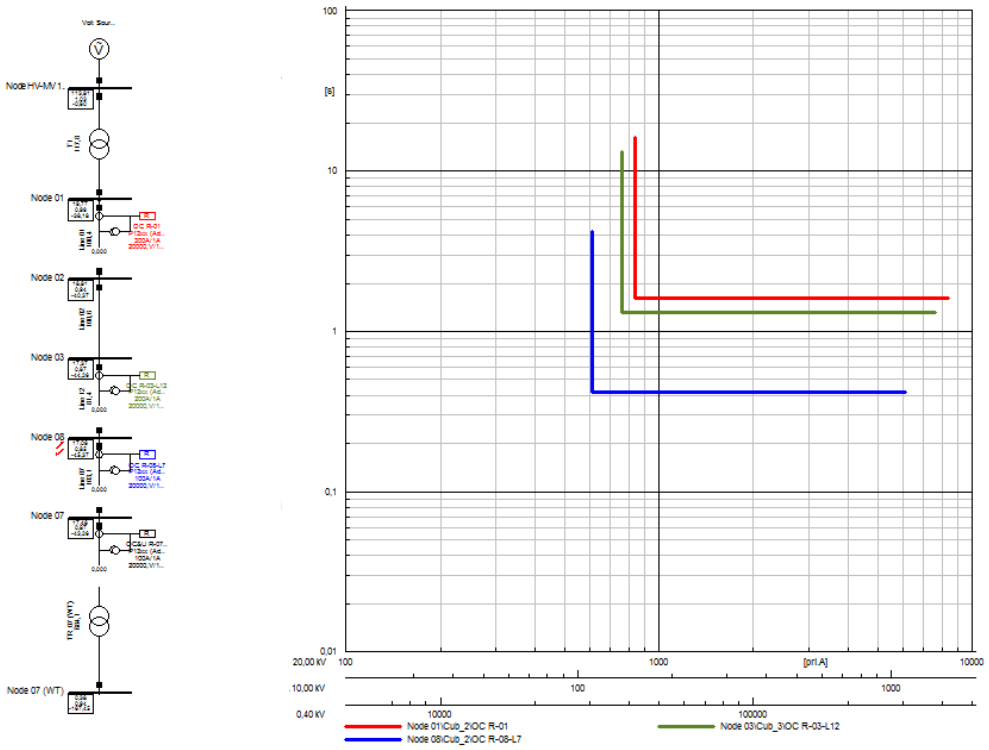

Figure 11–4: Tripping curves for the R08 relay

The wavelet decomposition for the faulted phase A (I_A) and the current I_0 is shown in Figure 11–5a and Figure 11–5b.

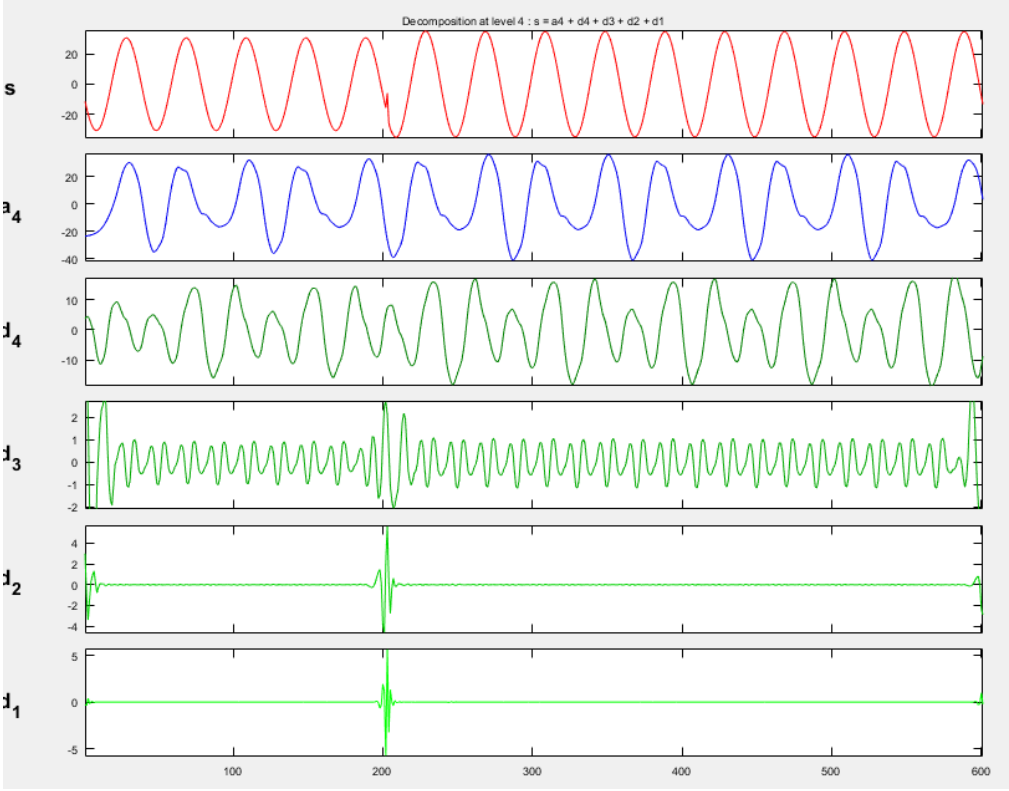

(a)

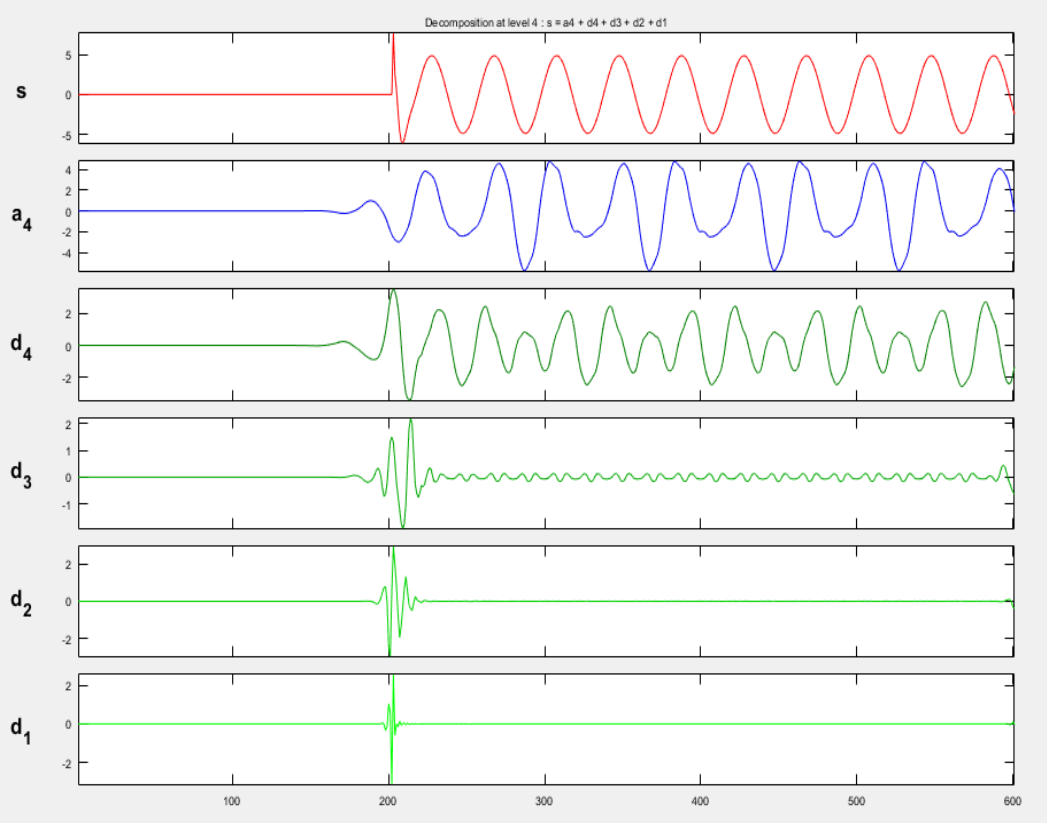

(b)

Figure 11–5: (a) Wavelet decomposition of currents I_A. (b) Wavelet decomposition of current I_0.

The summary results for the single-phase faults in the system are shown in Table 11-3.

Entropy \ Fault type	AG	BG	CG
I_A	**236.51**	2.73	8.37
I_B	1.15	**114.51**	10.13
I_C	0.16	2.43	**689.00**
I_0	**32.96**	**21.00**	**156.00**

Table 11-3: Absolute value of entropy of D1 coefficients for normal operation conditions

It can be seen that the faulted phase and the zero sequence current have a value of entropy that is noticeably larger than the value of the entropy of the current in the other phases, what is useful to detect what type of fault has occurred (single-phase to ground) and the affected phase.

11.3.3 Phase to Phase Faults

Results from the phase to phase and phase-to-phase to ground faults are summarized Table 11-4 and Table 11-5, where the faulted phases are also easily detectable by the increase in the entropy value.

Entropy \ Fault type	AB	BC	AC
I_A	**435.28**	0.53	**601.56**
I_B	**492.98**	**451.31**	1.57
I_C	0.97	**450.07**	**600.37**
I_0	1.63e-07	6.03e-07	3.20e-07

Table 11-4: Absolute value of entropy of D1 coefficients for phase to phase faults.

Entropy \ Fault type	ABG	BCG	ACG
I_A	**163.86**	2.08	**292.74**
I_B	**156.48**	**157.50**	3.11
I_C	2.90	**922.90**	**143.50**
I_0	**52.27**	**35.35**	**47.04**

Table 11-5: Absolute value of entropy of D1 coefficients for phase to phase to ground faults.

11.3.4 Three-Phase Faults

Results for the three-phase faults are summarized in Table 11-6.

Entropy \ Fault type	ABC
I_A	**284.80**
I_B	**112.46**
I_C	**1073.33**
I_0	0.00

Table 11-6: Absolute value of entropy of D1 coefficients for phase to phase faults.

As the system is balanced, in this specific topology the results concerning the case ABC-G are equal to those for the ABC case, because there is no zero sequence current flowing by the neutral conductor. However, as has been tested in the other unbalanced faults, the methodology can be easily extendable. It can be concluded that remarkable differences in the entropy of the D1 coefficient can be detected in case of faults. If there is a noticeable presence of entropy in the I_0 component, it is clear that the fault is grounded. According to the results of the simulations, the tripping thresholds could be settled in values of entropy in values around 100 for the phase currents and over 10 for the zero sequence current.

11.4 Conclusions

In this chapter, a methodology based on the use of the absolute value of the entropy for the D_1 coefficient of the wavelet transform, for the phase and zero sequence currents has been tested and validated. It has been applied to a single cell of the WoC that has been considered in other research developments within the ELECTRA project (i.e. the European CIGRE MV grid with distributed resources). From the results, it can be derived that the differences in the absolute value of the D_1 entropy between the faulted and non-faulted phases are very sharp, with differences of approximately a factor of 100 for the current in the phases compared with the values of the entropy with no fault. This simplifies the settlement of tripping thresholds that can be useful to complement

the standard protection schemes with an extra functionality for HIF that would be in the non-detection zone of the overcurrent relays. According to the WoC concept, the internal reconfiguration capabilities of the single cells are not foreseen often, even some reconfiguration capabilities at a WoC level are expected. The possibilities of getting different normal operating patterns to compare with the faulted patterns at a low computational cost makes this wavelet detection techniques of special interest for the future WoC, because the different thresholds for the different configurations can be easily calculated for the relays.

12 Conclusions and Recommendations

12.1 Summary of Major Achievements

This report has provided guidance for the key areas of protection research that will underpin the realisation of stable and efficient future power systems, particularly considering the proposed ELECTRA Web of Cells (WoC) control architecture.

It has been shown how distribution protection can be adapted in real-time to take advantage of additional measurements and communications to counter the impact of highly-distributed generation connected at MV and LV, and to optimise protection operation times. The adaptive overcurrent protection methods studied for both single cell and multi-cell networks ensures reliable network protection for high DER penetrations and islanded operation. Therefore, the safety margin of network components can be increased and some coordination problems due to the presence of DER can be mitigated. Additionally, it has been indicated that the central controller of a cell can successfully provide the proposed adaptive protection scheme combined with Post Primary Voltage Control (PPVC) operation.

Structured data sources, such as the Common Information Model (CIM) and IEC 61850 configuration files, provide opportunities for automated creation of power system control and protection systems, and it has been shown how such self-organising capabilities can be applied to the WoC concept. Moreover, the subdivision of a power system into a potentially large number of cells raises important interoperability requirements, which can be effectively tackled by the implementation of standardized communication protocols and data models.

The importance of fault ride through (FRT) functionality, considering large-scale deployment of wind energy, has been demonstrated. It has been shown that Primary Voltage Control (PVC) must be carefully coordinated with FRT control to ensure stability, due to the similar timescales of operation.

An elegant wide area protection implementation, leveraging the wealth of measurements in future power systems to provide correct and timely supervisory protection functionality, has been demonstrated. The key characteristics of the proposed approach are: 1) resiliency to missing measurements, 2) adaptability to varying system conditions, such as changes in topology, changes in generation and demand, and changes in tie-line flows, and 3) scalability to many measurement locations due to efficient computational design. The WoC architecture provides a convenient division of a large grid into smaller areas that can accommodate the low-latency requirements of wide area protection; the corresponding wide area protection scheme architecture for the WoC, including protection of tie-lines, has been proposed.

It has been shown how the end-to-end latency of PMU measurements can be characterised, and how this information can be exploited to enable a new class of realistic, but efficient, cross-domain simulations. This is important for validating and realising distributed control of power systems that fundamentally depend on communications.

A new method for efficient and accurate fault location, which is suitable for use with distribution systems with a high penetration of renewable energy sources and long rural overhead lines, has been developed and presented. This is important to enable self-healing systems, and it has been shown that PPVC can be negatively impacted if internal system models are not correctly updated for automation and restoration processes.

The prevalence of renewable energy sources, connected to the grid via power electronic converters and enabling the flexibility required for distributed control, will fundamentally change the

voltage and current waveforms measured during disturbances such as faults, and conventional assumptions used for protection settings and coordination can no longer be used. It has been shown how the wavelet transform can be used to detect and characterise faults, and provide a new type of fault indicator, particularly for high-impedance faults.

In summary, based on the simulations in this report, the impact of disturbances on voltage control is typically minor and local, particularly if the faulted part of the feeder can be separated quickly and supply be restored to the remaining part of the network. This may require reconfiguration of the cell network. In particular, the simulations showed that the developed control functions for PPVC operated as expected.

12.2 Recommendations

The adaptive overcurrent protection scheme can be extended by increasing the number of overcurrent relays (OCRs) in a cell by placing OCRs at each node. However, it increases the complexity of relay coordination and it is recommended to use three or four series OCRs to provide more efficient overcurrent protection with safe grading margins.

Within a cell, wide area protection schemes could be deployed as a backup at transmission level, or as primary protection at distribution level. It is, however, recommended that these wide area schemes (within each cell) are separated due to the differing protection requirements for transmission and distribution systems, and the likelihood that distribution systems involve significantly more potential measurement locations and lower bandwidth communications.

It is recommended that the open source tools for real-time latency characterisation, presented in Chapter 9, be further used to provide measurement data of real (or representative) utility communications systems. This will form a very useful dataset to enhance future smart grid R&D activities, which commonly depend on communications.

From an ICT interoperability perspective, it is recommended that the high number of cells which will form the structure of future power systems, as proposed by ELECTRA, be managed with standardised protocols and data models, such as IEC 61850 and the CIM. While this will help in achieving interoperable systems, it will also require significant implementation efforts from the point of view of data modelling and implementation of new processes for the correct management of such standardised artefacts. While ENTSO-E already implements many processes based on the CIM, the WoC concept requires their implementation on a much more distributed scale.

12.3 Opportunities for Further Research

Similar to the combined testing of adaptive protection and PPVC, balance control functions can be simulated with adaptive protection operations in order to observe the interactions between frequency stability and protection operations. In this case, the provision of additional active power reserves may have impact on the calculation of new relay setting parameters. Furthermore, the validation of adaptive protection algorithms can be proven using real-time simulation. Laboratory testing of adaptive protection may require to also investigate possible communications and information standards, taking cybersecurity issues into account.

Similarly, further research is required to validate the wide area protection method in Chapter 9 under realistic communications delays. Although the wide area protection framework introduced in Chapter 9 is designed to be computationally efficient, the limit – in terms of the maximum number of measurement locations which can feasibly be accommodated in real-time – remains to be quantified. These factors will influence the open question of the appropriate size of a cell in the WoC paradigm. This will also govern the operation time of the wide area protection scheme;

excessive operation time may negatively interact with WoC control functions due to the requirements to identify the event location as part of the Balance Restoration Control (BRC) algorithm and to activate fast-acting BRC reserves as early as possible. This potential interaction between protection and BRC should be studied in more detail. Furthermore, validation using more diverse power system models, such as “weak” distribution systems, is required.

Regarding ICT interoperability, the actual applicability of the major IEC standards related to smart grids (IEC 61850 and the CIM) should be validated by considering the highly distributed nature of the WoC concept compared to the present-day centralised control approach. New research-based software tools are required to deliver this vision.

The developed protection algorithms have been tested to some extent by simulations in the case of standalone ELECTRA use cases (balance and voltage control). More investigation is needed to test their performance and impact on voltage and balancing control, focusing on the integration of multiple use cases within test networks and providing further validation in realistic multi-domain laboratory environments.

13 Appendix: Analysis of Objectives

To support the definition of this work, as described in Chapter 2, Table 13-1 compares the text from the ELECTRA IRP DoW with the interpretation by the report authors.

Original DoW Text	**Notes and interpretation**
Sub-task 6.3.1: Adaptive protection providing dynamic emergency system response	
Self-healing characteristics, as part of the safety net that nowadays relies on protection systems, play an important role in minimising the impact of disturbances on the network. Therefore, protection systems that are flexible enough to deal with a highly flexible network are needed. Adaptive protection techniques should be employed to identify abnormal operating states at local and system wide levels. The behaviour of the protection system would dynamically change to reflect the prevailing power system state, but at the same time maintains the desired performance. Performance targets can also change to better align with the system's operational state. At any given time, dependable protection operation may be favoured over secure operation and vice versa. The results of this sub-task describe real-time performance indicators that protection functions can use to adapt their behaviour accordingly. These indicators will focus mainly on information derived from wide area measurements. This deliverable will also determine the appropriate actions by adaptive protection in response to different system condition categories – these can be in the form of flexible scheme logic and signalling and dynamic protection characteristics.	In this context, it is assumed that "emergency system response" refers to the role conventionally associated with "power system protection". Grids need to become more self-healing. Although existing provisions such as conventional frequency response and System Integrity Protection Schemes (SIPS) are deployed in today's systems, future systems will be significantly architecturally different – requiring new approaches for disturbance detection and location. The term "disturbance" is assumed to mean "power system fault" in the context of Task 6.3, but could also be interpreted as including harmonics, flicker, power swings, power system outages, or communications outages. "Performance" could be determined by, for example: accuracy of fault location, correct protection device coordination, reduced tripping times, and minimised isolated zone. The trade-off between dependable protection operation and secure operation is a potential "control" conflict. "Real-time performance indicators" could be measurements from power system components or controller outputs. In this task, it should be assumed that communications systems are available, and that it is not required to depend entirely on local measurements. "Different system conditions" could include: fault levels; inertia levels (which are typically related to fault levels); network topologies; DERs connected/disconnected; overall system state (i.e. the traffic light system); and communications operational/degraded. "Flexible scheme logic and signalling and dynamic protection characteristics" – i.e. adaptive protection.
Sub-task 6.3.2: New protection philosophies utilising flexible controls for inherent fault detection and mitigation	
Advanced switching equipment respond quickly to emerging problems by using strategies like promptly changing flow patterns and voltage levels. Protection delivery mechanisms will make use of inherent controllability of network assets such as converters, fault current limiters and FACTS. This will complement protective relaying based approaches. The ability of these resources to inherently provide fast responses to network events is advantageous in impeding the development of disturbances into catastrophic system failures. The purpose is to establish the capabilities of individual devices (especially power electronic based) to maintain network resilience during faults and disturbances through the active control of fault levels and power flows. The control actions of these devices can be in response to local or system wide disturbances. It will also investigate the ability to identify the onset of a disturbance by monitoring the response of network	It can be assumed that, within the context of ELECTRA, radical new system operational states are permitted or available, including: low fault levels, islanding, bi-directional power flows, and very high penetration of sensors and associated communications infrastructure. "Advanced switching equipment" is assumed to refer to power electronic technologies. "Inherent controllability..." implies *proactive* control of network devices to optimise protection operation. "...fast responses to network events..." – could refer to grid codes i.e. the role of power electronic devices during faults, and settings requirements for frequency- and ROCOF-based protection. "...active control..." – rather than a strictly-defined fault behaviour specified in a grid code, i.e. some flexibility can be assumed. In the same way that cell-wide inertia or frequency response may need to be controlled, cell-wide protection

devices during transient conditions.	settings may need to be adapted. "...ability to identify the onset of a disturbance" could be assumed to refer to condition monitoring, or data mining of historical events. However, in terms of this task, real-time protection is assumed to be the focus.
Sub-task 6.3.3: Utilising ubiquitous automation, self-healing and dynamic ratings for system resilience	
A full complement of automatic control and active network management schemes will be deployed to counteract the impact of disturbances in real-time (seconds or minutes). These measures can help alleviate post disturbance constraints by dynamically releasing additional available network capacity, restoring supplies and managing network constraints in the wake of a disturbance. The results of this sub-task will determine the required post disturbance functions described. It will also describe the necessary coordination to spread the required response across different functions in a way that better serves system performance and avoids conflict.	"...coordination to spread the required response across different functions in a way that better serves system performance and avoids conflict" – implies coordinated wide-area control, rather than just device-specific actions. The focus of this sub-task is post-fault/disturbance action, such as network restoration. There may be some overlap with the control schemes defined in Task 6.2 for WoC operation. Therefore, this sub-task needs to identify areas which are not catered for by the existing defined frequency and voltage controls in Task 6.2 – and potentially involves more "exotic" or device-specific schemes.

Table 13-1: Process of Task 6.3 objective refinement

14 References

[1] L. Martini, H. Brunner, E. Rodriguez, C. Caerts, T. Strasser, and G. Burt, “The grid of the future & the need for a decentralized control architecture: the web-of-cells concept,” in *International Conference & Exhibition on Electricity Distribution (CIRED)*, 2017.

[2] Bell Labs, “Bell Labs Advisory Service for Smart Grid Network Transformation,” 2014.

[3] P. Wall, N. Shams, V. Terzija, V. Hamidi, C. Grant, D. Wilson, S. Norris, K. Maleka, C. Booth, Q. Hong, and A. Roscoe, “Smart frequency control for the future GB power system,” in *IEEE PES ISGT Europe*, 2016.

[4] S. M. Blair, G. Burt, A. Lof, S. Hänninen, B. Kedra, M. Kosmecki, J. Merino, F. R. Belloni, D. Pala, M. Valov, B. Lüers, and A. Temiz, “Minimising the impact of disturbances in future highly-distributed power systems,” in *CIGRE B5 Colloquium*, 2017.

[5] G. Radman, “Wide area frequency based generation trip event location estimation,” in *2012 IEEE Power and Energy Society General Meeting*, 2012, pp. 1–6.

[6] H. Zhang, F. Shi, Y. Liu, and V. Terzija, “Adaptive Online Disturbance Location Considering Anisotropy of Frequency Propagation Speeds,” *IEEE Trans. Power Syst.*, vol. 31, no. 2, pp. 931–941, Mar. 2016.

[7] CIGRE WG C6.04 Task Force C6.04.02, “Benchmark Systems for Network Integration of Renewable and Distributed Energy Resources,” 2014.

[8] Alstom Grid, *Network Protection & Automation Guide*. Alstom Grid, 2011.

[9] C.-R. Chen and C.-H. Lee, “Adaptive overcurrent relay coordination for off-peak loading in interconnected power system,” *Int. J. Electr. Power Energy Syst.*, vol. 63, pp. 140–144, Dec. 2014.

[10] F. Belloni, C. Chiumeo, C. Gandolfi, and S. Pugliese, “Simulation model of a protection scheme for active distribution networks,” in *International Conference on Renewable Energies and Power Quality*, 2013.

[11] M. Delfanti, E. Fasciolo, V. Olivieri, and M. Pozzi, “A2A project: A practical implementation of smart grids in the urban area of Milan,” *Electr. Power Syst. Res.*, vol. 120, pp. 2–19, Mar. 2015.

[12] A. Dede, D. Della Giustina, F. Franzoni, and A. Pegoiani, “IEC 61850-based logic selectivity scheme for the MV distribution network,” in *2014 IEEE International Workshop on Applied Measurements for Power Systems Proceedings (AMPS)*, 2014, pp. 1–5.

[13] A. Gashi, G. Kabashi, S. Kabashi, S. Ahmetaj, and V. Veliu, “Simulation the Wind Grid Code Requirements for Wind Farms Connection in Kosovo Transmission Grid,” *Energy Power Eng.*, vol. 4, no. 6, pp. 482–495, Nov. 2012.

[14] A. J. Roscoe, M. Yu, R. Ierna, J. Zhu, A. Dyśko, H. Urdal, and C. Booth, “A VSM (virtual synchronous machine) convertor control model suitable for RMS studies for resolving system operator/owner challenges,” in *15th Wind Integration Workshop*, 2016.

[15] V. Terzija, G. Valverde, Deyu Cai, P. Regulski, V. Madani, J. Fitch, S. Skok, M. M. Begovic, and A. Phadke, “Wide-Area Monitoring, Protection, and Control of Future Electric Power Networks,” *Proc. IEEE*, vol. 99, no. 1, pp. 80–93, Jan. 2011.

[16] E. G. Sansano, M. H. Syed, A. Roscoe, G. Burt, M. Stanovich, and K. Schoder, “Controller HIL testing of real-time distributed frequency control for future power systems,” in *IEEE PES Innovative Smart Grid Technologies, Europe*, 2016.

[17] CIGRE Working Group B5.14, “Wide area protection & Control technologies,” 2016.

[18] IEEE Power System Relaying Committee (PSRC) Working Group C-14, “Use of Synchrophasor Measurements in Protective Relaying Applications,” 2013. [Online].

Available: http://www.pes-psrc.org/Reports/Use of Synchrophasor Measurements in Protective Relaying Applications_final.pdf.

[19] NERC, “Real-Time Application of Synchrophasors for Improving Reliability,” 2010. [Online]. Available: http://www.nerc.com/docs/oc/rapirtf/RAPIR final 101710.pdf.

[20] EURAMET, “EURAMET Smart Grids II,” 2017. [Online]. Available: http://www.smartgrids2.eu/.

[21] NASPI PMU Applications Requirements Task Force, “PMU Data Quality: A Framework for the Attributes of PMU Data Quality and a Methodology for Examining Data Quality Impacts to Synchrophasor Applications,” 2017.

[22] A. von Meier, E. Stewart, A. McEachern, M. Andersen, and L. Mehrmanesh, “Precision Micro-Synchrophasors for Distribution Systems: A Summary of Applications,” *IEEE Trans. Smart Grid*, pp. 1–1, 2017.

[23] NASPI Time Synchronization Task Force, “Time Synchronization in the Electric Power System,” 2017.

[24] M. Biswal, S. M. Brahma, and H. Cao, “Supervisory Protection and Automated Event Diagnosis Using PMU Data,” *IEEE Trans. Power Deliv.*, vol. 31, no. 4, pp. 1855–1863, Aug. 2016.

[25] M. Kezunovic, A. Esmaeilian, T. Becejac, P. Dehghanian, and C. Qian, “Life Cycle Management Tools for Synchrophasor Systems: Why We Need Them and What They Should Entail,” *IFAC-PapersOnLine*, vol. 49, no. 27, pp. 73–78, 2016.

[26] C. HUANG, F. LI, D. ZHOU, J. GUO, Z. PAN, Y. LIU, and Y. LIU, “Data quality issues for synchrophasor applications Part I: a review,” *J. Mod. Power Syst. Clean Energy*, vol. 4, no. 3, pp. 342–352, Jul. 2016.

[27] T. J. Overbye, “Visualization enhancements for power system situational assessment,” in *2008 IEEE Power and Energy Society General Meeting - Conversion and Delivery of Electrical Energy in the 21st Century*, 2008, pp. 1–4.

[28] A.-J. Nikkilä, M. Kuivaniemi, and J. Seppänen, “Using wide area measurements to improve situational awareness and power system analytics in Finnish power system,” *NASPI International Synchrophasor Symposium*, 2016. [Online]. Available: https://www.naspi.org/sites/default/files/2016-10/fingrid_nikkila_wide_area_measurements__20160322.pdf.

[29] D. Dorr and T. Geist, “Improving Electric Power System Situational Awareness,” *Electric Power Research Institute*, 2015. [Online]. Available: http://smartgrid.epri.com/doc/Leveraging Information Bursts.pdf.

[30] B. J. Pierre, F. Wilches-Bernal, D. A. Schoenwald, R. T. Elliott, J. C. Neely, R. H. Byrne, and D. J. Trudnowski, “Open-loop testing results for the pacific DC intertie wide area damping controller,” in *2017 IEEE Manchester PowerTech*, 2017, pp. 1–6.

[31] S. M. Blair, C. D. Booth, B. De Valck, D. Verhulst, C. Kirasack, K. Y. Wong, and S. Lakshminarayanan, “Validating Secure and Reliable IP/MPLS Communications for Current Differential Protection,” in *Developments in Power System Protection (DPSP)*, 2016.

[32] M. Begovic, D. Novosel, D. Karlsson, C. Henville, and G. Michel, “Wide-Area Protection and Emergency Control,” *Proc. IEEE*, vol. 93, no. 5, pp. 876–891, May 2005.

[33] E. Udren, “Principles for Practical Wide-Area Backup Protection with Synchrophasor Communications,” in *CIGRE Paris Session B5*, 2014.

[34] Y. Gong, Y. Huang, and N. N. Schulz, “Integrated Protection System Design for Shipboard Power System,” *IEEE Trans. Ind. Appl.*, vol. 44, no. 6, pp. 1930–1936, 2008.

[35] J. Tang and P. G. McLaren, “A Wide Area Differential Backup Protection Scheme For Shipboard Application,” *IEEE Trans. Power Deliv.*, vol. 21, no. 3, pp. 1183–1190, Jul. 2006.

[36] M. K. Neyestanaki and A. M. Ranjbar, “An Adaptive PMU-Based Wide Area Backup Protection Scheme for Power Transmission Lines,” *IEEE Trans. Smart Grid*, vol. 6, no. 3, pp. 1550–1559, May 2015.

[37] S. Brahma, “Advancements in Centralized Protection and Control within a Substation,” *IEEE Trans. Power Deliv.*, vol. PP, no. 99, pp. 1–1, 2016.

[38] A. Johnsson, J. E. Soderstrom, P. Norberg, and A. Fogelberg, “Standard platform for integrated soft protection and control,” in *2010 IEEE PES Innovative Smart Grid Technologies Conference Europe (ISGT Europe)*, 2010, pp. 1–6.

[39] M. Kezunovic, “Translational Knowledge: From Collecting Data to Making Decisions in a Smart Grid,” *Proc. IEEE*, vol. 99, no. 6, pp. 977–997, Jun. 2011.

[40] I. Dorofeyev, “Software Based Protection & Control System,” *PAC World magazine*, 2013. [Online]. Available: https://www.pacw.org/issue/december_2012_issue/russian/software_based_protection_control_system/complete_article/1.html.

[41] Y. Liu, S. You, W. Yao, Y. Cui, L. Wu, D. Zhou, J. Zhao, H. Liu, and Y. Liu, “A Distribution Level Wide Area Monitoring System for the Electric Power Grid–FNET/GridEye,” *IEEE Access*, vol. 5, pp. 2329–2338, 2017.

[42] V. Miranda, “Excess of Data, Lack of Models,” *IEEE PowerTech Conference*, 20017. [Online]. Available: http://sites.ieee.org/pes-powertech/files/2017/07/PowerTech-2017-Vladimiro-Miranda.pdf.

[43] H. Gharavi and B. Hu, “Synchrophasor Sensor Networks for Grid Communication and Protection,” *Proc. IEEE*, vol. 105, no. 7, pp. 1408–1428, Jul. 2017.

[44] X. Liang, S. A. Wallace, and D. Nguyen, “Rule-Based Data-Driven Analytics for Wide-Area Fault Detection Using Synchrophasor Data,” *IEEE Trans. Ind. Appl.*, vol. 53, no. 3, pp. 1789–1798, May 2017.

[45] IEEE PES Power System Relaying Committee, “Centralised Substation Protection and Control,” 2015.

[46] S. Brahma, R. Kavasseri, H. Cao, N. R. Chaudhuri, T. Alexopoulos, and Y. Cui, “Real-Time Identification of Dynamic Events in Power Systems Using PMU Data, and Potential Applications—Models, Promises, and Challenges,” *IEEE Trans. Power Deliv.*, vol. 32, no. 1, pp. 294–301, Feb. 2017.

[47] J. C. Tan, P. A. Crossley, D. Kirschen, J. Goody, and J. A. Downes, “An expert system for the back-up protection of a transmission network,” *IEEE Trans. Power Deliv.*, vol. 15, no. 2, pp. 508–514, Apr. 2000.

[48] J. C. Tan, P. A. Crossley, P. G. McLaren, P. F. Gale, I. Hall, and J. Farrell, “Application of a wide area backup protection expert system to prevent cascading outages,” *IEEE Trans. Power Deliv.*, vol. 17, no. 2, pp. 375–380, Apr. 2002.

[49] S. Pati, C. K. Panigrahi, and P. R. Pattanaik, “A Superimposed Components based Fault Detector for Power System Applications,” *Indian J. Sci. Technol.*, vol. 9, no. 13, Apr. 2016.

[50] R. K. Aggarwal, Y. Aslan, and A. T. Johns, “New concept in fault location for overhead distribution systems using superimposed components,” *IEE Proc. - Gener. Transm. Distrib.*, vol. 144, no. 3, p. 309, 1997.

[51] A. P. Apostolov, D. Tholomier, and S. H. Richards, “Superimposed components based sub-cycle protection of transmission lines,” in *IEEE PES Power Systems Conference and Exposition, 2004.*, 2004, pp. 508–513.

[52] M. M. A. Mahfouz and M. M. Eissa, “New high-voltage directional and phase selection protection technique based on real power system data,” *IET Gener. Transm. Distrib.*, vol. 6, no. 11, pp. 1075–1085, Nov. 2012.

[53] Y. Seyedi and H. Karimi, “Coordinated Protection and Control Based on Synchrophasor Data Processing in Smart Distribution Networks,” *IEEE Trans. Power Syst.*, 2017.

[54] I. Abdulhadi, F. Coffele, and C. Booth, “Testing of Distribution Network Fault Passage Indicators to Facilitate Enhanced Network Automation,” in *PAC World Conference*, 2015.

[55] R. Guo, V. Vankayala, C. Qu, E. Crozier, S. Allen, K. Adeleye, V. Dabic, P. Found, and N. Shah, “Fault Location, Isolation and Service Restoration -- Optimizing Field Operations for Utilities,” in *2016 IEEE Rural Electric Power Conference (REPC)*, 2016, pp. 33–41.

[56] K. Sun, Q. Chen, and Z. Gao, “An Automatic Faulted Line Section Location Method for Electric Power Distribution Systems Based on Multisource Information,” *IEEE Trans. Power Deliv.*, vol. 31, no. 4, pp. 1542–1551, Aug. 2016.

[57] J.-H. Teng, W.-H. Huang, and S.-W. Luan, “Automatic and Fast Faulted Line-Section Location Method for Distribution Systems Based on Fault Indicators,” *IEEE Trans. Power Syst.*, vol. 29, no. 4, pp. 1–10, 2014.

[58] F. Yu, C. Booth, and A. Dyśko, “Backup Protection Requirements in Future Low-Inertia Power Systems,” in *51st International Universities’ Power Engineering Conference*, 2016.

[59] Z. Galijasevic and A. Abur, “Fault location using voltage measurements,” *IEEE Trans. Power Deliv.*, vol. 17, no. 2, pp. 441–445, Apr. 2002.

[60] M. M. Eissa, M. E. Masoud, and M. M. M. Elanwar, “A Novel Back Up Wide Area Protection Technique for Power Transmission Grids Using Phasor Measurement Unit,” *IEEE Trans. Power Deliv.*, vol. 25, no. 1, pp. 270–278, Jan. 2010.

[61] Z. Zhang, X. Kong, X. Yin, Z. Yang, and L. Wang, “A novel wide-area backup protection based on fault component current distribution and improved evidence theory.,” *ScientificWorldJournal.*, vol. 2014, p. 493739, 2014.

[62] J.-A. Jiang, Ching-Shan Chen, and Chih-Wen Liu, “A new protection scheme for fault detection, direction discrimination, classification, and location in transmission lines,” *IEEE Trans. Power Deliv.*, vol. 18, no. 1, pp. 34–42, Jan. 2003.

[63] F. Zhang and L. Mu, “Wide-area protection scheme for active distribution networks based on phase comparison,” in *2015 5th International Conference on Electric Utility Deregulation and Restructuring and Power Technologies (DRPT)*, 2015, pp. 927–932.

[64] Q. Jiang, X. Li, B. Wang, and H. Wang, “PMU-Based Fault Location Using Voltage Measurements in Large Transmission Networks,” *IEEE Trans. Power Deliv.*, vol. 27, pp. 1–1, 2012.

[65] P. Orr, G. Fusiek, P. Niewczas, C. D. Booth, A. Dysko, F. Kawano, T. Nishida, and P. Beaumont, “Distributed Photonic Instrumentation for Power System Protection and Control,” *IEEE Trans. Instrum. Meas.*, vol. 64, no. 1, pp. 19–26, Jan. 2015.

[66] L. Nordström, “Open measurements for new applications,” *DPSP 2014 Keynote*, 2014. [Online]. Available: https://www.kth.se/files/view/larsno/5836d24012b51d1042596725/DPSPNordstrmrevised20140401.pdf.

[67] M. Khan, P. M. Ashton, M. Li, G. A. Taylor, I. Pisica, and J. Liu, “Parallel Detrended Fluctuation Analysis for Fast Event Detection on Massive PMU Data,” *IEEE Trans. Smart Grid*, vol. 6, no. 1, pp. 360–368, Jan. 2015.

[68] M. Kezunovic, “Fault location estimation based on matching the simulated and recorded waveforms using genetic algorithms,” in *7th International Conference on Developments in Power Systems Protection (DPSP 2001)*, 2001, vol. 2001, pp. 399–402.

[69] M. Kezunovic, “Smart Fault Location for Smart Grids,” *IEEE Trans. Smart Grid*, vol. 2, no. 1, pp. 11–22, Mar. 2011.

[70] M. Pignati, L. Zanni, P. Romano, R. Cherkaoui, and M. Paolone, “Fault Detection and

Faulted Line Identification in Active Distribution Networks Using Synchrophasors-Based Real-Time State Estimation," *IEEE Trans. Power Deliv.*, vol. 32, no. 1, pp. 381–392, Feb. 2017.

[71] J. Zare, F. Aminifar, and M. Sanaye-Pasand, "Synchrophasor-Based Wide-Area Backup Protection Scheme with Data Requirement Analysis," *IEEE Trans. Power Deliv.*, vol. 30, no. 3, pp. 1410–1419, Jun. 2015.

[72] S. R. Firouzi, L. Vanfretti, A. Ruiz-Alvarez, H. Hooshyar, and F. Mahmood, "Interpreting and implementing IEC 61850-90-5 Routed-Sampled Value and Routed-GOOSE protocols for IEEE C37.118.2 compliant wide-area synchrophasor data transfer," *Electr. Power Syst. Res.*, vol. 144, pp. 255–267, 2017.

[73] M. Kanabar, M. G. Adamiak, and J. Rodrigues, "Optimizing Wide Area Measurement System architectures with advancements in Phasor Data Concentrators (PDCs)," in *2013 IEEE Power & Energy Society General Meeting*, 2013, pp. 1–5.

[74] IEC TC 57, "Communication networks and systems for power utility automation - Part 90-12: Wide area network engineering guidelines," 2015.

[75] Y. Wu, L. Nordström, A. Saleem, K. Zhu, N. Honeth, and M. Armendariz, "Perspectives on Peer-to-Peer Data Delivery Architectures for Next Generation Power Systems," in *ISAP2013*, 2013.

[76] Yiming Wu, A. Saleem, and L. Nordstrom, "IEC61850 logical node lookup service using distributed hash tables," in *ISGT 2014*, 2014, pp. 1–5.

[77] P. T. Myrda, J. Taft, and P. Donner, "Recommended Approach to a NASPInet Architecture," in *2012 45th Hawaii International Conference on System Sciences*, 2012, pp. 2072–2081.

[78] P. T. Myrda and K. Koellner, "NASPInet - The Internet for Synchrophasors," in *2010 43rd Hawaii International Conference on System Sciences*, 2010, pp. 1–6.

[79] R. B. Bobba, J. Dagle, E. Heine, H. Khurana, W. H. Sanders, P. Sauer, and T. Yardley, "Enhancing Grid Measurements: Wide Area Measurement Systems, NASPInet, and Security," *IEEE Power and Energy Magazine*, vol. 10, no. 1, pp. 67–73, Jan-2012.

[80] R. Bobba, E. Heine, H. Khurana, and T. Yardley, "Exploring a tiered architecture for NASPInet," in *2010 Innovative Smart Grid Technologies (ISGT)*, 2010, pp. 1–8.

[81] L. Zhao and A. Abur, "Multiarea State Estimation Using Synchronized Phasor Measurements," *IEEE Trans. Power Syst.*, vol. 20, no. 2, pp. 611–617, May 2005.

[82] Z. Zhong, C. Xu, B. J. Billian, L. Zhang, S.-J. S. Tsai, R. W. Conners, V. A. Centeno, A. G. Phadke, and Y. Liu, "Power System Frequency Monitoring Network (FNET) Implementation," *IEEE Trans. Power Syst.*, vol. 20, no. 4, pp. 1914–1921, Nov. 2005.

[83] L. Qin, Y. Wang, C. Hao, and M. Li, "Multi-Agent System wide area protection considering distributed generation impact," in *2011 International Conference on Advanced Power System Automation and Protection*, 2011, pp. 549–553.

[84] E. O. Schweitzer, A. Guzmán, H. J. Altuve, and D. A. Tziouvaras, "Real-Time Synchrophasor Applications for Wide-Area Protection, Control, and Monitoring," in *3rd International Conference on Advanced Power System Automation and Protection*, 2009.

[85] J. Zare, F. Aminifar, and M. Sanaye-Pasand, "Communication-Constrained Regionalization of Power Systems for Synchrophasor-Based Wide-Area Backup Protection Scheme," *IEEE Trans. Smart Grid*, vol. 6, no. 3, pp. 1530–1538, May 2015.

[86] H. A. Tokel, G. Alirezaei, S. Baig, and R. Mathar, "An optimization framework for planning of WAMS with a heterogeneous communication network," in *2016 IEEE International Conference on Smart Grid Communications (SmartGridComm)*, 2016, pp. 521–526.

[87] R. Khan, K. McLaughlin, D. Laverty, and S. Sezer, "Design and Implementation of Security Gateway for Synchrophasor based Real-time Control and Monitoring in Smart Grid," *IEEE*

Access, pp. 1–1, 2017.

[88] A. Derviskadic, P. Romano, M. Pignati, and M. Paolone, “Architecture and Experimental Validation of a Low-Latency Phasor Data Concentrator,” *IEEE Trans. Smart Grid*, pp. 1–1, 2016.

[89] S. P. Pokharel and S. Brahma, “Optimal PMU placement for fault location in a power system,” in *41st North American Power Symposium*, 2009, pp. 1–5.

[90] Xiaoping Xiong, Jiancheng Tan, and Xiangning Lin, “Study on Communication Architecture Design of Wide-Area Measurement System,” *IEEE Trans. Power Deliv.*, vol. 28, no. 3, pp. 1542–1547, Jul. 2013.

[91] K. Zhu, L. Nordstrom, and A. T. Al-Hammouri, “Examination of data delay and packet loss for wide-area monitoring and control systems,” in *2012 IEEE International Energy Conference and Exhibition (ENERGYCON)*, 2012, pp. 927–934.

[92] K. L. Lo, H. S. Ng, and J. Trecat, “Power systems fault diagnosis using Petri nets,” *IEE Proc. - Gener. Transm. Distrib.*, vol. 144, no. 3, p. 231, 1997.

[93] Bai-Lin Qin, A. Guzman-Casillas, and E. O. Schweitzer, “A new method for protection zone selection in microprocessor-based bus relays,” *IEEE Trans. Power Deliv.*, vol. 15, no. 3, pp. 876–887, Jul. 2000.

[94] K. Kangvansaichol, “Multi-zone differential protection for transmission networks,” in *Eighth IEE International Conference on Developments in Power System Protection*, 2004, vol. 2004, pp. 428–431.

[95] Bai-Lin Qin, A. Guzman-Casillas, and E. O. Schweitzer, “A new method for protection zone selection in microprocessor-based bus relays,” *IEEE Trans. Power Deliv.*, vol. 15, no. 3, pp. 876–887, 2000.

[96] S. M. Blair, “rapid61850,” 2012. [Online]. Available: https://github.com/stevenblair/rapid61850.

[97] S. M. Blair, F. Coffele, C. D. Booth, and G. M. Burt, “An Open Platform for Rapid-Prototyping Protection and Control Schemes with IEC 61850,” *IEEE Trans. Power Deliv.*, vol. 28, no. 2, pp. 1103–1110, 2013.

[98] A. Guzman, S. Samineni, and M. Bryson, “Protective Relay Synchrophasor Measurements During Fault Conditions,” in *2006 Power Systems Conference: Advanced Metering, Protection, Control, Communication, and Distributed Resources*, 2006, pp. 83–95.

[99] Synchrophasor Measurements for Power Systems Working Group, “C37.118.1a-2014 - IEEE Standard for Synchrophasor Measurements for Power Systems -- Amendment 1: Modification of Selected Performance Requirements,” 2014.

[100] IEEE, “1588-2008 IEEE Standard for a Precision Clock Synchronization Protocol for Networked Measurement and Control Systems.” 2008.

[101] S. M. Blair, “Real-time measurement of PMU reporting latency,” 2017. [Online]. Available: https://doi.org/10.5281/zenodo.400934.

[102] S. M. Blair, C. D. Booth, B. De Valck, D. Verhulst, and K.-Y. Wong, “Modelling and Analysis of Asymmetrical Latency in Packet-Based Networks for Current Differential Protection Application,” *IEEE Trans. Power Deliv.*, pp. 1–1, 2017.

[103] S. Abourida, J. Bélanger, and V. Jalili-Marandi, “Real-Time Power System Simulation: EMT vs. Phasor,” 2016.

[104] S. M. Blair, C. D. Booth, J. Michielsen, and N. Joshi, “Application of MPLS-TP for transporting power system protection data,” in *2016 IEEE International Conference on Smart Grid Communications (SmartGridComm)*, 2016, pp. 619–624.

[105] P. M. Ashton, “Exploiting phasor measurement units for enhanced transmission network

operation and control," 2014.

[106] P. Castello, C. Muscas, P. A. Pegoraro, and S. Sulis, "Automated test system to assess reporting latency in PMUs," in *2016 IEEE International Instrumentation and Measurement Technology Conference Proceedings*, 2016, pp. 1–6.

[107] M. Lehtonen, *Edison - research programme on electricity distribution automation 1993-1997 : interim report 1995*. Technical Research Centre of Finland, 1996.

[108] ELECTRA IRP, "European Liaison on Electricity Committed Towards long-term Research Activity - Integrated Research Programme," 2013. [Online]. Available: http://www.electrairp.eu/.

[109] ELECTRA Web-of-Cells Task Force, "The ELECTRA Web-Of-Cell Architecture in a Nutshell," 2015.

[110] Finnish Meteorological Institute, "Open data manual," 2014. [Online]. Available: http://en.ilmatieteenlaitos.fi/open-data-manual.

[111] R. Zimmerman and R. Lincoln, "Python Interior Point Solver (PIPS)," 2011. [Online]. Available: https://rwl.github.io/PYPOWER/api/pypower.pips-module.html.

[112] Fraunhofer IWES and University of Kassel, "pandapower," 2016. [Online]. Available: http://pandapower.readthedocs.io/en/v1.4.0/index.html.

[113] A. Ghaderi, H. L. Ginn, and H. A. Mohammadpour, "High impedance fault detection: A review," *Electr. Power Syst. Res.*, vol. 143, pp. 376–388, Feb. 2017.

[114] Z. Liang, "High impedance fault detection in power distribution systems with impedance-based methods in frequency domain," University of British Columbia, 2016.

[115] M. M. Ghalei, H. K. Kargar, and M. G. M. M. G. M. Zanjani, "High impedance fault detection of distribution network by phasor measurement units," in *Electrical Power Distribution Networks (EPDC), 2012 Proceedings of 17th Conference on*, 2012, vol. 4, no. Proceedings of 17th Conference on, pp. 1–5.

[116] A. Ghaderi, H. A. Mohammadpour, H. L. Ginn, and Y. J. Shin, "High-impedance fault detection in the distribution network using the time-frequency-based algorithm," *IEEE Trans. Power Deliv.*, vol. 30, no. 3, pp. 1260–1268, Jun. 2015.

[117] I. Baqui, I. Zamora, J. Mazón, and G. Buigues, "High impedance fault detection methodology using wavelet transform and artificial neural networks," *Electr. Power Syst. Res.*, vol. 81, no. 7, pp. 1325–1333, Jul. 2011.

[118] MathWorks, "Matlab Wavelet Toolbox User Guide," 2017.

[119] S. A. Rana, A. Ahmad, and M. N. Quadri, "Faults Detection And Classification On Long Transmission Line Using Wavelet Analysis," *Int. J. Res. Eng. Adv. Technol.*, vol. 2, no. 3, 2014.

[120] N. S. A. . Taujuddin, R. Ibrahim, and S. Sari, "Wavelet Coefficients Reduction Method Based on Standard Deviation Concept for High Quality Compressed Image," *J. Theor. Appl. Inf. Technol.*, vol. 79, no. 3, pp. 380–388, 2015.

[121] A. M. El-Zonkoly, "Fault diagnosis in distribution networks with distributed generation," *Electr. Power Syst. Res.*, vol. 81, no. 7, pp. 1482–1490, Jul. 2011.

[122] O. A. Rosso, S. Blanco, J. Yordanova, V. Kolev, A. Figliola, M. Schürmann, and E. Başar, "Wavelet entropy: a new tool for analysis of short duration brain electrical signals.," *J. Neurosci. Methods*, vol. 105, no. 1, pp. 65–75, Jan. 2001.

[123] A. von Meier and R. Arghandeh, "Chapter 34 – Every Moment Counts: Synchrophasors for Distribution Networks with Variable Resources," in *Renewable Energy Integration*, L. E. Jones, Ed. 2014, pp. 429–438.

[124] Joe-Air Jiang, Jun-Zhe Yang, Ying-Hong Lin, Chih-Wen Liu, and Jih-Chen Ma, "An adaptive

PMU based fault detection/location technique for transmission lines. I. Theory and algorithms," *IEEE Trans. Power Deliv.*, vol. 15, no. 2, pp. 486–493, Apr. 2000.

[125] A. H. Al-Mohammed and M. A. Abido, "A Fully Adaptive PMU-Based Fault Location Algorithm for Series-Compensated Lines," *IEEE Trans. Power Syst.*, vol. 29, no. 5, pp. 2129–2137, Sep. 2014.

[126] A. H. Al-Mohammed and M. A. Abido, "Fault location based on synchronized measurements: a comprehensive survey.," *ScientificWorldJournal.*, vol. 2014, p. 845307, Feb. 2014.

15 Disclaimer

The ELECTRA project is co-funded by the European Commission under the 7th Framework Programme 2013.